FABRIC STRUCTURE STRENGTH AND STRUCTURAL INTEGRITY OF LARGE AREA MAINTENANCE SHELTERS (LAMS)

by

Todd Preston Fittro, Jr.

A Thesis Submitted to the Graduate Faculty of
Auburn University
in partial fulfillment of the
requirements for the Degree of
Master of Science

Auburn, Alabama
May 4, 2019

Approved by

Dr. James S. Davidson, Committee Chair, Professor of Civil Engineering
Dr. Justin D. Marshall, Associate Professor of Civil Engineering
Dr. David B. Roueche, Assistant Professor of Civil Engineering
Dr. Alessandra Bianchini, Airbase Recovery and Acquisition Subject Matter Expert, Air Force Civil Engineer Center

VITA

Todd Preston Fittro, Jr., son of Todd and Kathleen Fittro, was born January 25, 1994, in Birmingham, Alabama. In May of 2012, he graduated from Homewood High School in Homewood, Alabama. He graduated from Auburn University with a Bachelor of Civil Engineering in May of 2017. He entered graduate school at Auburn University in August of 2017 seeking a degree of Master of Science in Civil Engineering (Structures).

ABSTRACT

Large Area Maintenance Shelters (LAMSs) are deployed worldwide by the United States Air Force. The U.S. Air Force uses LAMSs as storage facilities and hangars for vehicles and aircrafts alike. The inherent low weight and mobility of these structural systems make them a key asset to the U.S. Air Force. The lightweight material used as the roofing system on LAMSs has proved inadequate in cases of high wind events which has caused worry within the U.S. Air Force. Through material testing of four types of fabric structures used in the industry as roofing systems and a verification process using finite element analysis, this research provides an operable engineering model. The engineering model predicts the strength and serviceability requirements a fabric structure must provide to withstand high wind events as instructed by the Departments of Defense's Unified Facilities Criteria on Structural Engineering.

ACKNOWLEDGEMENTS

I would like to take this time to thank Dr. Davidson for his continuous support throughout my research. I would also like to thank Casey O'Laughlin with Jacobs, Serge Ferrari, and Seman Corporation for providing fabric structure samples for testing and prior material test data, and Ramsis Farag and the Auburn mechanical engineering department for the use of their material testing equipment. Finally, I would like to thank the United States Air Force and ORISE for the funding provided to make this research possible.

TABLE OF CONTENTS

LIST OF TABLES

LIST OF FIGURES

CHAPTER 1

INTRODUCTION

1.1. BACKGROUND

The Air Force deploys large area maintenance shelters (LAMSs) domestically and abroad to protect assets from weather and ultraviolet (UV) rays. LAMSs range in utility from lunch halls to storage shelters for equipment and aircrafts, with their structural integrity being of highest importance when sheltering people or multi-million dollar aircrafts. Through personal communication with personal at the Air Force Civil Engineer Center the Air Force began to notice a large number of their LAMS structures failing due to wind gusts. The failure was a bursting of the cover fabric structure. Most manufacturers claimed that this failure was due to a rare wind event; however, the Air Force continued to notice these types of failures to multiple LAMSs and began to question the reliability of the fabrics used by the manufacturers.

The following research describes the development of an engineering model (Excel worksheet) to evaluate the strength and deflection limits of different fabric structures used on LAMSs. Once initial conditions are set and material properties are populated, an algorithm will commence in search of the maximum tension force and midspan deflection a certain fabric structure can attain before failure. In addition to this primary objective, a finite element model was developed and material properties were gathered from multiple fabric structures to validate

the engineering model. The analytical results generated from both models will be used to validate the manufacturer's claim of fabric structure strength and serviceability.

1.2. OBJECTIVES

The objective of this research is to develop an engineering model used to predict the strength and serviceability of fabric structures used by the U.S. Air Force for LAMSs.

1.3. RESEARCH APPROACH

Microsoft Excel was used to formulate the engineering model and algorithm assuming a simple cable of catenary action with a uniformly distributed load to represent the fabric structure resisting a uniform wind load. MathCAD was used to validate equations used within the engineering model. ANSYS Mechanical was used to formulate finite element models for further validation. Once validated, the results were analyzed.

1.4. THESIS OUTLINE

Chapter 2 provides a review of literature and previous research related to fabric structures used on LAMSs and a synthesis of the overall review. Chapter 3 discusses the material testing procedure and results from tests run at Auburn University using equipment from the mechanical engineering department. The development of the engineering model is covered in Chapter 4. Chapter 5 presents the development of the finite element models used to validate the engineering model. A design example using the engineering model is covered in Chapter 6. A summary of the research and relevant conclusions are presented in Chapter 7.

As stated by the objective, the engineering model developed by this research is primary with material testing and finite element modeling being ancillary objectives meant to aid in the development and validation of the engineering model.

CHAPTER 2

LITERATURE REVIEW AND SYNTHESIS

2.1. INTRODUCTION

In this literature review, previous research completed in the area of fabric structures and LAMSs will be explored. An introduction to tensioned fabric structures and the make-up of LAMSs will be discussed. Following this introduction, fabric structures which are the focus of this research and the material properties associated with fabric structures will be reviewed.

2.2. TENSIONED FABRIC STRUCTURES

What is a tensioned fabric structure? The term invokes connotations of a tent like structure which does not lead to the thought of a permanent or semi-permanent structure. Tensioned fabric structures are covers or enclosures in which fabric is preshaped and pretensioned to provide a shape that is stable under environmental loads. They are high tech forms that boldly display the machinery of their construction functioning similar to that of timber, steel, or concrete structures with much smaller material self-weight.

The focus of this research is on LAMSs, which are smaller structures in the realm of tensioned fabric structures. Flat fabric profiles are only possible on small structures or those with a tightly modulated supporting structure that supports the fabric at close intervals. In the latter type of application, the fabric is more of a cladding material than a true structural element. For

the purpose of this research, fabrics used on LAMSs will be considered cladding, transferring their load directly to the supporting frame due to the tight modularity of structural supports.

2.3. RESEARCH REVIEW

Bridgens and Birchall's research on the form and function of tensile fabric structures provides insight into the significance of material properties used for the design of tensile fabric structures. Due to the inherent efficiency of fabric structures, there is an increasing tendency to use them as cost effective substitutes for roofs and façades. The performance and structural action of membrane material differs from the rigid construction it replaces. Bridgens and Birchall state that three fundamental fabric structure forms can be developed by manipulating the boundary conditions of an initially flat fabric structure as seen in Figure 2-1. The structural action of tensile structures depends on curvature rather than span allowing for the efficient use of fabric structures over large spans (Bridgens and Birchall 2012).

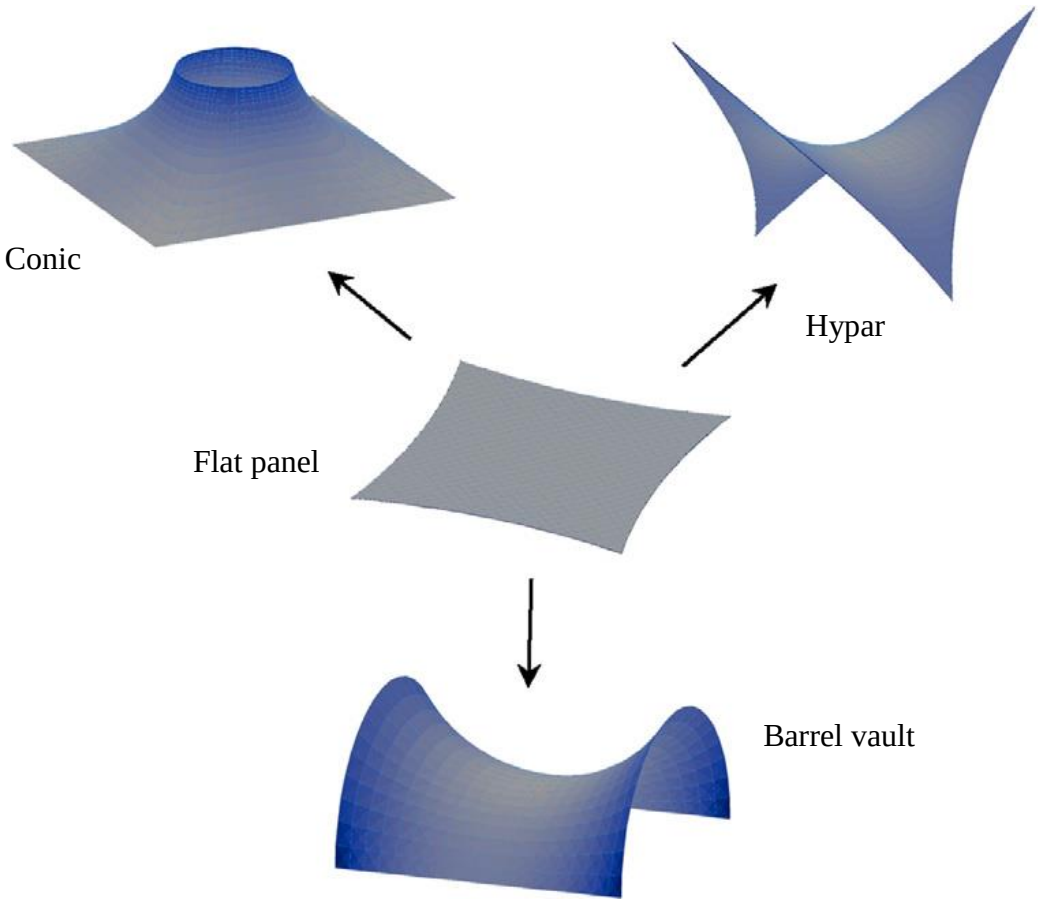

Figure 2-1: Fundamental tensile forms through boundary condition manipulation (Bridgens and Birchall 2012)

To reduce the number of parameters in their research, Bridgens and Birchall applied a constant pretension and linear elastic material constants. Critical load cases for fabric structures include wind and snow loading. Accurate representation of wind loading for fabric structure forms is difficult. Currently, there is very limited design guidance and wind tunnel testing is used routinely for major projects. For Bridgens and Birchall's work, a simplified approach of assigning a reasonable snow load and wind uplift load is taken. The modeling and analysis of the fabric structure is performed in two stages. First, boundary conditions are set and form finding properties are defined. The form finding software applied provides a membrane geometry and

pretension load. Next, a new model is created with the form found geometry that is used for the analysis stage. Last, material properties and loads are then applied, and a geometrically nonlinear analysis is carried out using membrane elements with zero bending and compression stiffness. Due to geometric nonlinearity, the results from different load cases cannot be combined or factored. Each load case is analyzed separately and a permissible stress approach is used to assess the required membrane strength. For architectural design, the dip of the fabric structure as seen in Figure 2-2 is significant in determining the level of coverage and aesthetics of the canopy. A dip to span ratio of 1:6 is often a rule of thumb for efficient and aesthetically pleasing design (Bridgens and Birchall 2012).

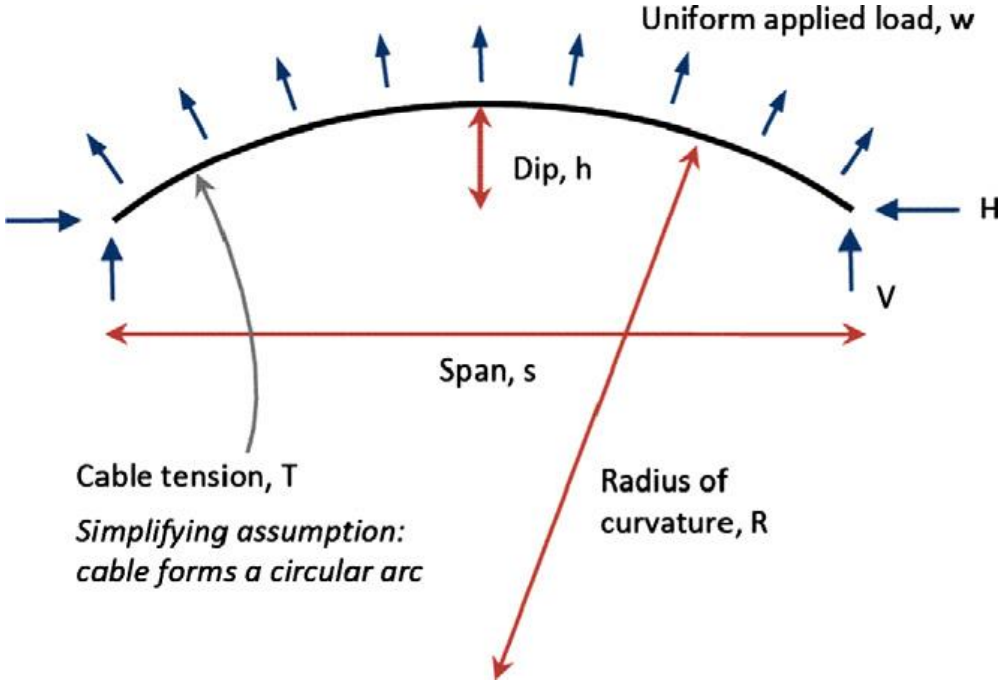

Figure 2-2: Edge cable curvature (Bridgens and Birchall 2012)

Bridgens and Birchall discuss multiple dip to span ratios with a lower ratio leading to a very large cable force as seen in section "A" of Figure 2-3 and a higher ratio allowing for lower cable forces. A dip ratio greater than 0.1 ensures low cable forces as seen in section "C" of Figure 2-3

following the rule of thumb of a 1:6 ratio mentioned above. Section "B" in Figure 2-3 may be used if the designer requires an increase in coverage; however, a ratio in this region will double the forces in the fabric structure.

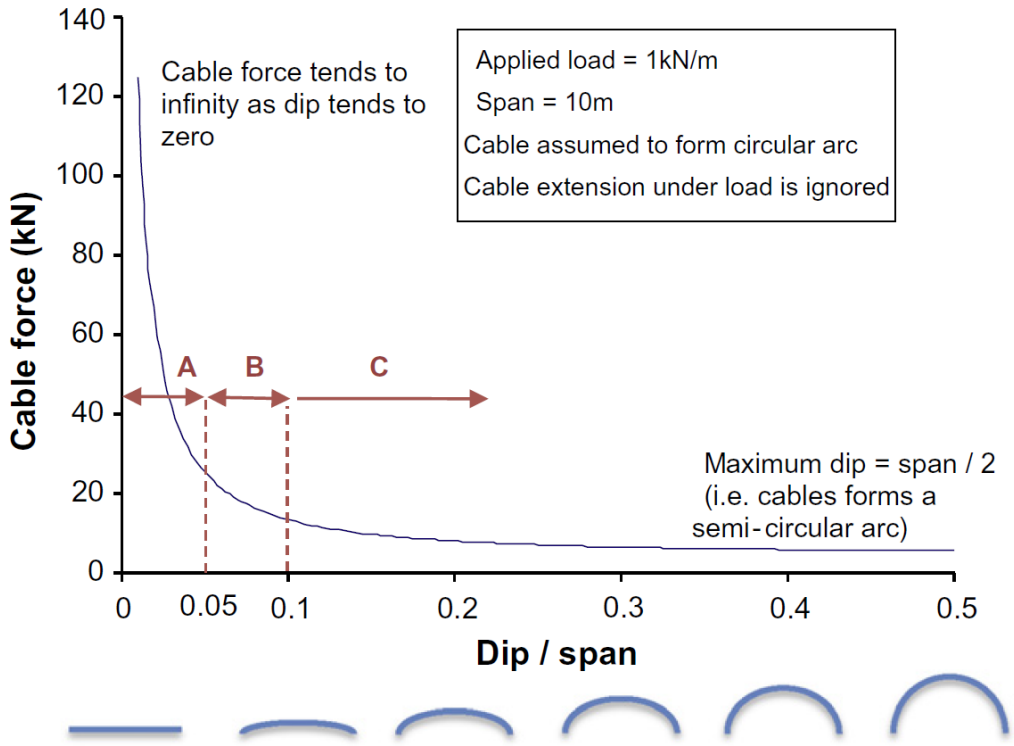

Figure 2-3: Cable force vs. curvature (Bridgens and Birchall 2012)

Bridgens and Birchall continue discussing the varying forms and their functions as the radius of curvature is increased. The LAMSs discussed in this research follow the form of a barrel vault fabric structure. A LAMS is a rigid frame holding two sides of a fabric structure as straight lines and the two perpendicular sides as curved over the arches of a LAMS. This action allows the fabric structure to span between the edges of the aches rather than its corners. A higher radius of curvature in the barrel vault provides an efficient design with low values in stress and deflection. As the barrel vault flattens and tends towards a flat plate, the fabric stresses and deflections increase by a factor of between 2 and 3 as seen in Figure 2-4 (Bridgens and Birchall 2012).

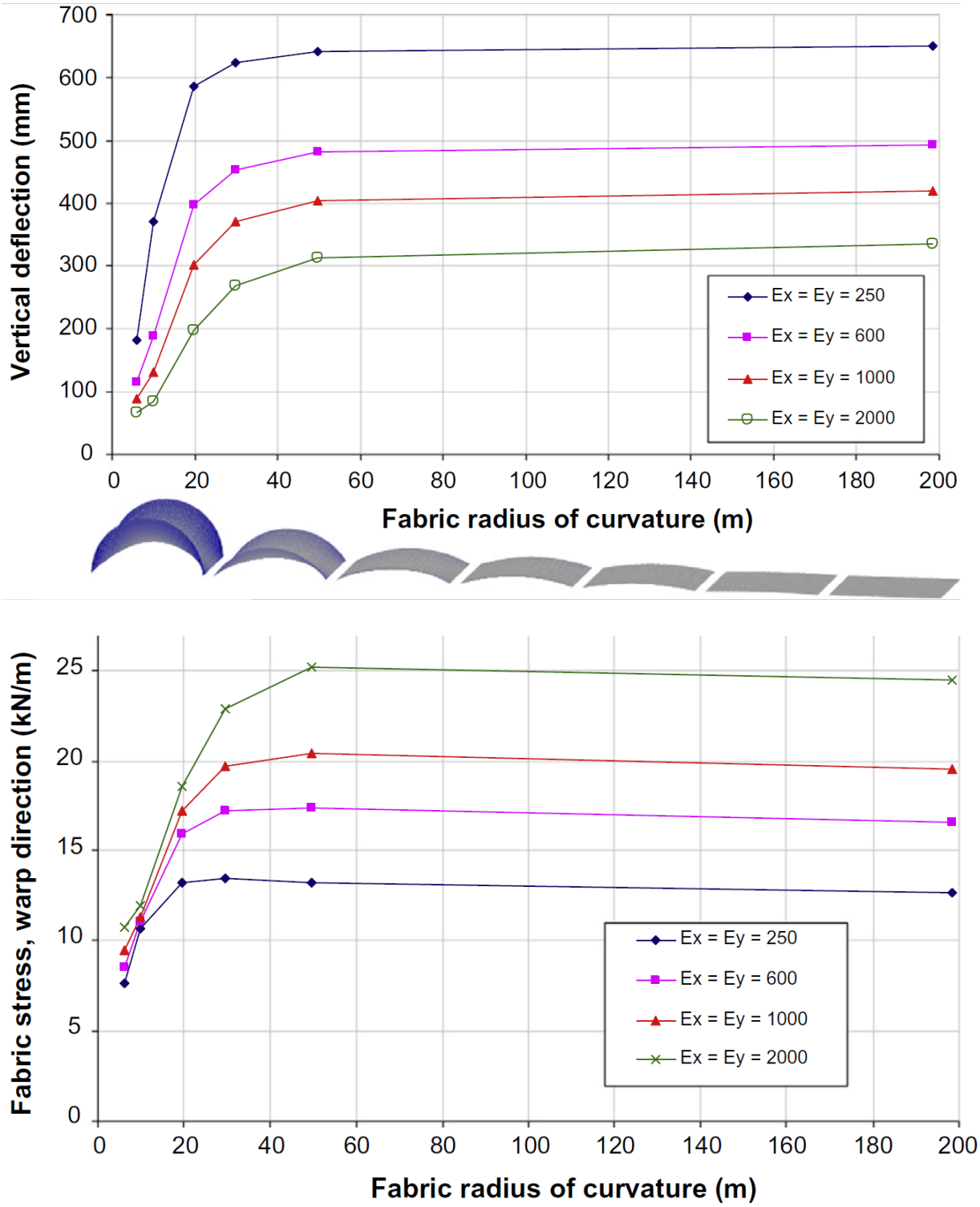

Figure 2-4: Barrel vault fabric structure variations (Bridgens and Birchall 2012)

The results for the barrel vault clearly show that highly curved structures work efficiently and robustly with low stress and deflections, which show minimal variation for a wide range of material stiffness values. Similarly, for cables holding the edge of the fabric structure in place the greater the level of curvature the lower the cable force, with the relationship being highly nonlinear. With a dip to span ratio less than 0.1, the cable force increases dramatically leading to larger cables and larger connection details which are at odds with the lightweight minimalist aesthetics that fabric structures set out to achieve (Bridgens and Birchall 2012).

Once a LAMS is erected, the fabric structure mirrors a flat plate structure, which transforms into a barrel vault structure as load is applied. This action calls for careful engineering analysis to successfully use these elements. An extensive amount of research preformed on fabric structures has been directed towards tensile fabric structures that take the shape of a conic or hypar, as shown in Figure 2-1 due to their use over large spans for roofs or shades installed on malls, airports, and sports complexes. LAMSs are much smaller structures, and to date, research solely on LAMSs is very limited.

2.4. LARGE AREA MAINTENANCE SHELTERS

Since LAMSs require neither interior beams nor columns for support, they can create large, open spaces completely protected from the outside. These interior spaces are perfect for conducting repairs and maintenance on vehicles and heavy machinery. The U.S. military uses these shelters for two basic purposes: aviation maintenance and ground-vehicle maintenance (Big Top Shelters n.d.). The U.S. Air Force's primary use of LAMSs includes aircraft shelter and storage facilities for assets domestically and abroad. Using LAMSs to cover aircraft while on the tarmac increases the aircrafts life span and decreases the heat level inside the cockpit prior to a pilot's

deployment. LAMSs are quick, relatively easy to deploy and have the ability to be very mobile. Figure 2-5 is a typical type of LAMS used on the tarmac to shelter Air Force fighter jets.

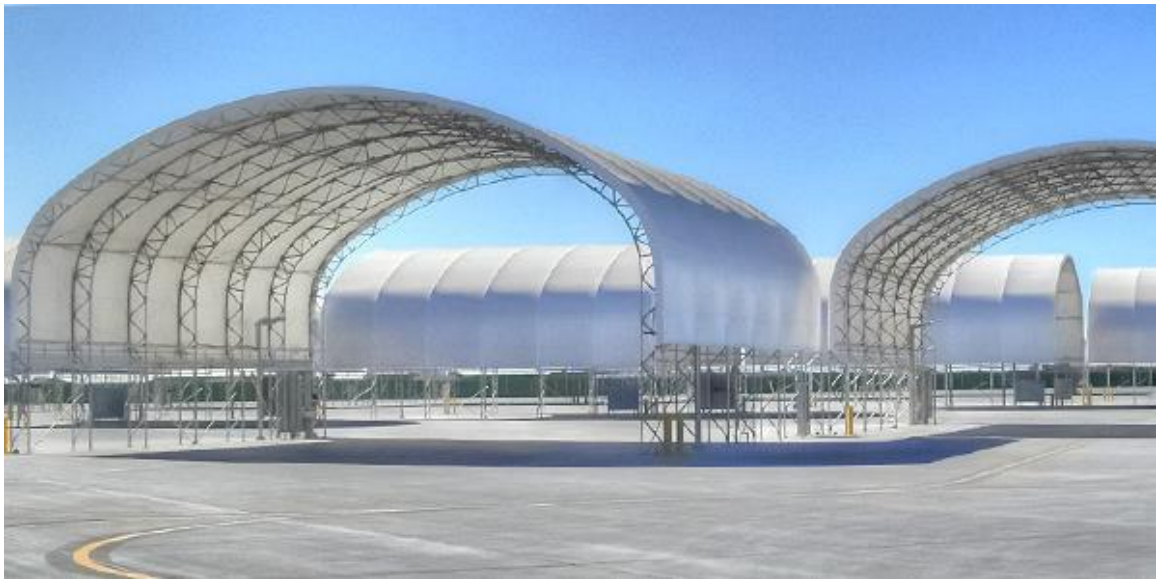

Figure 2-5: LAMS Fighter Jet Hanger (Big Top Shelters n.d.)

In short, LAMSs are tensioned fabric structures pulled tautly over a self-supporting steel frame structure. The steel frame is arched at the top eliminating the need for columns throughout the interior of the structure. After the steel frame is erected, it is secured to the ground by some form of a foundation. Foundations can range from driving large stakes into the ground to attaching a LAMS to cargo containers acting dually as walls and foundations. Once the steel frame is erected and secured to the foundation, a fabric structure is pulled tautly over the frame and secured to the steel frame itself as well as the foundation in some cases. Each company that produces LAMSs provides their clients with erection instructions and most will send a team to supervise or provide support during the erection process if needed.

2.4.1. SUPPORTING ELEMENTS

Fabric structures, like all tensioned-based structural elements, require compression and bending elements to bring their loads down to grade. Various types of structural materials have been used for supporting elements; however, the majority of fabric structures are supported by structural steel. Structural steel has a relatively high compression and bending capacity, can be easily transported, and in most cases, is the more economical option than aluminum or concrete. Structural steel has the ability to be shaped to any form through shop fabrication, making it ideal to interface with a carefully patterned fabric structure. As a material, steel can be readily formed into varying cross-sections such as cast, cut, bent, rolled, punched, welded, or bolted. Above all else, it is a material that allows for the demand of complex connections of fabric structures (Huntington 2004).

2.5. DESIGN AND CONSTRUCTION PROCESS

Most structures constructed in the United States today are designed by a team of engineer specialists working under the direction of an architectural generalists. Once the design is completed, a general contractor will construct the structure, which will be inspected by both the engineer and architect. The design and construction process discussed above works for most contemporary structures, but the tensioned fabric structure is not most structures. With the vast majority of contemporary structures being rectilinear in geometry, the general design of structural members is fairly predictable to most architects. However, the means by which tensioned fabric structures stand up and the way it looks are inseparable, with the structural engineer and architect to work in tandem when designing a tensioned fabric structure. The unusual structural properties of the fabrics used for these structures must be also carefully considered during the design phase. With very minimal thickness, the fabrics used have

negligible resistance to bending or compression. Due to these limitations, the fabrics must be shaped in a precise manner to carry all of the structural loads in pure tension. This causes a more complex process when designing the shape of a tension fabric structure, forcing the architect to rely heavily on the structural engineer specialized in the area of tensioned fabric structures (Huntington 2013).

2.5.1. DESIGN PARAMETERS AND ANALYSIS TECHNIQUES

In all structural systems, the designer must consider an array of failure modes. Fabric structures support load in a pure tension fashion in order to withstand any failures. Fabric structures are typically pretensioned high enough to remove any looseness or slack to eliminate the possibility of a sudden change in load causing a snap through effect of the fabric structure, known as fluttering, which can be very destructive. As the pretension levels are increased, fabrication tolerances and patterning become more critical to the design. Wind loads are critical when considering a design, however, establishing consistent design pressures over a fabric structure can be difficult. Wind tunnel testing can be done for more abnormally shaped membrane structures, but LAMSs are typically normally shaped tensile membrane structures as seen when comparing Figure 2-5, a LAMS used as an aircraft hangar, to Figure 2-6, the SkySong tensile fabric structure located on Arizona State University's Scottsdale campus.

Figure 2-6: SkySong the ASU Scottsdale innovation center (SkySong Center n.d.)

Supporting members deflection do not typically influence fabric structure design and can be modeled as fixed or linked to a rigid body of motion. Fabric structure reactions from an analysis can be used as the design loads for the supporting structural elements. Generally, the supporting structure is designed to resist the maximum probable load the fabric structure can transfer and to remain stable in the event of a sudden failure of the fabric structure (Huntington 2013).

2.5.2. SYSTEM CONSTRUCTION

During construction and erection of tensioned fabric structures, the structural engineer's work includes many roles. The engineer must respond to contractor RFIs, review the contractor's erection scheme, pay attention to the stability of supporting members during erection where supports rely on the tension of the fabric structure or cables, and for larger structures check loading conditions that occur only during erection. The engineer must perform regular inspections of the foundations and supporting members, tensioned cable, and fabric structure for any defects or tears that may occur during construction. Following the final erection stage, the

fabric structure at those points in contact with the support members should be assessed under loaded conditions. LAMSs steel frame does not rely on the tension of the fabric structure both during and after erection, making the erection process slightly easier. The steel frame of a LAMS must be erected first and secured to the foundations. The fabric structure is pulled tautly over the steel frame, functioning as cladding on the steel structure (Huntington 2013).

2.5.3. FABRIC STRUCTURE SEQUENCING

In general, installation of the fabric structures onto the support structure takes three steps: layout, fastening, and tensioning. During the layout phase, the fabric structure is unpacked and laid loosely over the supporting structural elements. Amid this stage, the fabric structure is most vulnerable to weather-related events and can be severely damaged if caught in a wind storm. The fabric structure is not the only element at risk; workers holding onto or securing the fabric structure during this stage are at risk as well. Generally it is recommended not to start the layout process if winds exceed 15 mph.

Two basic components of weaving are warp and weft. Warp is the thread held in tension in the longitudinal direction by a frame or loom. Weft is the thread drawn through and inserted over and under the warp threads in order to form a fabric structure as seen in Figure 2-7.

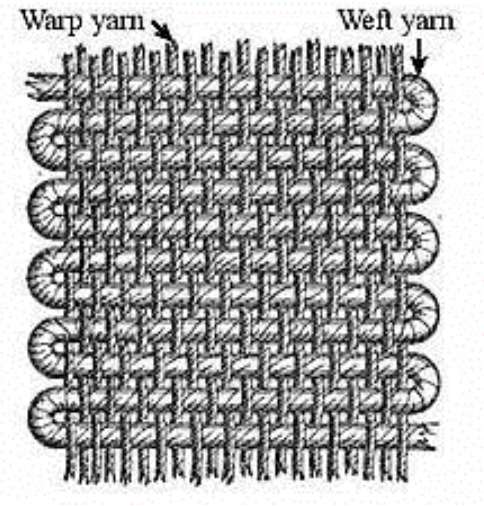

Figure 2-7: Warp and Weft fabric structure (Sewingplums 2010)

When fastening, it is desirable to first attach the warp direction of the material to its boundaries, which reasonably control the fabric structure in case of inclement weather. The system is then tensioned by typically pulling the warp direction orthogonal to the parallel arches and fastening it down. Following this, the installer traverses each side of the fabric structure and stretch the fill direction into the finished position. The permanent attachment points must be precisely placed to allow the fabric structure to fit to the support structure properly. Any misfits that occurs from improper attachment results in an improper and unexpected structural response in the system when external loads are applied and can lead to severe damage. Pretension should be developed gradually during the tensioning phase in stages and uniformly around the entire structure. During the final tensioning, the final pretension is developed and wrinkles eliminated. Following installation, fabric structures have proven to be relatively trouble free. Occasionally a structure may require re-tensioning due to creep of the fabric structure; however; LAMSs will follow a similar sequencing with the direction of the fabric structure's warp and fill yarns on the steel structure assigned by the manufacturer (Huntington 2013).

2.6. FABRIC STRUCTURES

Architectural fabrics are typically woven materials in which small orthogonal bundles of fibers are interlaced and then coated. The coatings primary function is to provide an impervious, watertight finish. Additionally, the coating acts as a protective layer for the interlaced fibers preventing tears and limiting ultraviolent radiation exposure (Huntington 2004). Fabric structures are an integral part of all LAMSs and key components in the functionality of any LAMS. In general, the fibers, typically a polyester type fibers which are the base component of a fabric structure, used are not long or thick enough to be used as a structural material until they are combined in various ways to make a yarn. Fibers are laid parallel and then twisted together creating a yarn that allows for larger elongation, which creates more flexible woven fabrics. Once the yarns are made, they are combined in various types of ways to create a fabric structure. Fabric structures exhibit far different properties and functionalities from typical structural material such as steel, wood, or concrete. Fabric structure material has in-plane stiffness but does not have any flexural stiffness. The additional stress that occurs in fabric under load is inversely proportional to the curvature in the deflected fabric shape. The large deflections that fabric structures experience under load tend to increase curvature in a manner that improves their ability to resist a given load. Fabric shapes with little or no curvature under pretension are generally most practical on small canopies with fabric spans limited to 32 feet or less. In the same manner that curvature in the suspension cables that support a bridge deck provides resistance to the vertical loads acting perpendicular to the bridge deck, the curvature in fabric provides resistance to the wind or live loads that act out of the plane of the fabric (Huntington 2004). The pretension and the geometry gives membranes out-of-plane stiffness when stretched between supporting structures and fastened down via cables are attached to the edge of

membrane surfaces. (Fujikake, Kojima, and Fukushima 1989). A fabric structure installed on a LAMS uses this out-of-plane stiffness produced from pretensioning to resist external loads including snow and wind loads.

The fabric structure on a LAMS is coated with a form of polymer, usually a PVC "polyvinyl chloride" material. Among the fabrics used is civil engineering, PVC-coated polyester is the most popular material mainly due to its favorable price. Furthermore, PVC-coated polyester fabrics can easily be folded and unfolded, which is an important aspect for temporary structures (Galliot and Luchsinger 2009). Coated fabrics behavior during deformation differs from uncoated fabrics behavior. It is well known that the fabrics become stiffer after coating, because coating material fills the spaces between the yarns and cements the warp and weft threads together. Coating changes all the fabrics properties. It increases tensile modulus and bending rigidity, especially in the warp direction (Masteikaite and Sacevičiene 2004). During the manufacturing process, in the weft/fill direction, the fibers must be stretched straight before any of the fabric begins to stiffen and carry a significant load. This is known as crimp interchange and can have adverse effects, causing fill fabrics to creep into a straighter profile under pretension creating a loss of initial tension. Some manufacturers have sought to combat crimp interchange through laid weaves (placing fabrics one on top of another without interweaving), stitched weaves (stitching together the warp and fill direction weaves at defined intervals), or a panama weave (interwoven material at every second to fourth strand). Both warp and fill directions can be held in tension during the weaving process, so the material has similar properties in both directions and limited crimp interchange. This is similar to a standard linear orthotropic material (Huntington 2004). If the weave is tight, a cloth is formed while a loose material forms a shade net. The shade net offers greater transparency and translucency along

with a higher tear strength due to the amount of PVC coating needed. A tight weave, while less transparent, offers a higher tensile strength and an easier surface for bonding to the PVC. Once a fabric structure is woven together, it can be coated with PVC material. If the yarns start breaking down, then the structural integrity of the entire cover is in question. Protecting the yarns from damage is one of the main functions of the exterior coating compound (Shelter-Rite n.d.).

The process discussed above is a very basic understanding of how manufactures produce the fabric structures used on LAMSs. All manufacturers have different techniques when designing and constructing their fabric structures. Ferrari fabrics have a special manufacturing process where the fabric is prestressed during the coating. Because of multiple manufacturing processes each fabric structure has unique material properties associated with it. To quantify one fabric structure and assume all other fabric structures have similar properties is a costly misconception.

2.6.1. FABRIC COATINGS

There are several coating options for fabric structures. In general, coating and fabric structure cannot be interchanged, as the two elements form a powerful composite material. The most common coating PVC is relatively soft and pliable enabling it to work well with tensile structures. PVC is typically applied to polyester fibers and is fairly resistant to UV rays, having to be replaced after 15 years due to brittleness. PVC coatings are available in a variety of colors, have the ability to be inserted with a blackout layer for any non-translucent applications, and can be printed on or painted similar to outdoor billboards. PVC alone attracts dirt and can seal in this dirt causing the fabric structure to look visually unattractive. To avoid this, a series of top-coatings have been developed. These coatings improve the fabric's self-cleaning properties and serve as a protective layer from UV rays. Another common coating is PTFE (Polytetrafluoroethylene), also known as Teflon, which is chemically inert, thus proving

resistance to dirt and demonstrating excellent flame resistive characteristics. PTFE coating is combined with a fiberglass fabric to form the fabric structure. PTFE also proves to have moderate translucencies with a high tensile strength and modulus of elasticity (Huntington 2013).

2.6.2. BEHAVIOR OF FABRIC STRUCTURES

The combination of fabrics, coatings, and toppings forms a fabric structure which is the primary external load resisting system of a LAMS. Many different qualities have an impact on the selection of a fabric structure including fire resistance, translucency, life span, tensile strength, and workability. Today LAMSs are made of one of two architectural fabrics: PVC coated polyesters or PTFE coated fiberglass.

2.6.2.1. MECHANICAL PROPERTIES

Based on work by Huntington (2004), (2013), the critical mechanical properties of fabric structures are related to tensile strength, tear strength, and stiffness. Tensile strength measures the direct pull force required to rupture the fabric structure and measures the fabric structures ability to resist the forces acting on it from pretensioning to external loads. Tear strength measures the resistance of the fabric structure to propagation of slits or cuts. The stress/strain (stiffness) behavior of a fabric structure is a complex phenomenon that cannot be reduced to a single variable. The orientation, type of weave, and the effect of crimp interchange all impact the stiffness of the fabric structure. Understanding the complex stiffness properties of fabric structures is definitely important for their design and fabrication.

The tensile strength of a fabric structure is one of the main criteria for selecting the fabric structure used on a LAMS. Several tests have been developed to model the stress/strain properties of fabric structures. The cut strip method, further discussed in Chapter 3, is a test

commonly used for quantifying the tensile strength of a fabric structure. This is a uniaxial test of a biaxial material (material simultaneously acted on in both the x and y direction), but it can be used as a good approximation of how the material will respond in the field. The stress and strain properties resulting from the cut strip method differ in the warp and fill directions and also on the subsequent application of high loads. The scope of this research only focused on the stress/strain (stiffness) values when determining material properties for analyzing fabric structures in a nonlinear fashion. This research tested new and used fabric structures to compare their material properties and effects on the engineering model. The cut strip tensile test will be used for determining material properties, as found in Chapter 3.

2.6.2.2. DURABILITY AND WICKING

The durability of a fabric structure is a complex variable to quantify. The effects of ultraviolent radiation, wicking (water absorbing into the woven fibers), and attacks from algae or other organic matter, are a few of the factors to consider when determining durability. The most reliable source for measuring the durability of a fabric structure is by evaluating the performance of fabric structures already erected. In general, PVC fabric structures have ample records of performance data already established. Some materials impacted by wicking will be degraded due to freeze-thaw action of the fabric structure in cold environments. Wicking also provides an environment for mildew growth, leading to fabric and seam degradation along with a permanent discoloration to the fabric structure. Wicking is easily prevented by an adequate PVC coating thickness (Huntington 2004).

2.6.2.3. FIRE RESISTANCE

All fabric structures are at a minimum fire resistive and some are considered non-combustible. Standard tests within the U.S. have been developed to determine the fire resistance of each fabric

structure. ASTM (American Society for Testing and Materials) E84, "Standard test methods for surface burning characteristics of building materials" known as the flame spread or tunnel test, determines the relative burning behavior of the material by observing how the flames spread along the specimen. ASTM E108, "Standard test methods for fire tests of roof coverings" known as the burning brand test determines the ability of the roof covering material to resist fire penetration from the exterior to the underside of the roof deck. ASTM E108 is specifically designed for roof coverings over a roof deck, and its application to an unsupported roof, such as a membrane roof, poses a problem. Other tests such as the NFPA (National Fire Protection Association) 701, "Standard methods of fire tests for flame propagation of textiles and films," determines the difficulty of igniting flame resistant textiles and the difficulty of the flame propagating beyond the ignition point. In the case of LAMSs, the NFPA 701 test would be a more accurate representation of the fire resistance rating when compared to the ASTM E108 test. In general, fiberglass and PTFE based fabrics are able to achieve non-combustible ratings, while polyester based fabrics meet fire resistive ratings. Most LAMSs, being a polyester based PVC fabric structure, would therefore reach a fire resistive rating (Huntington 2013).

2.6.2.4. TRANSLUCENCY

Fabrics range from 0 to 95 percent translucency, allowing 95 percent to 0 percent of the outdoor light shine through. Some fabric structures are selected purely for their translucency. Others, such as polyester paired with PVC fabric structures, are often selected for their blackout capabilities. These fabric structures have a translucency that ranges from 4 to 15 percent, depending on the manufacturer. The tightness of the yarns and thickness of the coating material heavily impacts the fabric structures translucency. As mentioned previously, differing material used for a membrane roof has the ability to produce translucency upwards of 90 percent.

However, for this research LAMSs have a relatively low level of translucency due to the polyester paired with PVC fabric structure that is used for its higher tensile properties (Huntington 2013).

2.6.2.5. LIFESPAN

The life span of a fabric structure is defined by its manufacturer and ranges from 10 to 30 and plus years, depending on the material used for its yarns and coatings. Generally, PVC fabrics have a shorter life span that PTFE or glass coated fabrics. Other factors, such as how deployable the structure is and whether it is a seasonal or permeant structure affect lifespan. The more deployable the structure the shorter the expected lifespan. LAMSs are relatively deployable; therefore, a shorter lifespan is to be expected for their fabric structures, depending on how the LAMS is used (Huntington 2013).

2.7. LOADS

The following sections on loads is credited to the work by Huntington (2013). All structures, with no exceptions made for tensile membrane structures, are subject to climatic, environmental, and service loads. Design loads are prescribed in ASCE (American Society of Civil Engineers) 7, “Minimum design loads for buildings and other structures" (2010). The application of ASCE 7 to tensile membrane structures such as LAMSs can be difficult, due to the uniqueness of these structures along with the inherent flexibility and large deflection capabilities of the fabric structures used. The large deflection behavior of the fabric structures allows for very high loads in relation to their self-weight, which is small and can be neglected in most cases. With negligible self-weight, seismic loads can be ignored due to the inherent low mass of the system. Wind loads prescribed in ASCE 7 can be difficult to determine due to the often unique surface

geometry of LAMSs and the fabric structures large deflection capabilities. Similarly, snow loads, where applicable, are often difficult to determine as well for similar, reasons to wind loads.

While the fabric structures are pretensioned across LAMSs, the pretension is a system characteristic and not considered a load. Due to the nonlinear system characteristic of fabric structures the use of superposition is invalid. All load combination must be considered as applied to the fabric structure. To date, there is no LRFD (Load Resistance Factor Design) standard method for tensile membrane structures. As with all structures, a load combination that produces the most unfavorable effect should be considered in design.

2.7.1. DEAD LOAD

LAMS are generally very lightweight when compared to modern steel and reinforced concrete structures. As in Figure 2-8, the thickness of the fabric structure material used is typically less than $1/16^{th}$ of an inch. Typical fabric structures not yet installed on their steel frame have a unit weight of 0.17 to 0.50 pounds per square foot, which for the most part is negligible when considering the most unfavorable loading condition. Any attached equipment such as light fixtures or speakers can be considered live loads.

Figure 2-8: Strip of fabric structure

2.7.2. LIVE LOAD

Tensile membrane structures are most commonly used as roofs or for partially or fully enclosed canopies. Per ASCE 7, the standard roof live load is to be assigned dependent on the tributary area supported by the members in question. There are also requirements for single point loads, with maintenance workers calling for a 300 pound point load. When considering the fabric structure, the tributary area can be measured as the region affected by the load application. LAMSs are supported fairly orthogonally in comparison to other tensile membrane structures; therefore, determining a tributary area is straightforward when task when assigning a roof live load.

2.7.3. WIND LOAD

Wind is the governing load for the majority of tensile membrane structures. Wind loads are transient, so careful attention must be paid to any slack in the fabric structure. Ample pretension must be applied to prevent any damage due to flutter. ASCE 7 addresses climatic and exposure parameters for determining wind loads. Determining surface pressures can be difficult for the majority of tensile fabric structures due to their double curvature shapes. The wind pressure coefficients in ASCE 7 are derived from hundreds of wind tunnel tests of various building shapes, almost all of which are rectilinear, barrel vaults, or spherical surfaces. This research is focused on LAMSs, which are rectilinear in shape with barrel vaulted roofs and fall in line with pressure coefficients developed in ASCE 7.

2.7.4. SNOW LOAD

Tension membrane structures have proven valuable in cold climates with the ability to resist significant snow loads. However, a consequence that must be taken into account is the effect of ponding due to the large deflection capabilities of fabric structures used, as seen in Figure 2-9.

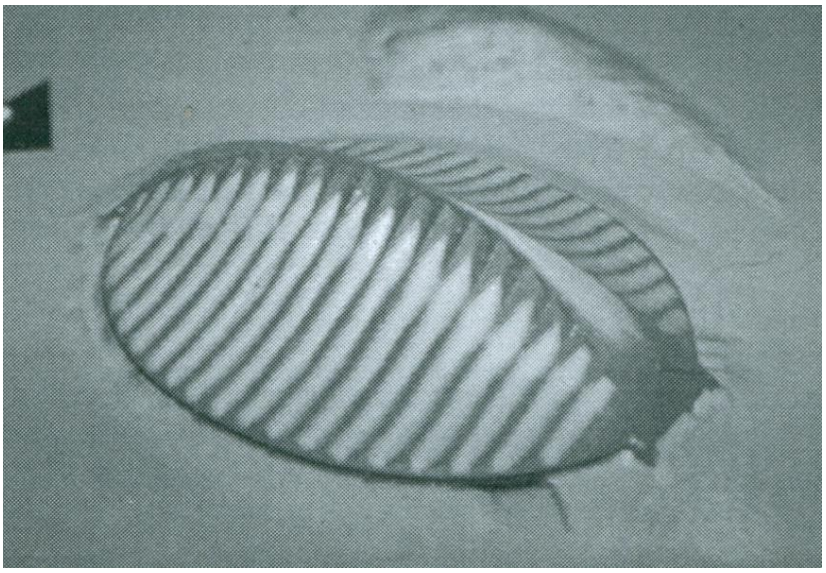

Figure 2-9: Snow drifting model for Lindsay Park roof (Huntington 2013)

Given basic site parameters, ASCE 7 provides snow loads; however, as with wind load pressure coefficients, these loads do not apply to the unique shape of tensile membrane structures. Due to the slick PVC coated fabric structures, low friction coefficients can cause potential consolidation of snow loads from sliding. As for LAMSs, their barrel-vaulted roofs provide difficult surfaces for snow to pond, but care should still be considered for LAMSs when utilized in snow-prone environments.

2.8. NONLINEAR RESPONSE TO APPLIED LOADS

The fabric structures on LAMSs under applied loads follow well established principles of mechanics. Unlike structural members with significant shear and flexural stiffness, geometric changes are too significant to ignore and must be considered when analyzing LAMSs. Consider a beam spanning between two supports with an applied load at the center, as seen in Figure 2-10. Once the load is applied, the beam transfers the load to its supports through its flexural stiffness characteristics. Performing a nonlinear analysis following minimal first order deflections will not provide any additional insight into the performance of the beam.

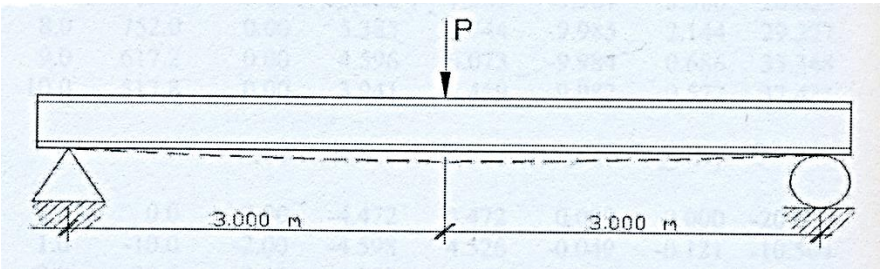

Figure 2-10: Loaded beam (Huntington 2013)

Next, consider a pretensioned cable with no initial sag spanning between the same two supports as seen in Figure 2-11. When a load is applied at the center, the cable grows taut and deflect, allowing a small load to cause a relatively large deflection. The deflection is not linearly proportional to the applied load due to the vertical resistance of the cable being dependent on the cable tension and deflection. A nonlinear analysis is in order to determine the deflection and tension. The fabric structures on LAMSs are represented well by analyzing them as a cable structure.

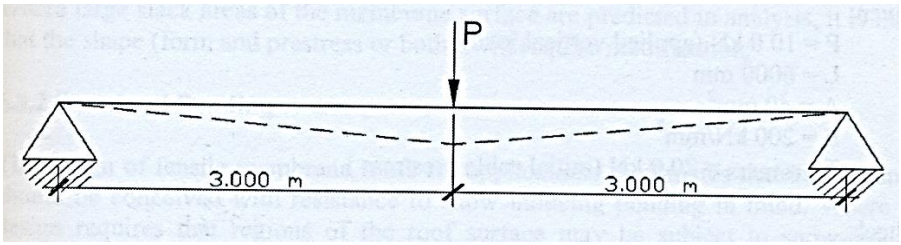

Figure 2-11: Loaded cable (Huntington 2013)

2.9. LOAD PERFORMANCE

Wind loads induce transient deformations in fabric structures that generally do not lead to any dynamic problems, as long as there is sufficient stress in the fabric structure under peak load conditions. The area of the fabric structure subjected to wind load should be reviewed for any slackness. More common is the problem of uniaxial slackness, where either the warp or fill direction of the fabric structure has no tension. Large regions of uniaxial slackness will result in

flutter during design wind events and can result in failure of the fabric structure. Snow and ponding effects should be considered on tensile membrane structures; however, LAMSs by nature shed snow easily due to their barrel vault roofs when compared to large tensile membrane structures with conic or hyper shaped roofs, and ponding of snow is relatively small in magnitude when compared to design wind loads.

2.10. MAINTENANCE, DURABILITY, AND INSPECTION

Design, materials, construction, and environment are all factors affecting the durability and maintenance of LAMSs. Design factors that influence durability and maintenance include determining appropriate loads to prevent overstresses in fabric structure and avoiding sharp points of contact with the support structure. UV rays are known sources of degradation for fabrics and must be considered when selecting a fabric structure for a specific life span. Care must be taken during packaging and placement of fabric structures to prevent any weakening of the material due to sharp folds or tears during erection.

Properly designed and constructed LAMSs generally require minimal maintenance until the effect of prolonged UV exposure sets in. Small tears in the fabric structure are typically easily repaired through patching measures. The manufacturer should be brought in if a tear or cut is too large to patch. Periodic inspections are recommended to check for any abrasions of the fabric structure, especially around points of contact with the supporting structure.

2.11. CONSLUSIONS

After reviewing previous works on the material properties of fabric structures, no constant material property can be determined due to the nature of how the material is manufactured. With material properties varying from manufacturer to manufacturer and even within the same manufacturer, lab testing is required to quantify the material properties of different fabric

structures. Chapter 3 covers material testing and the correct ASTM standards to use when quantifying a fabric structure's material properties.

CHAPTER 3

MATERIAL TESTING

3.1. INTRODUCTION

As discussed in Chapter 2, the fabric structures have varying material properties based on the manufacturing process. Chapter 3 provides the approach and standards used to quantify material properties from different fabric structure samples. Specific steps are also proposed for future material testing to evaluate any fabric structure in question. All material property data acquired for the purpose of this research is up to U.S. approved standards. The purpose of this chapter is not the evaluation of multiple fabric structures. The material properties acquired in this chapter are used as a tool for the development of the engineering model. When constructing LAMSs the orientation of the fabric structure must be known to account for the correct material properties from either the warp or fill direction.

3.2. BREAKING STRENGTH

Breaking strength, also known as ultimate tensile strength (UTS) and shortened to tensile strength (TS), is one of the key material properties this research seeks to obtain. With the design strength of fabric structures limited to a recommended 25 percent of the TS, most manufacturers do not test their material to failure when evaluating cyclic and biaxial loading based off the known maximum TS of their fabric structure. Therefore, this research quantified the TS through material testing. Stress vs. strain data to failure were captured as well during testing. All of the

recorded data are extremely valuable when analyzing the fabric structure using the algorithm developed in Chapter 4. The algorithm is an iterative process with the results dependent on raw data obtained from testing.

3.3. ASTM STANDARDS

ASTM provides standards for testing various types of coated fabrics in ASTM D751 (2006) "Standard Test Methods for Coated Fabrics." The tests for the breaking strength of a fabric structure are prescribed in the "Breaking Strength" section of ASTM D751. The two procedures used are the grab test method and the cut strip test method. For the purpose of this research, the breaking strength is determined by the cut strip test method. The testing machine for the cut strip test method has the following three main parts:

1. *Straining Mechanism* - A machine shall be used wherein the specimen is held between the two clamps and strained by a uniform movement of the pulling clamp. The machine shall have a uniform speed of 12 ± 0.5 inches per a minute.
2. *Load and elongation recording mechanisms* – A calibrated dial, scale, or chart shall be used to indicate applied load and elongation. The machine shall be adjusted or set so that the maximum load required to break the specimen will remain indicated on the computer interfaced with the testing machine after the test specimen has ruptured.
3. *Clamps for holding the specimen* – Clamps shall have gripping surfaces sufficiently flat and parallel to prevent the test specimen from slipping or moving between the gripping surface when held under pressure normal to operation. The dimension of all gripping surfaces parallel to the direction of application of the load shall be 1 inch; the dimensions perpendicular to this direction shall be 1inch for the face jaw and 2 inches or

more for the other. All edges that might cause a cutting action shall be rounded to a radius of not over 0.0156 inches. The pressure between the gripping surfaces, sufficient to clamp the specimen firmly before the testing load is applied and to prevent slippage during the progress of the test, shall be secured by any suitably constructed mechanical device operating on the member of the clamp. The distance between the clamps at the start of the test shall be 3 inches (ASTM-D751 2006).

3.4. ASTM PROCEDURE

The procedure set forth by ASTM-D751 is as follows:

The test specimens should be 1 inch in width and not less than 6 inches in length. Two sets of specimens will be required; one set for longitudinal breaking strength having the longer dimension parallel to the lengthwise direction of the specimen, and the other set for transverse breaking strength, having the longer dimension parallel to the crosswise direction of the specimen. Specimens shall be taken no nearer the selvage than one tenth the width of the coated fabric. Place the specimen symmetrically in the clamps of the machine with the longer dimension parallel to and the shorter dimension at right angles to the direction of application of the force. Report the average of the results of the individual tests in each direction as the longitudinal breaking strength and the transverse breaking strength of the fabric, respectively. If a specimen slips in the clamps, breaks in the clamps, breaks at the edges of the clamps, or if for any reason attributable to faulty operation, the result falls markedly below the average for the set of specimens. Discard

the results, take another specimen, and include the result of this break in the average. The 1 inch wide specimen shall be cut to obtain 1 inch of yarn (ASTM-D751 2006).

3.5. CUTTING SAMPLES

For the purpose of this research, samples for all of the fabric structures of interest were cut to 1 inch by 8 inches per ASTM D751 specs. A minimum of five warp direction samples were cut and eight weft direction samples were cut for each fabric structure. Each sample bears a label with the first number relating to a specific fabric structure, the second number relating to the sample number, and the letter at the end relating to the warp (machine) or weft (fill) direction. An example of this alpha numeric system is found in Figure 3-1.

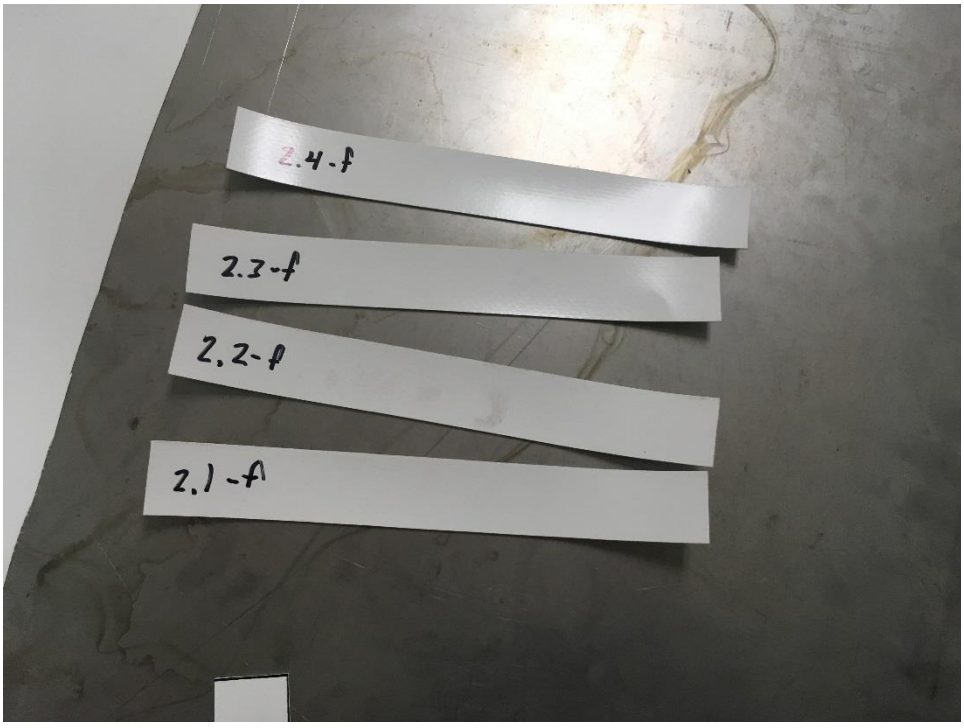

Figure 3-1: Cut samples with alpha numeric system

The material was cut down from rolls obtained from multiple companies and the Air Force. Once cut down to a manageable size, the material was cut into strips by marking dimensions and using

a straight edge T as seen in Figure 3-2. Overall, four different type fabric structures were tested taking into account the warp and fill directions for three of the four fabric structures. The fourth fabric structure obtained was already cut down into small square panels, which made it impossible to correctly assign a warp and fill direction.

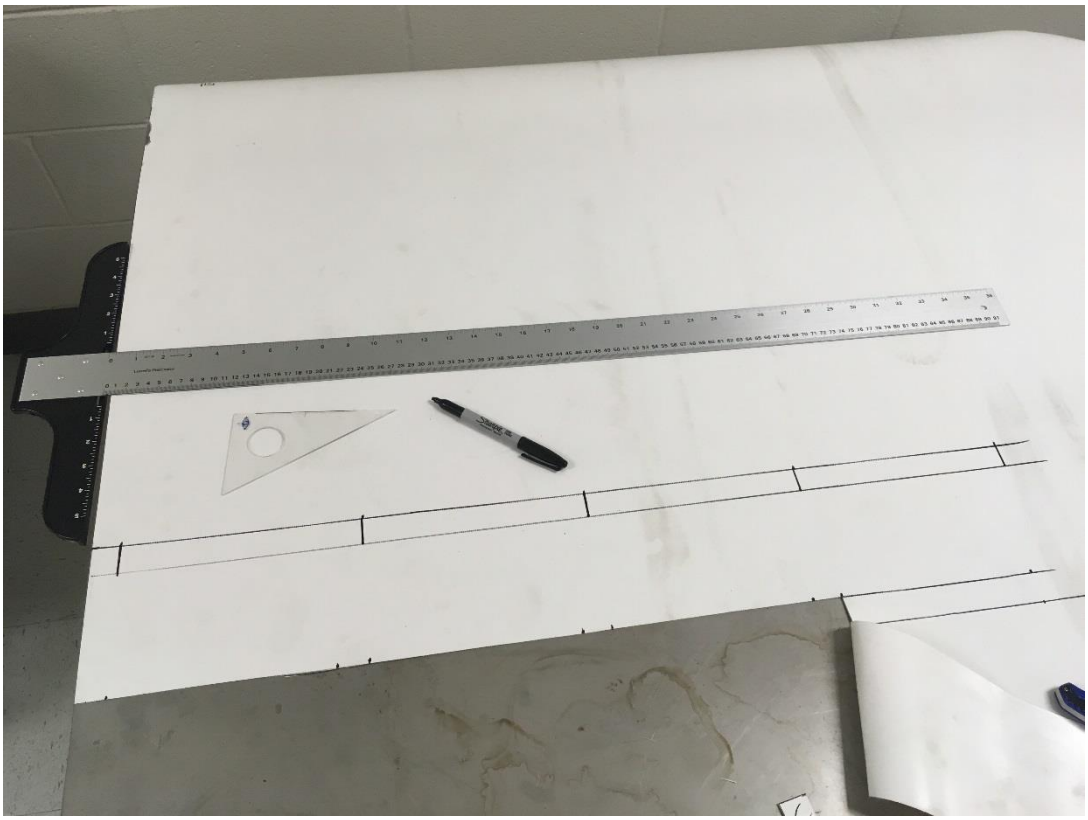

Figure 3-2: Fill direction cut strips

3.6. TESTING

The material testing was conducted using equipment from the mechanical engineering department of Auburn University. An Instron 5565 tensile testing machine was used for testing and can be seen in Figure 3-3. Initially, the hydraulic clamps were installed onto the straining mechanism and a three inch gauge length was set. Following the initial set up, the computer program to operate the machine was launched and the cut-strip method test, detailed in section

3.3, was selected. The only input needed was the thickness of each sample tested in order for the program to return stress and strain data. The thickness of each sample was measured until a consistent reading was returned using a TMI (Testing Machines Inc.) model 49-72 measuring machine precise to a micrometer seen in Figure 3-4.

Figure 3-3: Instron 5565 tensile testing machine

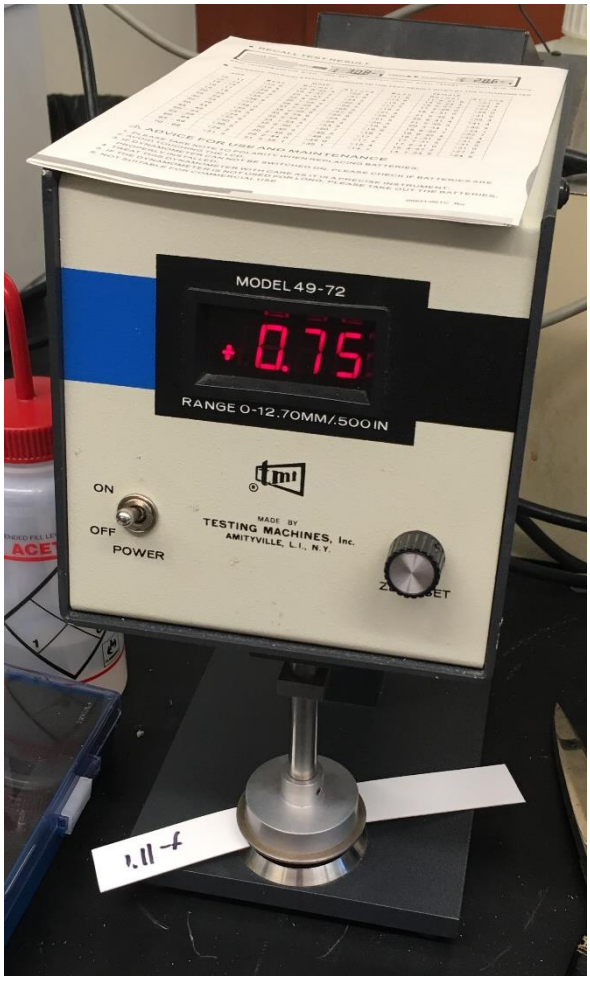

Figure 3-4: Machine to measure thickness

The data from each sample tested was recorded simultaneously as the machine strained each sample as seen in Figure 3-5. Every sample, following a thickness reading, was aligned and centered between the hydraulic clamps, which were then activated via a pedal close/open system. The initial set up can be seen in Figure 3-6. Once the sample was aligned, the start button was selected within the computer program and the test initiated at the rate prescribed in section 3.4 of 12 inches per minute. Depending on the alignment of the warp and fill fibers, each sample displayed a unique pattern as they were being strained, as seen in Figure 3-7.

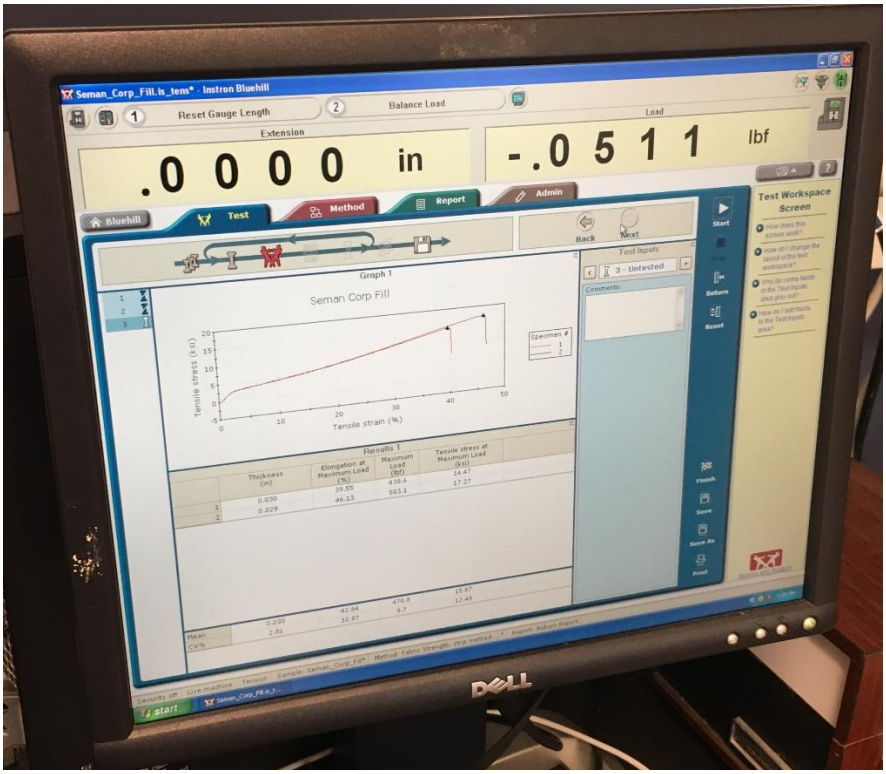

Figure 3-5: Computer program used to record ASTM data

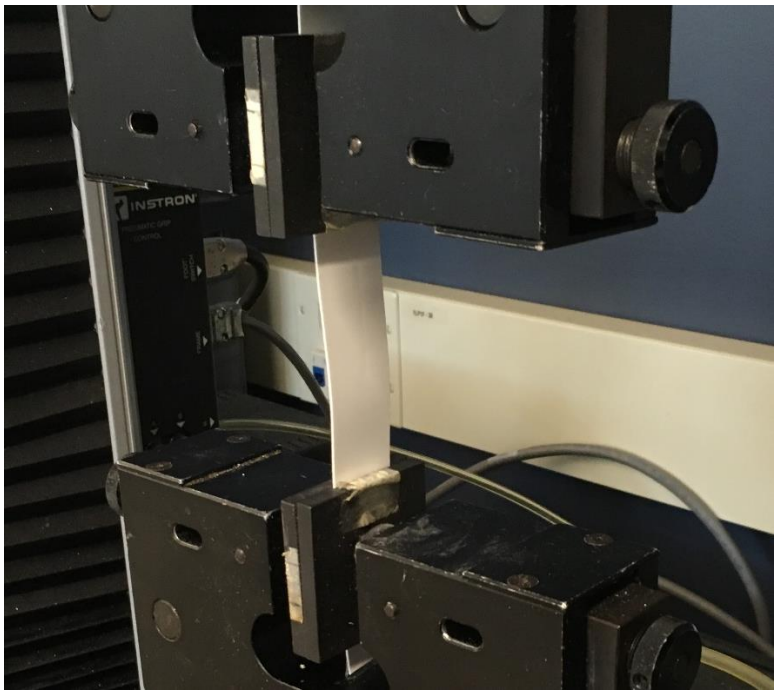

Figure 3-6: Clamped and ready for loading

Figure 3-7: Loading in progress with warp and fill directions visible

3.6.1. FAILURE MODES

Each specimen failed in under one minute with only one specimen slipping from the clamps. Each failure mode was noted as seen in Tables 3-1 through 3-4, and only the ideal or acceptable failures were used in the engineering algorithm and finite element models. Four fabric structures were tested with 6 to 10 samples taken in the warp direction and 8 to 10 samples taken in the weft/fill direction for the first three fabric structure. The orientation of the yarn in the fourth fabric structure were unknown therefore 6 samples were taken by varying the orientation of the sample as samples were cut out. The failures varied and the hydraulic clamps were adjusted

accordingly. When a sample failed at the clamp surface pressure was relieved at the interface to correct for the questionable failure mode. An ideal failure point was centered between the two clamps can be seen in Figure 3-8. Each set of samples tested had at least one ideal failure which could be used as a baseline to remove any unacceptable failure results. Other failures include failing near the clamps, considered an acceptable failure mode, as seen in Figure 3-9 and failing at the clamps, considered a questionable failure mode, as seen in Figure 3-10. Acceptable failure modes will represent the material properties well, however care must be taken to ensure questionable failure modes do not reflect an unacceptable failure before considering their material properties. Overall, the failures at the clamp surface produced very similar results to the ideal and acceptable failure modes.

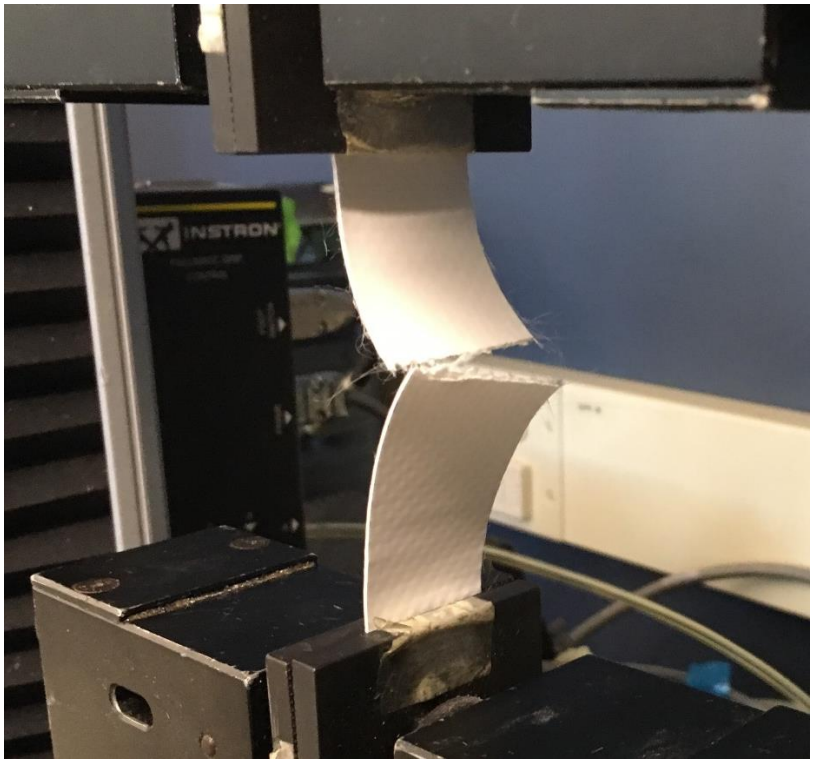

Figure 3-8: Ideal failure

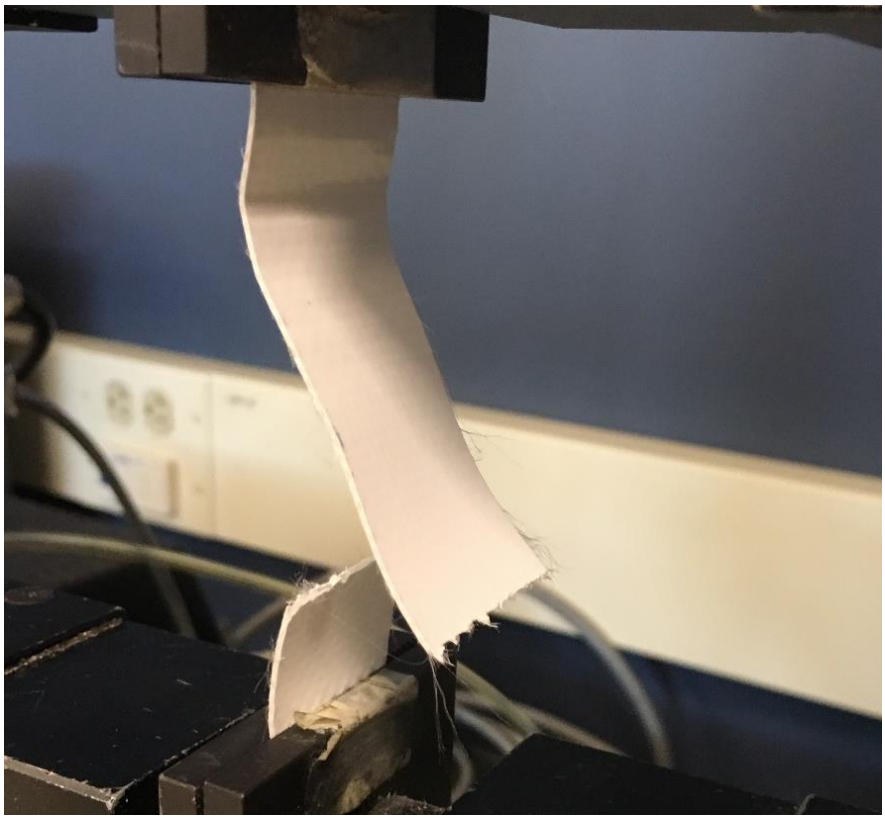

Figure 3-9: Acceptable failure

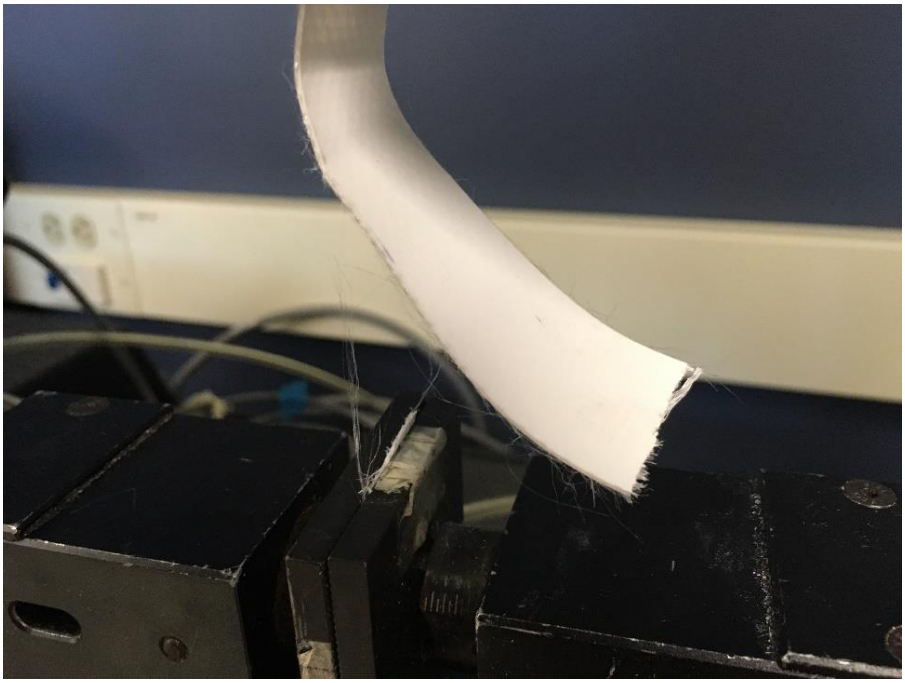

Figure 3-10: Questionable failure

Table 3-1: Material 1 failure modes

	Material 1		
	Warp	Max Strain	Max Stress (ksi)
1)	Acceptable	0.2761	13.18
2)	Acceptable	0.2988	14.46
3)	Questionable	0.2704	13.43
4)	Ideal	0.3023	15.20
5)	Acceptable	0.2909	14.96
6)	Acceptable	0.2968	15.57
	Fill	Max Strain	Max Stress (ksi)
1)	Questionable	0.2617	15.00
2)	Questionable	0.2448	14.87
3)	Ideal	0.2495	14.99
4)	Ideal	0.2507	14.84
5)	Acceptable	0.2520	15.28
6)	Acceptable	0.2745	16.66
7)	Questionable	0.2553	15.54
8)	Acceptable	0.2420	14.60

Table 3-2: Material 2 failure modes

	Material 2		
	Warp	Max Strain	Max Stress (ksi)
1)	Questionable	0.2403	17.77
2)	Questionable	0.0242	17.63
3)	Ideal	0.2553	18.03
4)	Questionable	0.2941	18.37
5)	Questionable	0.2595	18.27
6)	Acceptable	0.2929	17.00
7)	Acceptable	0.2972	17.06
8)	Acceptable	0.2857	16.93
	Fill	Max Strain	Max Stress (ksi)
1)	Ideal	0.3955	14.47
2)	Ideal	0.4613	17.27
3)	Ideal	0.4040	15.58
4)	Ideal	0.3872	12.56
5)	Questionable	0.3849	13.55
6)	Acceptable	0.3992	14.66
7)	Acceptable	0.3796	13.31
8)	Acceptable	0.3684	12.32
9)	Acceptable	0.4056	14.15
10)	Acceptable	0.4219	14.25

Table 3-3: Material 3 failure modes

	Material 3		
	Warp	Max Strain	Max Stress (ksi)
1)	Ideal	0.3011	9.32
2)	Questionable	0.3168	1.57
3)	Acceptable	0.3284	10.33
4)	Acceptable	0.2912	9.90
5)	Questionable	0.3329	10.74
6)	Questionable	0.3304	10.65
7)	Questionable	0.3173	10.42
8)	Ideal	0.2481	8.52
	Fill	Max Strain	Max Stress (ksi)
1)	Questionable	0.3033	8.47
2)	Questionable	0.3072	855.00
3)	Questionable	0.3129	8.92
4)	Questionable	0.2999	8.68
5)	Questionable	0.3125	8.76
6)	Questionable	0.3148	8.60
7)	Ideal	0.3344	9.29
8)	Acceptable	0.3920	9.20

Table 3-4: Material 4 failure modes

	Material 4		
	Direction Unknown	Max Strain	Max Stress (ksi)
1)	Grip Slipped	0.5407	15.99
2)	Ideal	0.3887	14.96
3)	Acceptable	0.4005	15.68
4)	Questionable	0.3732	13.63
5)	Acceptable	0.4009	15.01
6)	Acceptable	0.4043	15.73

All of the test results can be seen in Appendix-A with each set of samples with their own results graph. A similar trend can be observed of an initial high modulus followed by a lowering of the modulus to finish with relatively linear modulus. The relative linearity of the material properties as seen in Appendix-A prompted an investigation into a simplified linear analysis approach discussed in section 3.10.

3.7. CORRECTING AND SIMPLIFYING TEST RESULTS

Following the material tests of multiple fabric structures, each individual sample provided stress vs. strain data. The engineering model and finite element models only need one set of sample data to run. Therefore, the samples that displayed the most ideal break for each sample set are used in the engineering and finite element models. Given the raw test data for the most ideal failure, the values cannot simply be plugged straight into the engineering and finite element models. The data must be corrected and simplified for both engineering and finite element models to work efficiently and provide the most accurate results. First, at the beginning of every sample's data, a period of data collected before the sample engages must be removed. If not, these data create a strain situation where the modulus of elasticity is zero. To correct for this period, the data from this effect are removed and the remaining data are offset to the origin. This process is accomplished through analyzing the slope between data points until it remains constant. Once constant the slope is projected down to the x-axis and the data are offset to the origin.

Following this correction, representative data points are pulled from the data to create a multilinear plot which mirrors the test data to ease the process of inputting material properties into the finite element program and engineering model for interpolation purposes. Figure 3-11 shows the results of removing the slack data that occurs at the start of the material test. Following the removal of the slack data, the multilinear plot is fitted to the no slack curve. Each set of data used in the engineering and finite element models underwent a similar procedure to remove slack and simplify the data.

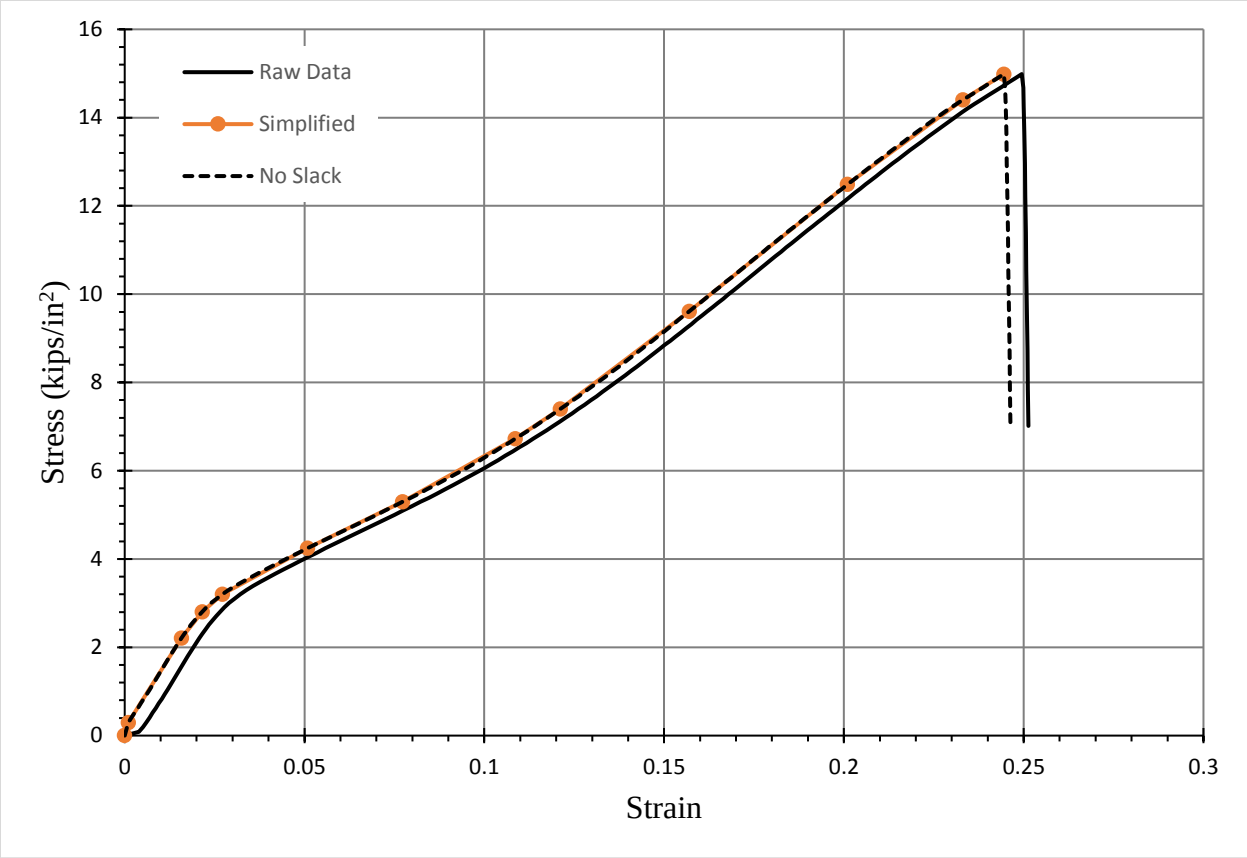

Figure 3-11: Removing slack and simplifying the data

The raw data from material testing, having successfully undergone a correction and simplification process, is now ready for use within the engineering and finite element models. The engineering model, similar to the finite element model, is able to linearly interpolate between known data points; therefore, the simplified multilinear data plot used for the finite element model is applicable to the engineering model as well.

3.8. TRUE STRESS AND TRUE STRAIN

To this point in the research, the material properties gathered are the engineering stress and engineering strain. Materials with strains exceeding 6 percent should bring about thoughts of a changing cross section due to Poisson's ratio and the elasticity of the material. As the material reaches the plastic region of material properties necking (localized deformations) occurs with an

increase in stress due to the decrease in the cross sectional area. Through the assumption of constant volume represented in Equation 3-1, the true stress and true strain of the material properties can be calculated:

$$V = A * L = A_0 * L_0 \tag{3-1}$$

Where V is the volume of the material, A_0 is the original undisturbed area, L_0 is the original undisturbed length, A is the true area instantaneous with the true stress and true strain, and L is the true length instantaneous with the true stress and true strain.

Using the constant volume assumption, the true stress can be formulated using Equations 3-2 and 3-3.

$$\sigma' = \frac{F}{A} = \frac{F * L}{A_0 * L_0} \tag{3-2}$$

$$\varepsilon = \frac{L - L_0}{L_0} = \frac{L}{L_0} - 1 \tag{3-3}$$

With F representing the force applied, σ' representing the true stress, and ε representing the engineering strain. Plugging Equation 3-3 into Equation 3-2 yields the Equation 3-4.

$$\sigma' = \frac{F}{A}(1 + \varepsilon) = \sigma(1 + \varepsilon) \tag{3-4}$$

Next, to calculate the true strain a similar process will be used following the constant volume assumption. The true strain is a change in length with respect to the instantaneous length as shown in Equations 3-5 and 3-6.

$$\varepsilon' = \int_{L_0}^{L} \frac{1}{L} d = \ln\left(\frac{L}{L_0}\right) \tag{3-5}$$

$$L = (1 + \varepsilon)L_0 \tag{3-6}$$

With ε’ representing the true strain. Plugging Equation 3-6 into Equation 3-5 will yield the true strain equation shown in Equation 3-7.

$$\varepsilon' = \ln(1+\varepsilon) \tag{3-7}$$

The engineering model discussed in the following chapter converts the engineering stress and strain obtained from testing into true stress and true strain by using Equation 3-4 and Equation 3-7. An example of this conversion is shown as a plot in Figure 3-12.

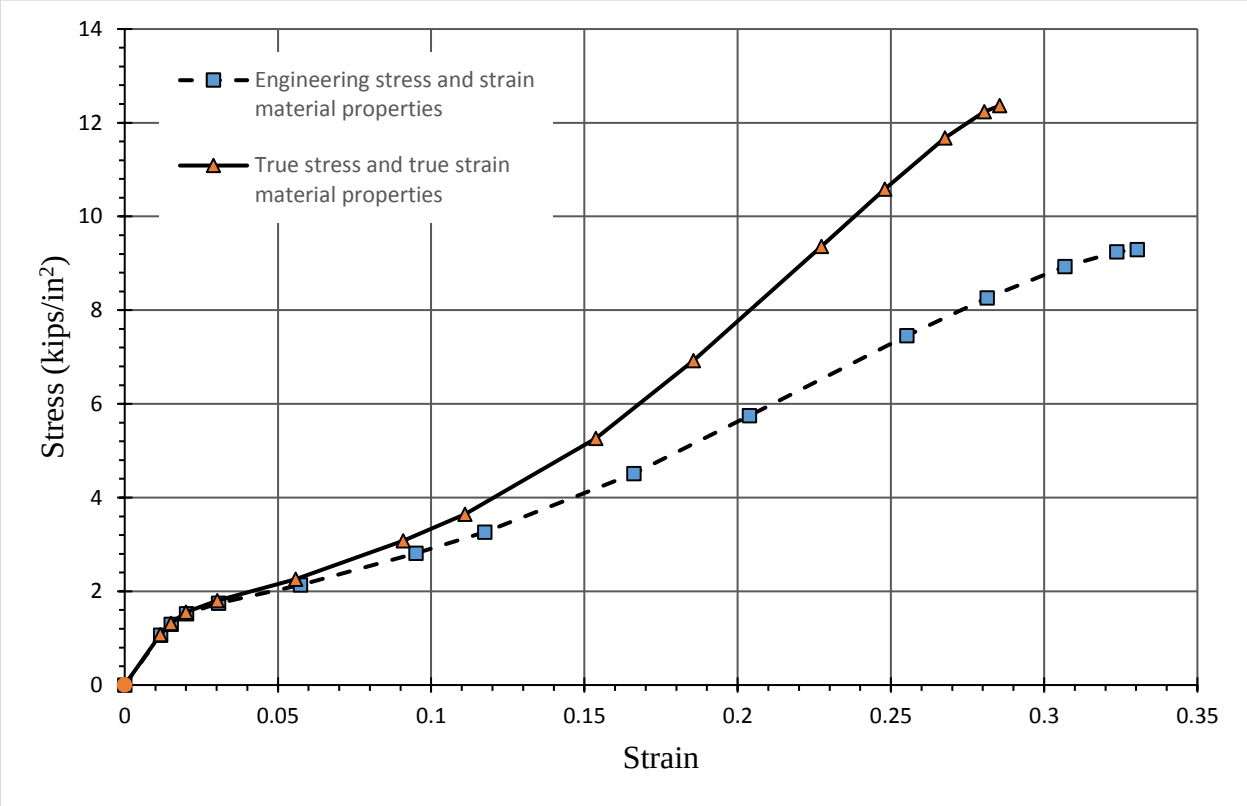

Figure 3-12: Material 3 fill: True stress/strain vs. engineering stress/strain

3.9. MATERIAL TEST RESULTS

Four fabric structures were tested following ASTM procedures discussed previously in this chapter. Each fabric structure, except material 4, were tested in the warp and fill directions.

Figures 3-13 through 3-116 show the simplified true stress and true strain values in both the warp and fill directions for each material.

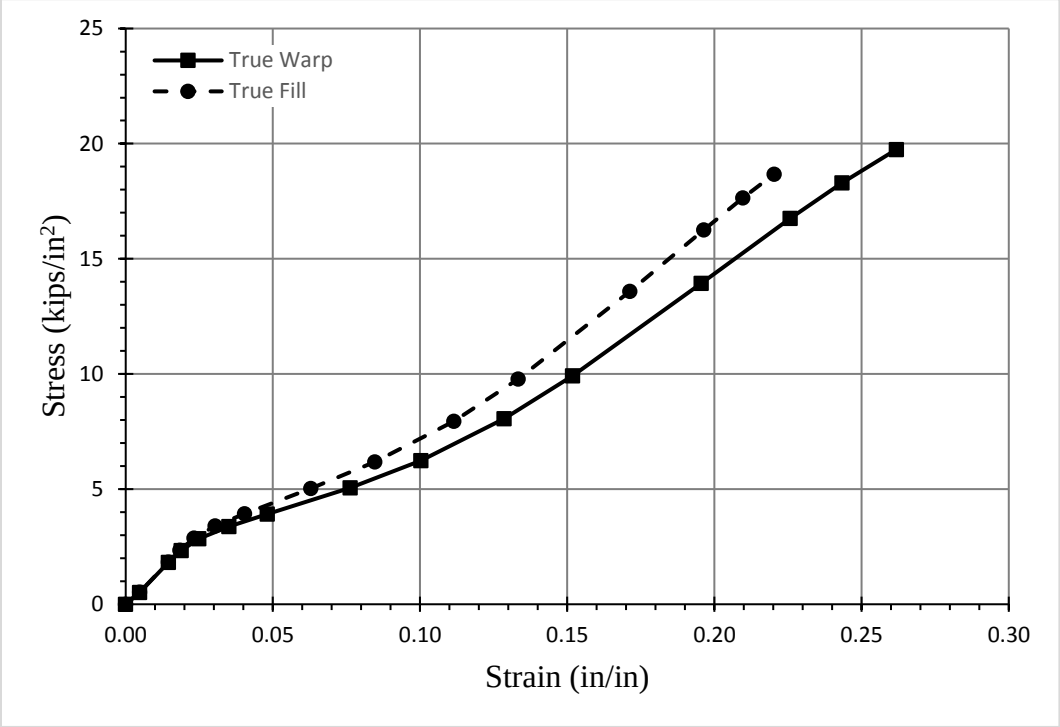

Figure 3-13: Material 1: True stress/strain for warp and fill directions

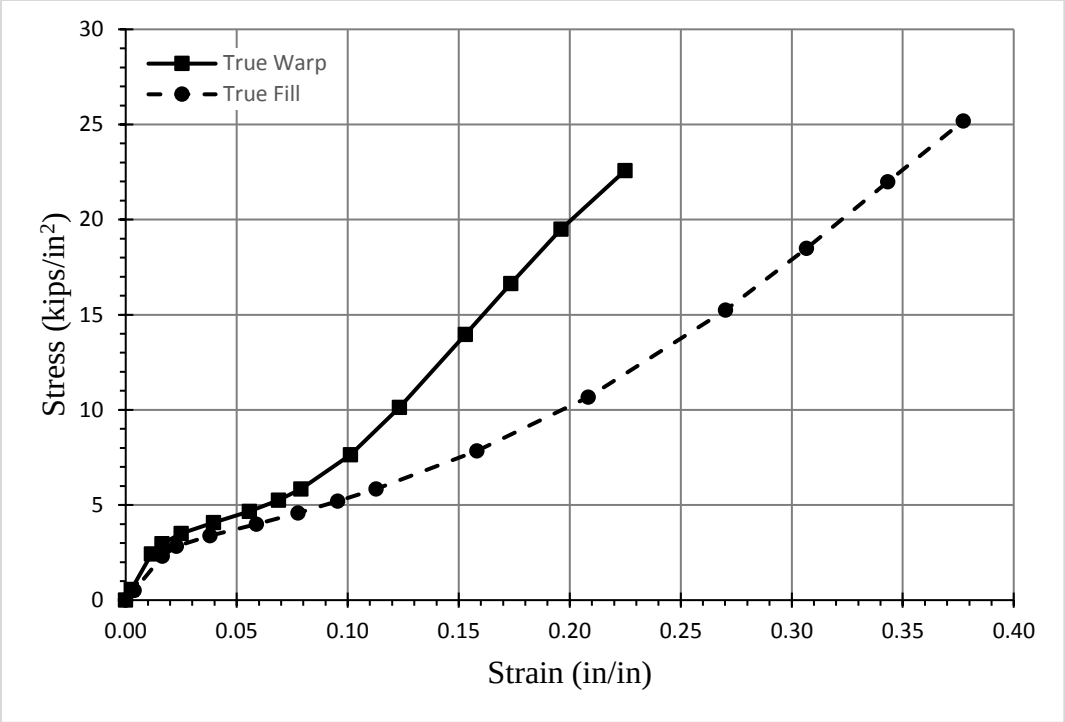

Figure 3-14: Material 2: True stress/strain for warp and fill directions

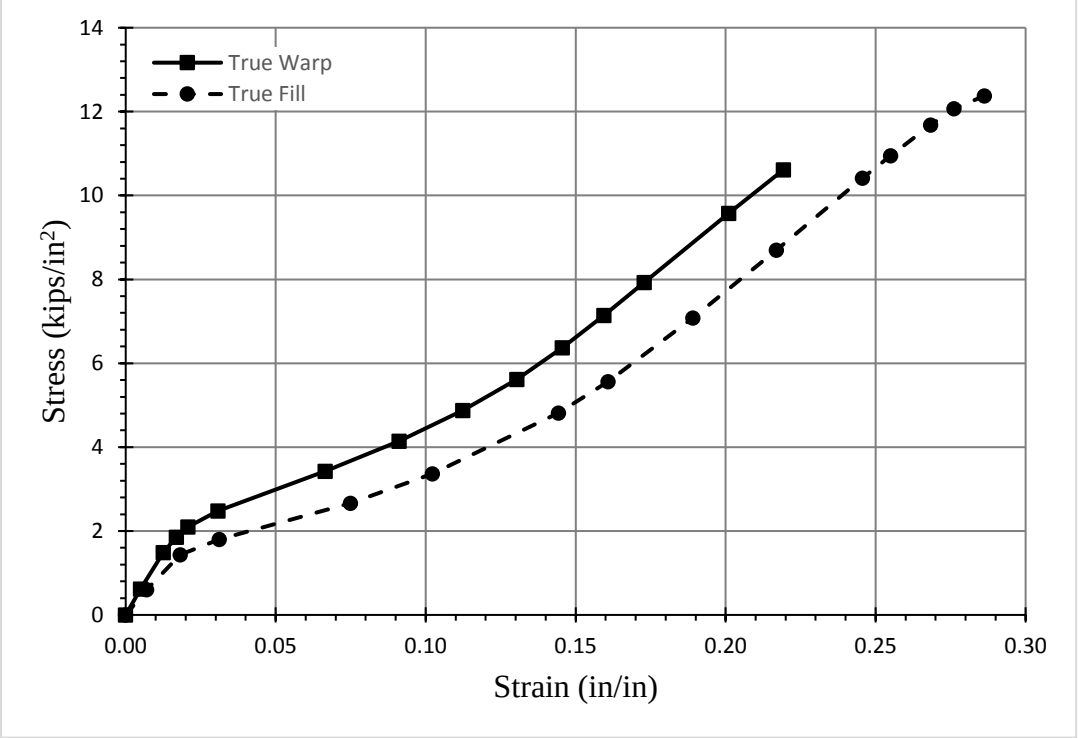

Figure 3-15: Material 3: True stress/strain for warp and fill directions

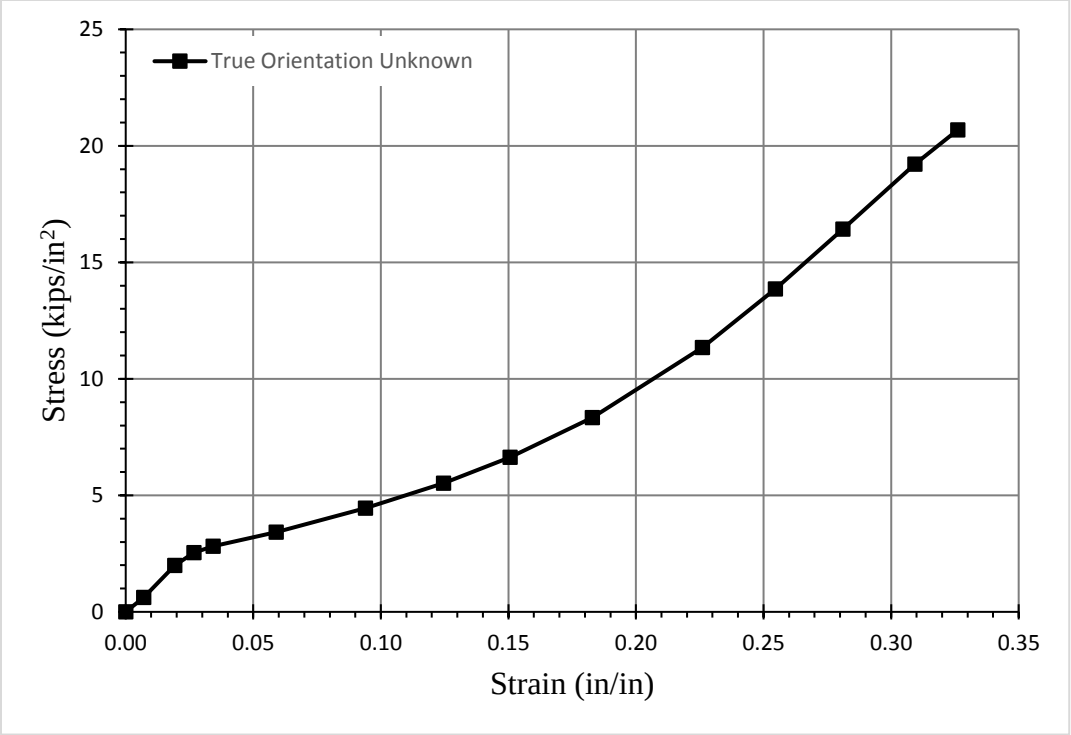

Figure 3-16: Material 4: True stress/strain

CHAPTER 4

DEVELOPMENT OF ALGORITHM

4.1. INTRODUCTION

Chapter 4 discusses the development and use of the engineering model/algorithm. The engineering model is developed on the basis of specific assumptions and mathematical approaches. From the users standpoint the engineering model consists of three sheets within a Microsoft Excel workbook with light green cells calling for input values. The first sheet is used to calculate the wind pressure exerted on a LAMS in accordance with ASCE 7-10 standards and UFC (Unified Facilities Criteria) 3-301-01 "Structural Engineering". UFC 3-301-01 calls for the use of ASCE 7-10 for all structural engineering applications and evaluates each chapter of ASCE 7-10 to determine if specification are up to standards set by the department of defense. If the department of defense requires any additions, deletions, or supplementation to sections within the specification they will be noted in UFC 3-301-01. Chapter 26 on wind loads within ASCE 7-10 requires no additions, deletions, or supplement information. The second sheet contains the iterative algorithm to evaluate the fabric structure on a LAMS. The third sheet contains the material properties determined by testing the fabric structure as covered in Chapter 3. All syntax used within Excel is available in Appendix B.

The purpose of this algorithm is to evaluate a fabric structure's performance against wind loading. The algorithm will calculate wind loads and apply them in an iterative process

accounting for the nonlinearity of the fabric structures geometry and material properties. The algorithm will return service and maximum values for breaking stress, tension force, and midspan deflection. The algorithm will also report back if the fabric structure passes ASCE 7-10 standards.

4.2. WIND ANALYSIS

A wind analysis must be conducted in order to determine the wind pressure exerted on a fabric structure. Chapter 26 of ASCE 7-10 covers the wind analysis portion of loading. Beginning with the risk category, a I through IV must be assigned based on the LAMS use and purpose as seen in Table 4-1 based on Table 1.5-1 from ASCE 7-10. The Air Force assigns a risk category of I for a LAMS used as equipment storage and a III for a LAMS used as aircraft hangar. Risk categories are developed to predict the time period of which the prescribed wind speeds will occur. A risk category of I has a 300 year time period while a risk category of III has a 1,700 year time period.

Table 4-1: Table of risk categories (ASCE/SEI Standard 7-10, 2010)

Use or Occupancy of Buildings and Structures	Risk Category
Buildings and other structures that represent a low risk to human life in the event of failure.	I
All buildings and other structures except those listed in Risk Categories I, III, and IV	II
Buildings and other structures, the failure of which could pose a substantial risk to human life. Buildings and other structures, not included in Risk Category IV, with potential to cause a substantial economic impact and/or mass disruption of day-to-day civilian life in the event of failure. Buildings and other structures not included in Risk Category IV (including, but not limited to, facilities that manufacture, process, handle, store, use, or dispose of such substances as hazardous fuels, hazardous chemicals, hazardous waste, or explosives) containing toxic or explosive substances where their quantity exceeds a threshold quantity established by the authority having jurisdiction and is sufficient to pose a threat to the public if released.	III
Buildings and other structures designated as essential facilities. Buildings and other structures, the failure of which could pose a substantial hazard to the community. Buildings and other structures (including, but not limited to, facilities that manufacture, process, handle, store, use, or dispose of such substances as hazardous fuels, hazardous chemicals, or hazardous waste) containing sufficient quantities of highly toxic substances where the quantity exceeds a threshold quantity established by the authority having jurisdiction to be dangerous to the public if released and is sufficient to pose a threat to the public if released. Buildings and other structures required to maintain the functionality of other Risk Category IV structures.	IV

After determining the risk category, the wind speed must be inputted based on the site location and risk category. The wind speeds used in ASCE 7-10 are three second gust wind speeds at thirty three feet above ground in terrain with open exposure. The wind speeds are established from years of collecting data in the regions and extensive statistical analysis. The wind speed can be identified from the wind speed maps in ASCE 7-10 as Figure 26.5-1A (Figure 4-1) or from the website http://windspeed.atcouncil.org/. For all military base applications within the U.S., the wind speed according to risk category can be found in Table E-1 of UFC 3-301-01. For all military base applications outside of the U.S., the wind speed according to risk category can be found in Table F-1 of UFC 3-301-01. An example of these tables is shown in Table 4-2.

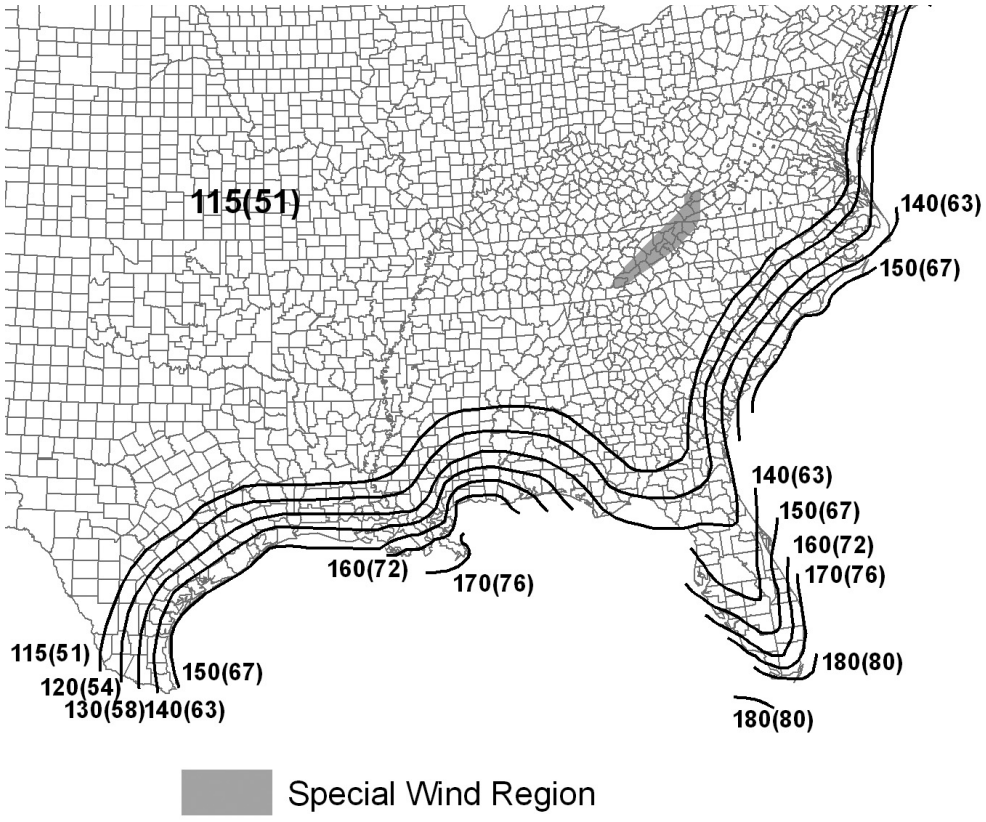

Figure 4-1: Example wind speed map (ASCE/SEI Standard 7-10, 2010)

Table 4-2: Example wind speed table from UFC 3-301-01 (Unified Facilities Criteria (UFC) 2013)

		Wind Speed (mph)				Wind Speed (km/h)			
		Risk Category				Risk Category			
State	**Base / City**	**I**	**II**	**III-IV**	**V**	**I**	**II**	**III-IV**	**V**
Alabama	Anniston Army Depot	**105**	**115**	**120**	**146**	**169**	**185**	**193**	**235**
	Birmingham	**105**	**115**	**120**	**146**	**169**	**185**	**193**	**235**
	Fort McClellan	**105**	**115**	**120**	**146**	**169**	**185**	**193**	**235**
	Fort Rucker	**112**	**120**	**128**	**156**	**180**	**193**	**206**	**250**
	Maxwell-Gunther AFB / Montgomery	**105**	**115**	**120**	**146**	**169**	**185**	**193**	**235**
	Mobile	**142**	**155**	**165**	**201**	**229**	**249**	**266**	**323**
	Redstone Arsenal / Huntsville	**105**	**115**	**120**	**146**	**169**	**185**	**193**	**235**
Alaska	Clear AS	**105**	**110**	**115**	**140**	**169**	**177**	**185**	**225**

Once the design wind speed is inputted into sheet one of the engineering model Excel worksheet, the wind directionality factor K_d must be assigned from Table 26.6-1 in ASCE 7-10 based on the structure type as shown in Table 4-3. This factor accounts for the reduced probability of maximum winds coming from any given direction and for the reduced probability of the maximum pressure coefficients occurring for any given direction.

Table 4-3: Table of wind directionality factors (ASCE Standard ASCE/SEI 7-10. 2010)

Structure Type	Directionality Factor K_d
Buildings Main Wind Force Resisting System Components and Cladding	 0.85 0.85
Arched Roofs	0.85
Chimneys, Tanks, and Similar Structures Square Hexagonal Round	 0.90 0.95 0.95
Solid Freestanding Walls and Solid Freestanding and Attached Signs	0.85
Open Signs and Lattice Framework	0.85
Trussed Towers Triangular, square, rectangular All other cross sections	 0.85 0.95

The next step in the wind analysis is to assign an exposure category based on the structure's surroundings. For each wind direction, the upwind exposure is based on the surface roughness determined by the topography, vegetation, and surrounding structures. Surface roughness is categorized in ASCE 7-10 as follows: "Surface Roughness B: Urban and suburban areas, wooded areas, or other terrain with numerous closely spaced obstructions having the size of single-family dwellings or larger. Surface Roughness C: Open terrain with scattered obstructions having heights generally less than 30 feet. This category includes flat open country and

grasslands. Surface Roughness D: Flat, unobstructed areas and water surfaces. This category includes smooth mud flats, salt lakes, and unbroken ice" (ASCE/SEI Standard 7-10, 2010). Knowing the surface roughness of the specified location, the exposure category is assigned and inputted into sheet one of the engineering model Excel worksheet. ASCE 7-10 categorizes exposure categories as follows: "Exposure B: For buildings with a mean roof height of less than or equal to 30 feet, exposure B shall apply where the ground surface roughness, as defined by surface roughness B, prevails in the upwind direction for a distance greater than 1,500 feet For buildings with a mean roof height greater than 30 feet, exposure B shall apply where surface roughness B prevails in the upwind direction for a distance greater than 2,600 feet or 20 times the height of the building, whichever is greater. Exposure C: Exposure C shall apply for all cases where exposure B or D do not apply. Exposure D: Exposure D shall apply where the ground surface roughness, as defined by surface roughness D, prevails in the upwind direction for a distance greater than 5,000 feet or 20 times the building height, whichever is greater, from an exposure D condition as defined in the previous sentence. For a site located in the transition zone between exposure categories, the category resulting in the largest wind force shall be used" (ASCE/SEI Standard 7-10, 2010). The commentary in ASCE 7-10 provides visual examples of different exposure categories for reference. These examples can be seen in Figures 4-2a to 4-2f.

EXPOSURE B SUBURBAN RESIDENTIAL AREA WITH MOSTLY SINGLE-FAMILY DWELLINGS. LOW-RISE STRUCTURES, LESS THAN 30 FT (9.1 M) HIGH, IN THE CENTER OF THE PHOTOGRAPH HAVE SITES DESIGNATED AS EXPOSURE B WITH SURFACE ROUGHNESS CATEGORY B TERRAIN AROUND THE SITE FOR A DISTANCE GREATER THAN 1500 FT (457 M) IN ANY WIND DIRECTION.

Figure 4-2a: Exposure category examples (ASCE/SEI Standard 7-10, 2010)

EXPOSURE B URBAN AREA WITH NUMEROUS CLOSELY SPACED OBSTRUCTIONS HAVING SIZE OF SINGLE FAMILY DWELLINGS OR LARGER. FOR ALL STRUCTURES SHOWN, TERRAIN REPRESENTATIVE OF SURFACE ROUGHNESS CATEGORY B EXTENDS MORE THAN TWENTY TIMES THE HEIGHT OF THE STRUCTURE OR 2600 FT (792 M), WHICHEVER IS GREATER, IN THE UPWIND DIRECTION.

Figure 4-2b: Exposure category examples (ASCE/SEI Standard 7-10, 2010)

EXPOSURE B STRUCTURES IN THE FOREGROUND ARE LOCATED IN EXPOSURE B. STRUCTURES IN THE CENTER TOP OF THE PHOTOGRAPH ADJACENT TO THE CLEARING TO THE LEFT, WHICH IS GREATER THAN APPROXIMATELY 656 FT (200 M) IN LENGTH, ARE LOCATED IN EXPOSURE C WHEN WIND COMES FROM THE LEFT OVER THE CLEARING.

Figure 4-2c: Exposure category examples (ASCE/SEI Standard 7-10, 2010)

EXPOSURE C FLAT OPEN GRASSLAND WITH SCATTERED OBSTRUCTIONS HAVING HEIGHTS GENERALLY LESS THAN 30 FT.

Figure 4-2d: Exposure category examples (ASCE/SEI Standard 7-10, 2010)

EXPOSURE C OPEN TERRAIN WITH SCATTERED OBSTRUCTIONS HAVING HEIGHTS GENERALLY LESS THAN 30 FT FOR MOST WIND DIRECTIONS, ALL 1-STORY STRUCTURES WITH A MEAN ROOF HEIGHT LESS THAN 30 FT IN THE PHOTOGRAPH ARE LESS THAN 1500 FT OR TEN TIMES THE HEIGHT OF THE STRUCTURE, WHICHEVER IS GREATER, FROM AN OPEN FIELD THAT PREVENTS THE USE OF EXPOSURE B.

Figure 4-2e: Exposure category examples (ASCE/SEI Standard 7-10, 2010)

EXPOSURE D A BUILDING AT THE SHORELINE (EXCLUDING SHORELINES IN HURRICANE-PRONE REGIONS) WITH WIND FLOWING OVER OPEN WATER FOR A DISTANCE OF AT LEAST 1 MILE. SHORELINES IN EXPOSURE D INCLUDE INLAND WATERWAYS, THE GREAT LAKES, AND COASTAL AREAS OF CALIFORNIA, OREGON, WASHINGTON, AND ALASKA.

Figure 4-2f: Exposure category examples (ASCE/SEI Standard 7-10, 2010)

After assigning an exposure category which dictates the amplification or reduction of the applied wind pressure on a structure, the topographic effect factor is assigned and inputted into sheet one of the engineering model Excel workbook. The topographic effect factor is accounts for wind speed-up effects over hills, ridges, and escarpments as seen in Figure 4-3 from Figure 26.8-1 in ASCE 7-10.

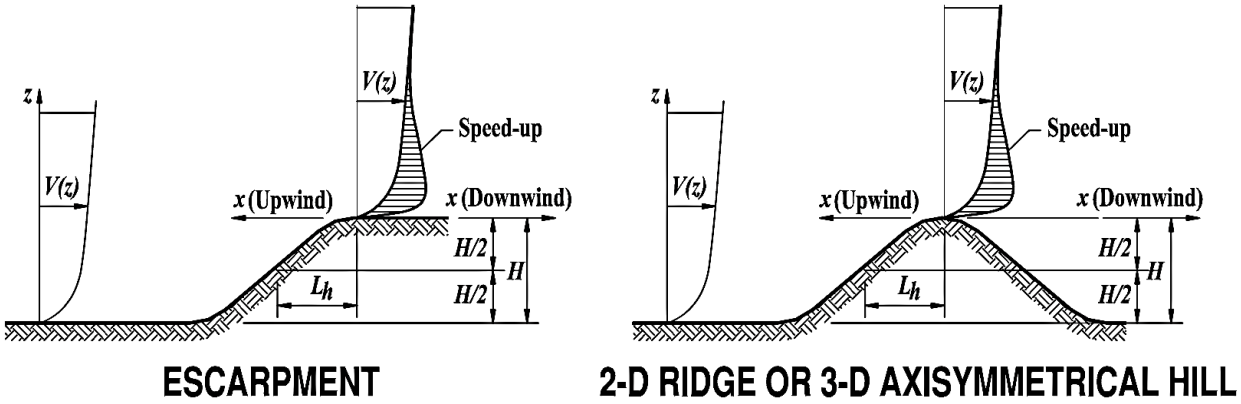

Figure 4-3: Topographic effect scenarios (ASCE/SEI Standard 7-10, 2010)

If the structure falls into a category listed in the topographic effects section of ASCE 7-10, then a topographic effect factor must be calculated. This research, assumes that the LAMSs are located primarily on airfields and relatively flat terrain; therefore, the topographic effect factor (K_{zt}) is 1.0.

Next, the gust-effect factor is taken as 0.85 due to all LAMSs being rigid in regard to structural flexibility. For taller structures with more mass that may not be classified as rigid, the gust effect section of ASCE 7-10 covers a process to determine the gust effect factor based on a structure's natural frequency.

All structures, unless fully open, will experience internal pressure effects due to wind. To determine the amount of internal pressure, an enclosure classification must be assigned from the enclosure classification section of ASCE 7-10. Knowing the enclosure classification, the internal

pressure coefficient (GC_{pi}) is assigned based off the enclosure classification Table 26.11-1 from ASCE 7-10 as seen in Table 4-4. From this table an open structure or partially enclosed structure, such as the LAMSs the Air Force uses, will have an internal pressure coefficient of 0.0 or 0.55 respectively.

Table 4-4: Internal pressure coefficient table (ASCE/SEI Standard 7-10, 2010)

Enclosure Classification	(GC_{pi})
Open Buildings	0.00
Partially Enclosed Buildings	+0.55 -0.55
Enclosed Buildings	+0.18 -0.18

ASCE 7-10 Chapter 30 covers wind loading on components and cladding of structures. This research is tasked with investigating fabric structures used on LAMSs. The fabric structures function as cladding, thus transferring their load to the metal frame system which functions as the main wind force resisting system (MWFRS). For this purpose, the wind pressure is calculated using the components and cladding section of ASCE 7-10. The velocity pressure is evaluated at all heights in pounds per foot squared using Equation 4-1 from equation 27.3-1 in ASCE 7-10.

$$q_z = 0.00256 * K_z * K_{zt} * K_d * V^2 \quad (4\text{-}1)$$

Where K_z is the velocity pressure exposure coefficient, K_{zt} is the topographic effect factor, K_d is the wind directionality factor, and V is the basic wind speed. K_z is assigned based on the

exposure and height of the structure using the velocity pressure exposure coeffcients table in ASCE 7-10 as seen in Table 4-5 from Table 27.3-1 in ASCE 7-10. The engineering model has this table built in and will asign K_z based on the exposure category assigned.

Table 4-5: Velocity pressure exposure coefficients (ASCE/SEI Standard 7-10, 2010)

Height above ground level, z		Exposure		
		B	C	D
ft	(m)			
0-15	(0-4.6)	0.70	0.85	1.03
20	(6.1)	0.70	0.90	1.08
25	(7.6)	0.70	0.94	1.12
30	(9.1)	0.70	0.98	1.16
40	(12.2)	0.76	1.04	1.22
50	(15.2)	0.81	1.09	1.27
60	(18)	0.85	1.13	1.31
70	(21.3)	0.89	1.17	1.34
80	(24.4)	0.93	1.21	1.38
90	(27.4)	0.96	1.24	1.40
100	(30.5)	0.99	1.26	1.43
120	(36.6)	1.04	1.31	1.48
140	(42.7)	1.09	1.36	1.52
160	(48.8)	1.13	1.39	1.55
180	(54.9)	1.17	1.43	1.58
200	(61.0)	1.20	1.46	1.61
250	(76.2)	1.28	1.53	1.68
300	(91.4)	1.35	1.59	1.73
350	(106.7)	1.41	1.64	1.78
400	(121.9)	1.47	1.69	1.82
450	(137.2)	1.52	1.73	1.86
500	(152.4)	1.56	1.77	1.89

Finally, the design wind pressure at all heights shall be calculated from Equation 4-2 as noted in the design wind pressures section of structures classified as open buildings or partially enclosed low rise buldings in the components and cladding section of ASCE 7-10.

$$p = q_z * (GC_p - GC_{pi}) \tag{4-2}$$

q_z was previously calculated per Equation 4-1, G is the gust factor assigned earlier, C_{pi} is the intenal pressure coefficient also assigned earlier, and C_p is the external pressure coefficient. C_p

for open building is asigned per the components and cladding net pressure coefficient Table 30.8-2 in ASCE 7-10 that specifies pitched roofs and open buildings as seen in Table 4-6.

Table 4-6: Net pressure coefficients (ASCE Standard ASCE/SEI 7-10. 2010)

Roof Angle θ	Effective Wind Area	C_N											
		Clear Wind Flow						Obstructed Wind Flow					
		Zone 3		Zone 2		Zone 1		Zone 3		Zone 2		Zone 1	
0°	$\leq a^2$	2.4	-3.3	1.8	-1.7	1.2	-1.1	1	-3.6	0.8	-1.8	0.5	-1.2
	$> a^2, \leq 4.0a^2$	1.8	-1.7	1.8	-1.7	1.2	-1.1	0.8	-1.8	0.8	-1.8	0.5	-1.2
	$> 4.0a^2$	1.2	-1.1	1.2	-1.1	1.2	-1.1	0.5	-1.2	0.5	-1.2	0.5	-1.2
7.5°	$\leq a^2$	2.2	-3.6	1.7	-1.8	1.1	-1.2	1	-5.1	0.8	-2.6	0.5	-1.7
	$> a^2, \leq 4.0a^2$	1.7	-1.8	1.7	-1.8	1.1	-1.2	0.8	-2.6	0.8	-2.6	0.5	-1.7
	$> 4.0a^2$	1.1	-1.2	1.1	-1.2	1.1	-1.2	0.5	-1.7	0.5	-1.7	0.5	-1.7
15°	$\leq a^2$	2.2	-2.2	1.7	-1.7	1.1	-1.1	1	-3.2	0.8	-2.4	0.5	-1.6
	$> a^2, \leq 4.0a^2$	1.7	-1.7	1.7	-1.7	1.1	-1.1	0.8	-2.4	0.8	-2.4	0.5	-1.6
	$> 4.0a^2$	1.1	-1.1	1.1	-1.1	1.1	-1.1	0.5	-1.6	0.5	-1.6	0.5	-1.6
30°	$\leq a^2$	2.6	-1.8	2	-1.4	1.3	-0.9	1	-2.4	0.8	-1.8	0.5	-1.2
	$> a^2, \leq 4.0a^2$	2	-1.4	2	-1.4	1.3	-0.9	0.8	-1.8	0.8	-1.8	0.5	-1.2
	$> 4.0a^2$	1.3	-0.9	1.3	-0.9	1.3	-0.9	0.5	-1.2	0.5	-1.2	0.5	-1.2
45°	$\leq a^2$	2.2	-1.6	1.7	-1.2	1.1	-0.8	1	-2.4	0.8	-1.8	0.5	-1.2
	$> a^2, \leq 4.0a^2$	1.7	-1.2	1.7	-1.2	1.1	-0.8	0.8	-1.8	0.8	-1.8	0.5	-1.2
	$> 4.0a^2$	1.1	-0.8	1.1	-0.8	1.1	-0.8	0.5	-1.2	0.5	-1.2	0.5	-1.2

C_p for partially enclosed buildings is asigned per the components and cladding external pressure coefficient figures in ASCE 7-10 seen in figure 30.4-2C for gable type roofs or figure 30.4-7 for domed roof structures. Figure 4-4 shows the chart used for gable type roof structures and Table 4-7 shows the table used for domed roofs.

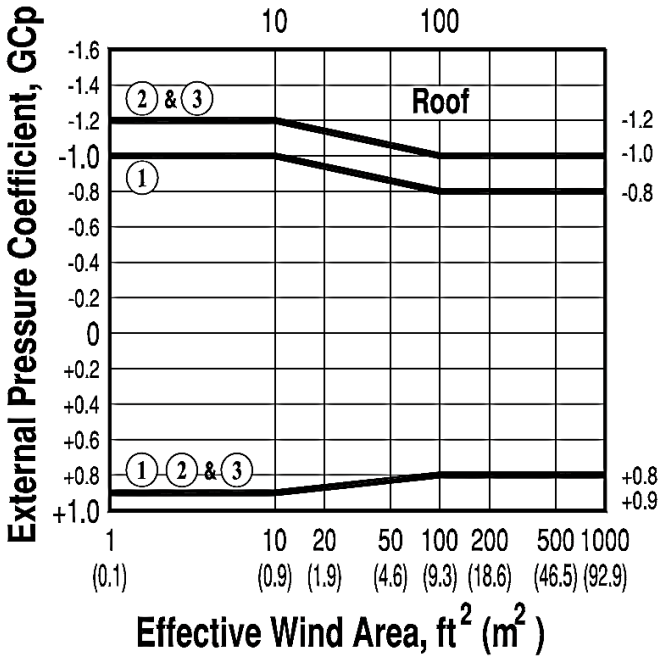

Figure 4-4: Gabled roof external pressure coefficients (ASCE Standard ASCE/SEI 7-10. 2010)

Table 4-7: Domed roof external pressure coefficients (ASCE Standard ASCE/SEI 7-10. 2010)

	Negative Pressure	Positive Pressure	Positive Pressure
Θ, degrees	0-90	0-60	61-90
GC_p	-0.9	+0.9	+0.5

The pressure coefficient varies based on roof pitch and the effective wind area. All LAMSs are not the same, some having domed roofs and others having pitched free roofs. The purpose of this research is to evaluate fabric structures used on LAMSs; therefore, a more conservative approach of assigning the worst possibility to the external pressure coefficient will prove the fabric structure is able to stand up to ASCE 7-10 standards. LAMSs are not all regularly shaped structures, and a more accurate representation of the wind load pressure applied could be

accomplished by the wind tunnel procedure of ASCE 7-10. This approach is outside the scope of this research. Once inserted all the wind parameters, the wind analysis sheet of the engineering model Excel workbook calculates wind pressures at increasing elevations up to 500 feet. Although LAMSs do not reach height of 500 feet, including this pressure in the analysis allows the algorithm to reach the breaking strength of stronger fabric structures.

4.3. ITERATIVE ALGORITHM

Sheet two of the engineering model Excel worksheet contains the bulk of the analysis process with the wind pressures and elevations as determined in from sheet one. The midspan deflection is incremented by 0.10 inches up to 100.00 inches. Fabric structures undergo large deformations under extreme wind load, and an accurate nonlinear analysis requires an iterative process. As a part of the iterative algorithm, linear interpolation is used for wind pressures and elevations not covered in the wind analysis section of ASCE 7-10 and sheet one of the engineering model Excel worksheet. Similar to the wind analysis section, there are more input cells which need to be populated by the operator before the algorithm runs as shown in Table 4-8.

Table 4-8: Input cells for iterative algorithm

"Input cell"	
Initial properties	
Thickness of material (in):	0.025197
Consistant Unit Width (ft):	1
Distance between longitudinal supports (ft):	12.5
Height of LAMS (ft):	40
Are max values below ASCE7-10 loads?:	YES
Are service values below ASCE7-10 loads?:	YES
Maximum Values	100%
Breaking Stress (kips/in^2):	12.36
Max Tension Force (kips/ft):	3.15
Max Midspan Deflection (in):	50.00
Service Values (% of Max):	25%
Service Stress (kips/in^2):	3.09
Service Tension Force (kips/ft):	0.93
Service Midspan Deflection (in):	28.80
Service Wind Pressure Failure (lb/ft^2)	103.74

The thickness of the material shall be taken from the material test results of the sample the operator selects as a best representation of the fabric structure in question. The distance between longitudinal supports (arches) shall be inputted based on the geometry of the structure. The input height is used to determine if the breaking and service values are acceptable per the manufacturer's standards based on prescribed ASCE 7-10 loads. The service value percentage shall be determined by the operator. Acceptable industry service values typically are in the range of 25 percent.

Industry practice is to use a factor of safety of 4.0 for pretension plus wind load. Using a life-cycle factor of 0.75 and a strength reduction factor returns an equivalent factor of safety of 4.04 for pretension plus wind load. Because of the low degree of accuracy to which membrane materials can be determined uniformly and because of the wide range and complexities of the loadings on tensile membrane structures, the standard is based on

past successful usage of safety factors in thousands of constructed projects. Accurate statistical and probabilistic methods for determining load and resistance factors currently are not possible because of the lack of data for each of them (ASCE Standard ASCE/SEI 7-10. 2010).

Once all input cells are populated, the algorithm will initiate assuming a catenary cable action of the fabric structure as seen in Figure 4-5. Huntington (2004) discovered that by modeling a strip of fabric as if it were a cable having equivalent axial stiffness returns a good approximation of the proper shaping and stress the fabric structure feels under a certain load.

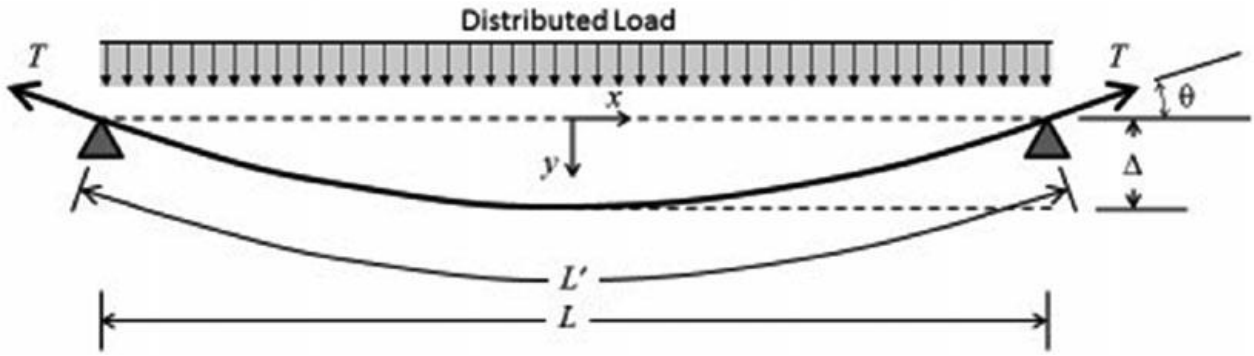

Figure 4-5**:** Distributed load on a cable (Gagnet at el. 2017)

Gagnet at el. (2017) presents multiple membrane resistance definitions and evaluates their accuracy when compared to a finite element model. Gagnet at el. (2017) evaluated the lateral pressure vs. deflection on a membrane and found that the parabolic deflection method closely resembles the finite element model results when considering all other methods presented in his research as seen in Figure 4-6. Therefore, this research will base calculations within the iterative algorithm on the parabolic deflection method.

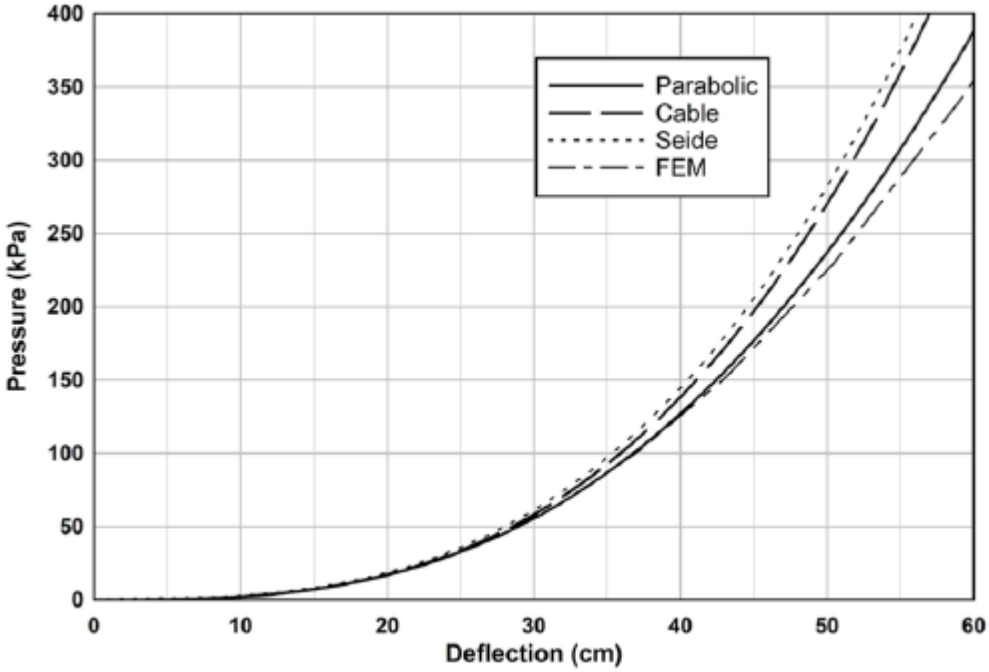

Figure 4-6: Linear material membrane resistance comparisons (Gagnet et al. 2017)

4.3.1. PARABOLIC DEFLECTION METHOD

The parabolic deflection method assumes a membrane deflects in a parabolic shape as load is applied. This method starts by formulating the deflection using geometric properties and then correlating the change in length to strain and stress to determine the corresponding pressure loading (Gagnet et al. 2017). The general deflection is represented by the following parabolic function:

$$y(x) = Ax^2 + Bx + C \tag{4-3}$$

Using Figure 4-5 as a basis for boundary conditions represented in Equations 4-4a, 4-4b, and 4-4c the unknown coefficients are solved for and the general deflection function is now represented by Equation 4-5.

$$y(x) = \Delta \text{ at } x = 0 \tag{4-4a}$$

$$y(x) = 0 \text{ at } x = \frac{L}{2} \tag{4-4b}$$

$$y'(x) = 0 \text{ at } x = 0 \tag{4-4c}$$

$$y(x) = -\frac{4\Delta}{L^2}x^2 + \Delta \tag{4-5}$$

Taking the derivative of the general deflection function returns the general slope function of the membrane represented by Equation 4-6.

$$y'(x) = -\frac{8\Delta}{L^2}x \tag{4-6}$$

The arc length L' as a function of the midspan deflection can then be solved for using arc length formula represented by Equation 4-7.

$$L' = 2\int_0^{\frac{L}{2}} \sqrt{1+(y'(x))^2}\,dx \tag{4-7}$$

Substituting the slope Equation (4-6) for y'(x), the arc length of the membrane is solved for represented by Equation 4-8.

$$L' = \frac{4\Delta}{L}\left[\sqrt{\frac{L^2}{4}+\frac{L^4}{64\Delta^2}} + \frac{L^3}{32\Delta^2} * \ln\left(\frac{L}{2}+\sqrt{\frac{L^2}{4}+\frac{L^4}{64\Delta^2}}\right) - \frac{L^3}{32\Delta^2} * \ln\left(\frac{L^2}{8\Delta}\right)\right] \tag{4-8}$$

The arc length is used to determine the strain in the membrane at each iterative step represented by Equation 4-9.

$$\varepsilon = \frac{L'-L}{L} \tag{4-9}$$

A nonlinear stress vs. strain definition is used to determine the membrane stress at each iterative step. Using the equilibrium conditions seen in Figure 4-5, the next step is to sum the forces in the y-direction in order to relate pressure to a known variable as represented in Equation 4-10.

$$\sum F_y = 0 = pL - 2T\sin(\theta) \tag{4-10}$$

Substituting the general slope function (4-6) in for Θ yields Equation 4-11

$$2T\sin\left(-\frac{8\Delta}{L^2}x\right) = pL \tag{4-11}$$

where T is represented as stress times the cross-sectional area (T=σA) in the membrane. If a unit width is considered, the cross-sectional area of the membrane can be reduced to t_s, the thickness of the membrane material. Since the angle of interest is at the ends of the membrane, L/2 is substituted for x and Equation 4-11 can be solved for the pressure p as represented by Equation 4-12 (Gagnet et al. 2017).

$$p = \frac{2\sigma t_s}{L}\sin\left(\frac{4\Delta}{L}\right) \tag{4-12}$$

these are the necessary engineering Equations in the iterative algorithm, of the engineering model. Incrementing the midspan deflection, the parabolic length is calculated based on Equation 4-8, with Δ equal to the midspan deflection (in inches) and L equal to the distance between longitudinal supports (undisturbed length) (in feet). The wind pressure is calculated based on Equation 4-12 with σ equal to the true stress of the membrane (in kips per square inch) and t_s equal to the thickness of the material (in inches). Knowing the wind pressure at each incremental step, the corresponding elevation (in feet) is interpolated based off the wind analysis sheet of the engineering model Excel worksheet.

The engineering model handles linear interpolation by utilizing the MATCH and INDEX functions within Excel. The MATCH function retrieves the position of an item in an array, returns a number representing a position in the lookup array. The syntax is as follows:

Position=MATCH(lookup_value, lookup_array, [match_type])

with lookup_value representing the value to match in the lookup array, lookup_array representing a range of cells or an array reference, and match_type representing how to match, specified as -1(greater than), 0(exact), or 1(less than). The INDEX function serves the purpose of retrieving a value in a list or table based on location and returns the value at a given location. The syntax is as follows:

Value=INDEX(array, row_num, [col_num], [area_num])

with array representing a range of cells or an array constant, row_num represents the row position in the reference or array, col_num represents the column position in the reference or array, and area_num represents the range in reference that should be used. Both col_num and area_num are optional and will not be used when linearly interpolating between material data points.

At each itterative step, the algorithim uses the calculated wind pressure form Equation 4-12 to retrieve the elevation value from the wind analysis sheet within the Excel worksheet that reflects the calculated wind pressure. This is accomplished through linear interpolation which uses Equation 4-13 in conjunction to the MATCH and INDEX functions.

$$y = y_1 + \frac{(x - x_1)(y_2 - y_1)}{(x_2 - x_1)} \tag{4-13}$$

First, the MATCH function searches for a value equal to or less than the calculated wind pressure for the itterative step in an array (table) of the wind analysis pressure and reports back the row number of that value. Then the INDEX function uses the reported row number to search the elevation array (table) to return the elevation value that coresponds to the row number of the calculated wind pressure.

Knowing the parabolic length and the initial undisturbed length of the fabric structure, the algorithm will calculate the srain at each itterative step based on Equation 4-9. The calculated stress follows the same interprolation process within Excel as the calculated elevation by referencing the calculated strain to the true strain and true stress arrays (tables) under the raw data sheet. Lastly, the tension force at each itterative step is calculated based on Equation 4-14.

$$T = \frac{\sigma * A}{\text{Unit Width}} \tag{4-14}$$

With A equal to the thickness of material multiplied by a unit width of one foot.

After the iterative process is complete, the model returns the breaking stress, maximum tension force, and maximum midspan deflection. The algorithm utilizes of the MAX function built into Excel to search the true stress column of the raw data tab to return the maximum/breaking stress. To find the maximum tension force and midspan deflection, the algorithm uses the INDEX and MATCH functions once again as shown in the following example: "=INDEX(H:H,MATCH(B11,J:J,1),1)." This function is first matching the breaking stress "B11" to column "J" to find a match equal to or less than the breaking stress "1". Once this cell is known, the index function is searching the column with the max deflection or force. For this example, assume "H:H," for the value that is in the same row as the breaking stress and returning its value which is found under the first "1" column in the INDEX statement. The maximum values are returned in the iterative algorithm sheet. Along with the maximum values, service values are also returned using the same process. Typical industry service values are in the range of 25 percent of the maximum breaking stress to prevent residual strains that would cause fluttering action if not addressed.

4.4. MATERIAL PROPERTIES

From Chapter 3, the material properties of the fabric structure are quantified and simplified. The material properties are copied and pasted into the raw data of the engineering model with the strain expressed as a unitless value (inch per inch) and stress expressed in kips per inch squared as seen in Table 4-9.

Table 4-9**:** Raw data input sheet

	Simplified multi-linear material properties	
	Strain (in/in)	Stress (kips/in^2)
INSERT MATERIAL → PROPERTY DATA HERE	0	0
	0.01172	1.064
	0.01519	1.294
	0.02013	1.522
	0.03067	1.748
	0.05733	2.138
	0.09507	2.813
	0.11746	3.264
	0.16613	4.512
	0.20387	5.751
	0.25519	7.457
	0.28146	8.259
	0.3068	8.933
	0.32374	9.246
	0.3304	9.293

The engineering model converts the engineering stress and strain into true stress and true strain using the Equations 3-4 and 3-7. An example is seen in Table 4-10.

Table 4-10**:** True stress/strain conversion

True stress and true strain material properties	
True Strain (in/in)	True Stress (kips/in^2)
0.0000	0.000
0.0117	1.076
0.0151	1.314
0.0199	1.553
0.0302	1.802
0.0557	2.261
0.0908	3.080
0.1111	3.647
0.1537	5.262
0.1855	6.923
0.2273	9.360
0.2480	10.584
0.2676	11.674
0.2805	12.239
0.2855	12.363

4.5. SIMPLIFIED LINEAR APPROACH

As discussed in Chapter 3, the material properties of fabric structures are nonlinear. However, representing the material properties as linear is an easier alternative to the hassle of iterating through nonlinear material properties as the fabric structure in analyzed. A comparison of the nonlinear material properties to the linear material properties is shown in Figure 4-7. ASCE 55-16 “Tensile Membrane Structures” discusses linearizing material properties through the least squares method, which forms a more accurate representation of the linear material properties. For the purpose of this research, linear material properties are taken from a point of zero stress and strain up to the breaking stress and strain of the material.

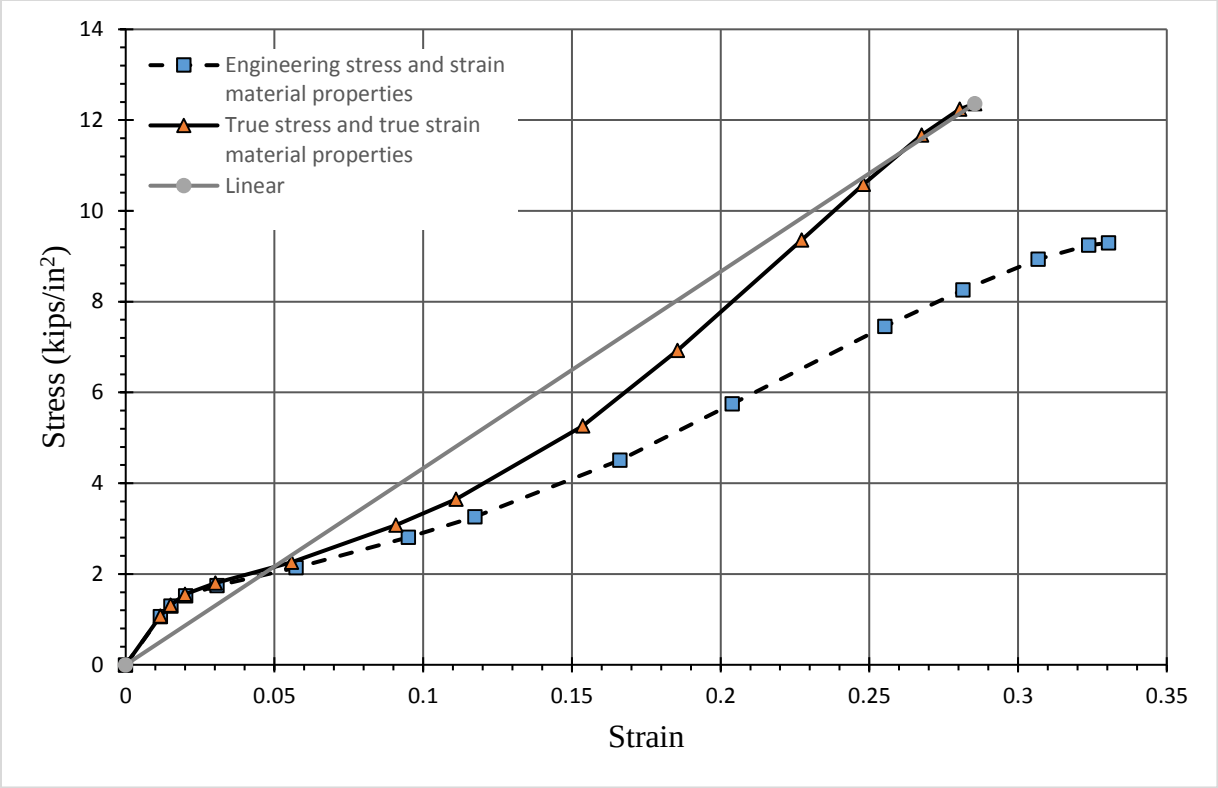

Figure 4-7**:** Material properties comparison

Based on the Figure 4-7, it becomes clear that initially the specimen undergoes a slight stiffening, most likely due to the PVC coating, then the material properties flatten out and follow a relatively linear path. Therefore, applying a constant modulus of elasticity should return similar, more conservative results to the nonlinear material properties. To test this theory, only the breaking stress and strain were inputted into the material properties as seen in Table 4-11, followed by the full nonlinear material properties inputted as seen in Table 4-12.

Table 4-11**:** Snapshot of linear material properties in the engineering model

True stress and true strain material properties	
True Strain (in/in)	True Stress (kips/in^2)
0.0000	0.000
0.2855	12.363

Table 4-12**:** Snapshot of NL material properties in the engineering model

True stress and true strain material properties	
True Strain (in/in)	True Stress (kips/in^2)
0.0000	0.000
0.0117	1.076
0.0151	1.314
0.0199	1.553
0.0302	1.802
0.0557	2.261
0.0908	3.080
0.1111	3.647
0.1537	5.262
0.1855	6.923
0.2273	9.360
0.2480	10.584
0.2676	11.674
0.2805	12.239
0.2855	12.363

For comparison purposes both linear and nonlinear material property engineering models were run with the same wind pressures and geometry inputs. The thickness of the material was set to 0.025 inches, the distance between longitudinal supports was set to 12.5 feet, and the height was set to 40 feet with service values limited to 25 percent. The iterative process ran through the calculations immediately returning the maximum and service values for each case. For comparison purposes, wind pressure up to 100 pounds per foot squared was plotted against the midspan deflection and tension force for both linear and nonlinear material property cases. As seen in Figure 4-8, the deflection results reflect a more conservative response when predicting the deflection of the fabric structure using only linear material properties up to a wind pressure of 50 pounds per square foot. Figure 4-9 shows a more conservative response from the nonlinear material properties up to 50 pounds per square foot for the tension force as well. This transition zone represents the point at which the nonlinear and linear material properties plots intersect seen

in Figure 4-7 at approximately a strain of 0.05. As a higher pressure is applied to the fabric structure the nonlinear material properties begin to soften, resulting in a larger deflection coupled with a lower tension force when compared to the linear material properties. As the linear and nonlinear material properties reach their breaking stress, the midspan deflection and tension force results begin to converge this convergence is reflected in Figure 4-10.

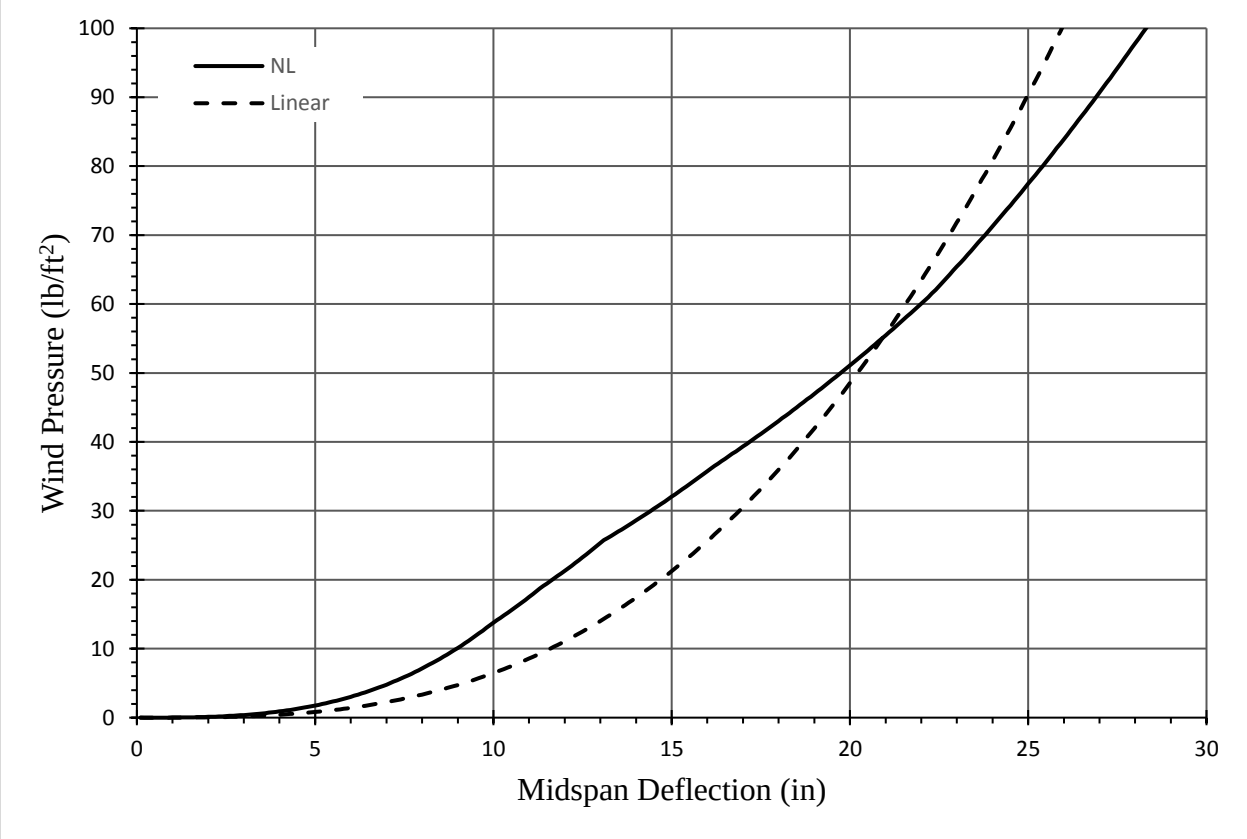

Figure 4-8**:** Linear vs. nonlinear material property deflection results

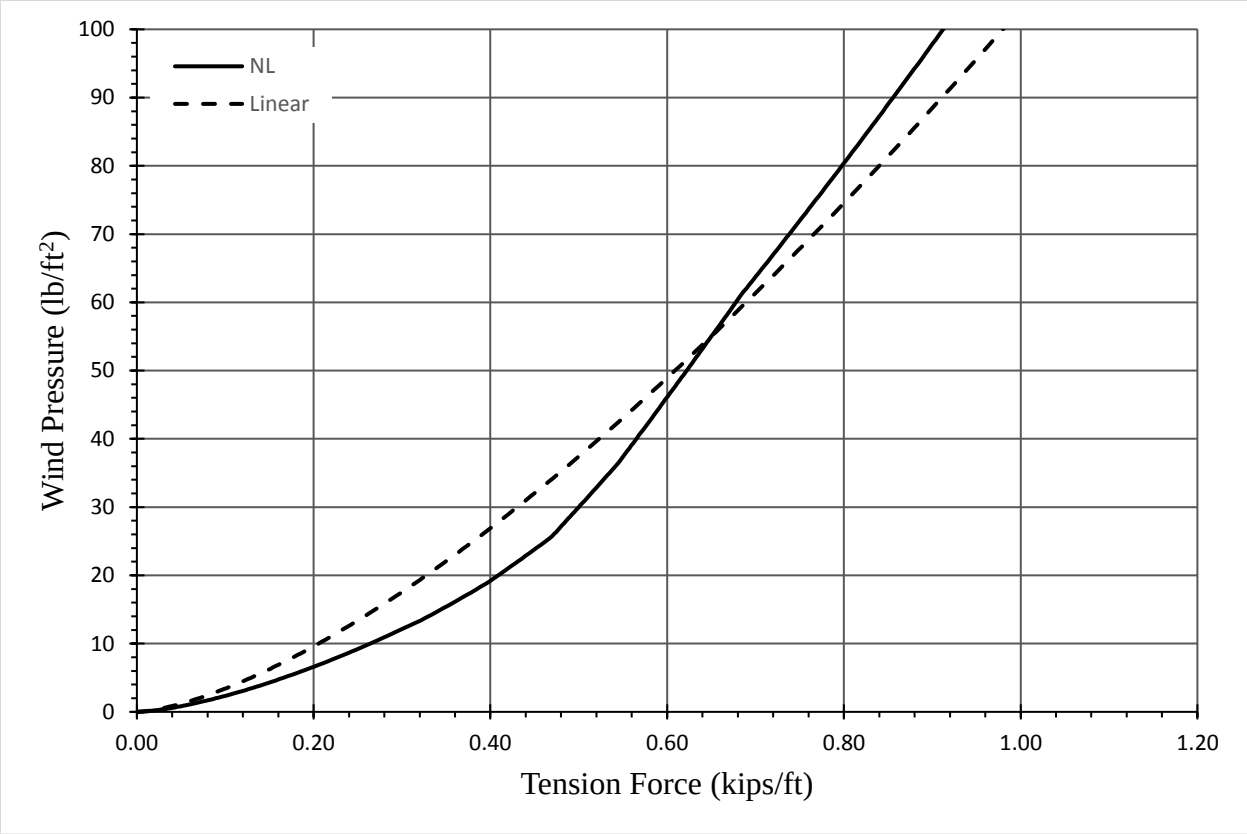

Figure 4-9**:** Linear vs. nonlinear material property tension force results

Applying linear material properties saves time and eliminates the need for testing samples if the manufacturer provides a breaking stress and breaking strain or modulus of elasticity. Using linear material properties is a quick way to check if the fabric structure will pass the manufacturers standards based on loads form ASCE 7-10 and determine the maximum and service midspan deflection and tension force.

Furthermore, the maximum wind pressure can be reduced to an explicit Equation using the breaking stress and breaking strain. This quick check will provide a starting point for the fabric structure analysis and allow the engineer to determine if a full nonlinear analysis is required. The explicit Equation is derived using pure statics of a uniformly loaded cable. Given

the breaking stress and strain of the fabric structure, the parabolic length and maximum tension force can be solved as represented by Equation 4-15 and Equation 4-16 respectively.

$$L_p = L + (\varepsilon * L) \tag{4-15}$$

$$T = \sigma * A \tag{4-16}$$

where L is the initial undisturbed length, ε is the breaking strain, σ is the breaking stress, and A is the cross-sectional area. From statics, the parabolic length of the cable can be approximated using Equation 4-17. Rearranging this equation and substituting in Equation 4-15, the midspan deflection Δ can be solved for as represented by Equation 4-18.

$$L_p = L + \frac{8 * \Delta^2}{3 * L} \tag{4-17}$$

$$\Delta = \frac{\sqrt{6} * L * \sqrt{\varepsilon}}{4} \tag{4-18}$$

The reactions in the x and y directions from Figure 4-5 are solved for based on Equations 4-19 and 4-20. The maximum tension force equation is represented by Equation 4-21. Substituting Equations 4-19 and 4-20 into Equation 4-21 yields Equation 4-22.

$$R_x = \frac{p * L^2}{8 * \Delta} \tag{4-19}$$

$$R_y = \frac{p * L}{2} \tag{4-20}$$

$$T = \sqrt{R_x{}^2 + R_y{}^2} \tag{4-21}$$

$$T = \sqrt{\left(\frac{p * L^2}{8 * \Delta}\right)^2 + \left(\frac{p * L}{2}\right)^2} \tag{4-22}$$

Finally Equations 4-16 and 4-18 are substituted into Equation 4-22, and the maximum wind pressure in pounds per square foot is represented by Equation 4-23.

$$p = \frac{2*\sqrt{6}*A*\sigma*\varepsilon*\sqrt{\frac{1}{\varepsilon}+6}}{L(1+6*\varepsilon)}*1200 \qquad (4\text{-}23)$$

Comparing the explicit equation for the maximum pressure to the engineering model, as shown in Figure 4-10, it reflects an accurte approximation of the breaking wind pressure on a fabric structure up to a wind load of 250 pounds per square foot then begins to tail off.

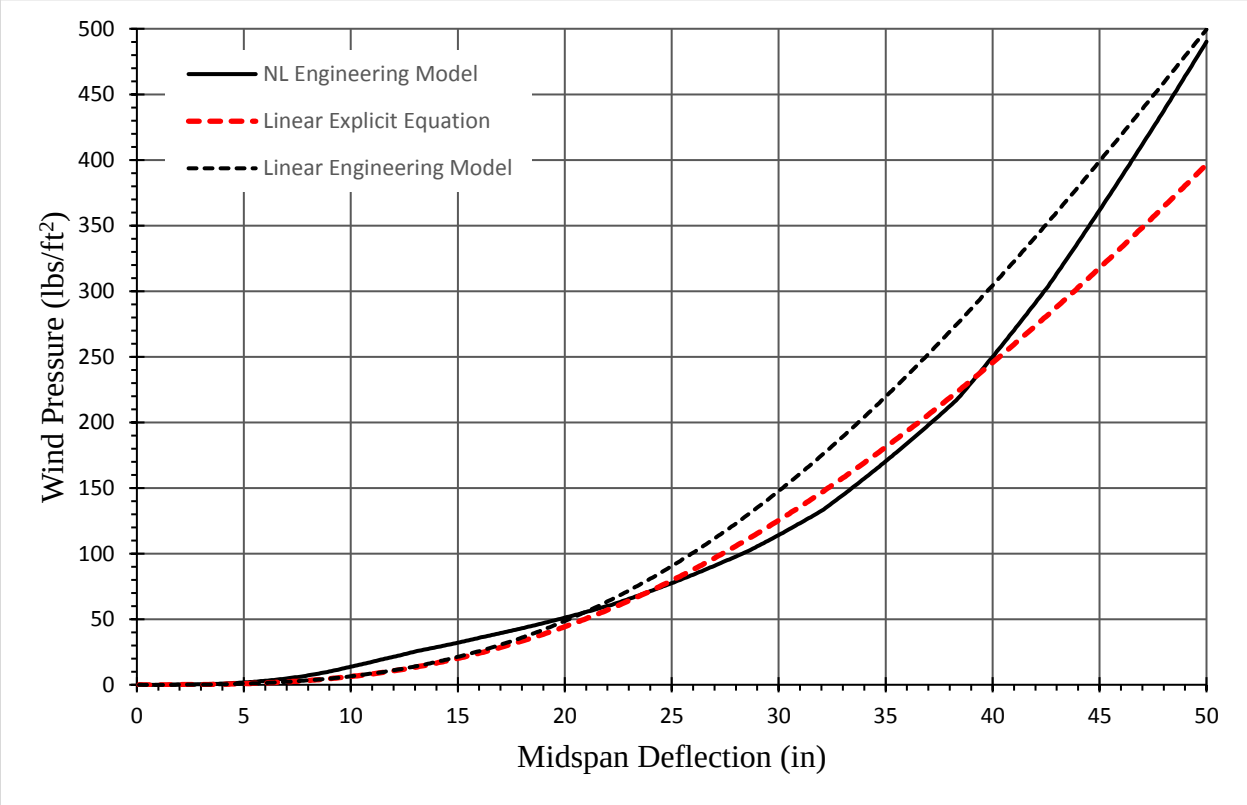

Figure 4-10**:** Explicit equation comparison

This explicit equation can be used to check against the ASCE 7-10 wind pressures that must be achieved. If this initial check does not pass the manufacturers standards, the engineering model will return more accurate results using a nonlinear itterative process.

CHAPTER 5

FINITE ELEMENT VALIDATION

5.1. INTRODUCTION

Chapter 5 discusses the development and use of the finite element models formulated in this research. The main objective of the finite element models is to validate the engineering model's calculations presented in Chapter 4. Further research must be conducted to fully represent fabric structures used on LAMSs as a complete finite element model. The engineering model treats the fabric structure as a catenary structure. Through the use of finite element a one foot strip of the fabric structure will be modeled as a membrane, loaded with a wind pressure, and analyzed to verify assumptions within the engineering model.

Finite element is a numerical method for solving engineering problems in structural analysis. To evaluate a structure, finite element software breaks the structural members down into tens to thousands of smaller finite elements. Each finite element, has degrees of freedom and a system of equations unique to the element. Each finite element is then assembled into a larger element representing the structure with its own system of equations that correctly models the original structure under evaluation. For the purpose of this research, ANSYS Mechanical APDL (ANSYS Parametric Design Language) is the program used for the finite element validation.

5.2. ANSYS MECHANICAL APDL

ANSYS Mechanical APDL allows the user to write a program needed to execute a finite element problem and is a powerful scripting for modeling and automation of common tasks.

5.3. MODEL VERIFICATION PROGRESION

5.3.1. LI NEAR MATERIAL PROPERTIES

To verify the engineering model discussed in Chapter 4, a finite element model needs to match it in every aspect. Beginning this verification, the easiest way to model the fabric structure was through a simple 2-D beam element with virtually no moment of inertia and a specified area matching the area inputted into the engineering model. The load of 16 pounds per square foot was selected as the applied load and was distributed into load steps in the finite element program to compare to the iterative algorithm. Since the beam element has no real surface area, the distributed load was distributed out into point loads distributed along the beam as seen in Figure 5-1.

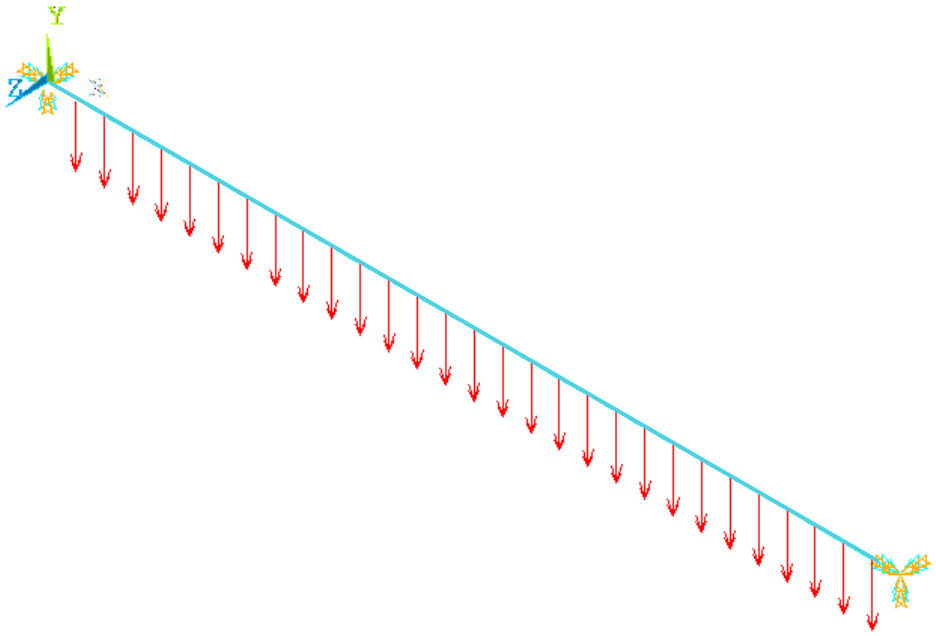

Figure 5-1: Beam elements FEM

Shell elements within ANSYS Mechanical are then investigated. Shell elements better represent the fabric structure as a whole. Taking a strip of the fabric structure and modeling it in ANSYS Mechanical as a shell element essentially parallels the engineering model approach. Shell elements are slightly different from beam elements. Shell elements will have to be modeled in two planes of direction when establishing the geometry. Once the geometry has been set, a thickness must be assigned to the shell element within ANSYS Mechanical. For comparison purposes and ease of modeling, the load of 16 pounds per square foot was again split up among the nodes acting in a similar fashion to the applied pressure load. The shell model, along with its applied loads, can be seen in Figure 5-2.

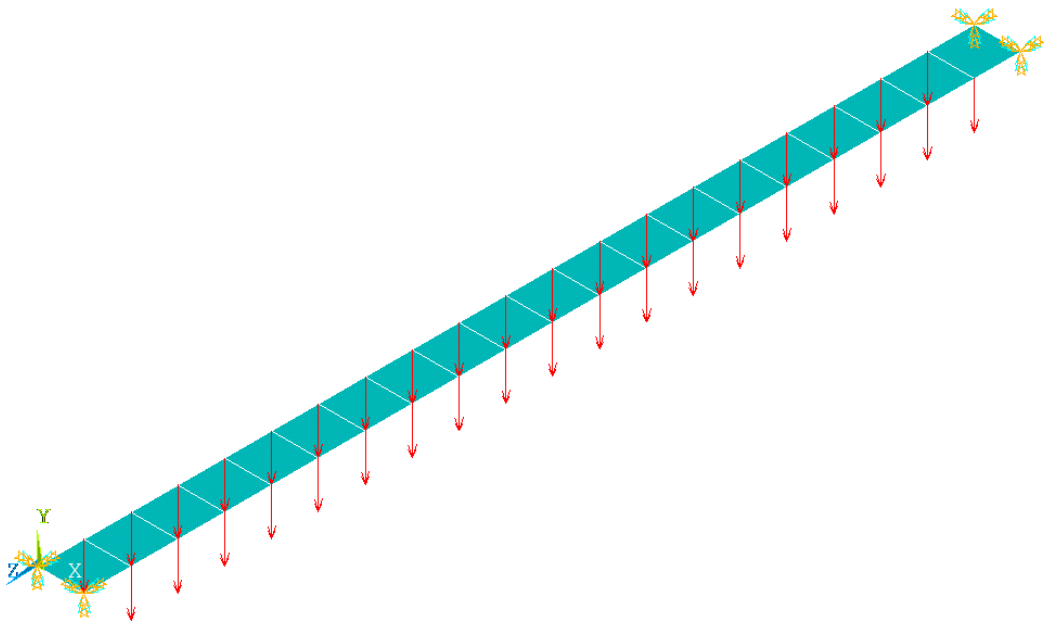

Figure 5-2: Shell elements FEM

Both beam element and shell element models follow the engineering model in regard to their modulus, cross sectional area, and span. As the models are loaded, their geometry changes posing the need for nonlinear solution controls within ANSYS Mechanical. Twenty sub steps (similar to iterations in the engineering model) are used for the loading process, and the iterations of each sub step are capped to assure the solution will converge. Each model is solved through the nonlinear solver within ANSYS Mechanical fairly quickly. The deformed shapes produced by ANSYS Mechanical proved reasonable, and the load step data for each model are exported for comparison to the engineering model. Figure 5-3 shows the results of both the beam and shell element models, along with the engineering model. At this point in the validation process, the models are linear elastic with a constant modulus of elasticity. Along the Y-axis, the load of 16 pounds per a square foot applied to all three models is normalized, and along the X-axis the deflection is reported. Comparing the three results, the engineering model slightly under reports

the beam finite element model, while slightly over reporting the shell element finite element model.

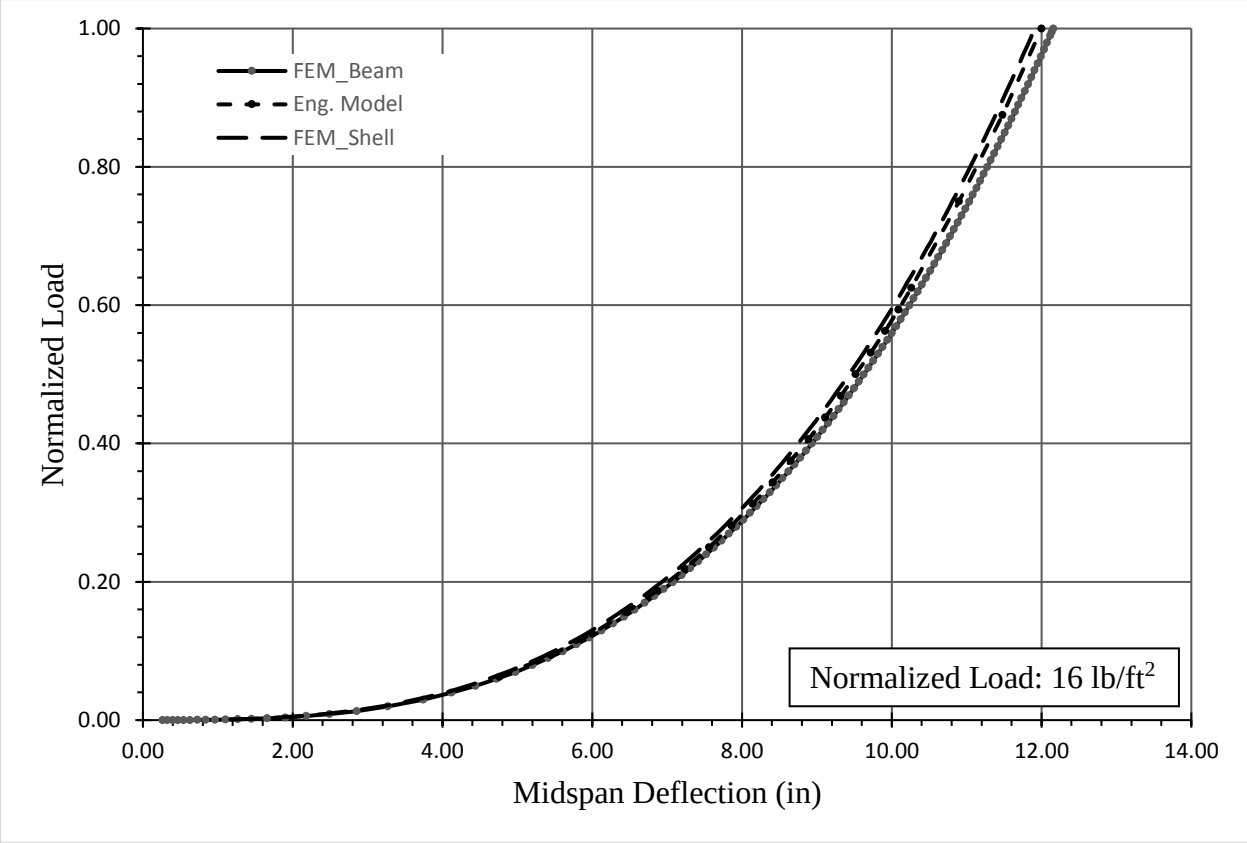

Figure 5-3: Linear material properties comparison

The results seen in Figure 5-3 are promising. Knowing that the real fabric structure closely reflects the finite element shell model, and possessing an engineering model that slightly over predicts the deflection of the finite element shell model, it is reassuring from the standpoint of safety and error. Successfully validating linear material property models within ANSYS mechanical that mirror the results of the engineering model is the first step in finite element validation of the engineering model. The next step this research sets out to accomplish is to validate the nonlinear material properties using the finite element shell model for comparison to the engineering model.

5.3.2. NONLINEAR MATERIAL PROPERTIES

Following some investigating within ANSYS Mechanical, nonlinear material properties work best with shell elements. The shell element model from the previous section with a few alterations is used to verify the engineering model when considering nonlinear material properties. Simplified nonlinear material properties from Chapter 3 are plugged into the ANSYS Mechanical model as seen in Figure 5-4. ANSYS Mechanical requires linear material properties as well to initialize the model. The model, using the linear material properties, will analyze the first load step to start the analysis process. The initial slope from the nonlinear material properties plot is used as the linear material properties. Following the first load step the initial deflected shape is used by ANSYS Mechanical to reference the nonlinear material properties and carry out the remainder of the load steps.

	STRAIN	STRESS
1	0.0117	1.064
2	0.0152	1.294
3	0.0201	1.522
4	0.0307	1.748
5	0.0573	2.138
6	0.0951	2.813
7	0.1175	3.264
8	0.1661	4.512
9	0.2039	5.751
10	0.2552	7.457
11	0.2815	8.259
12	0.3068	8.933
13	0.3237	9.246
14	0.3304	9.293

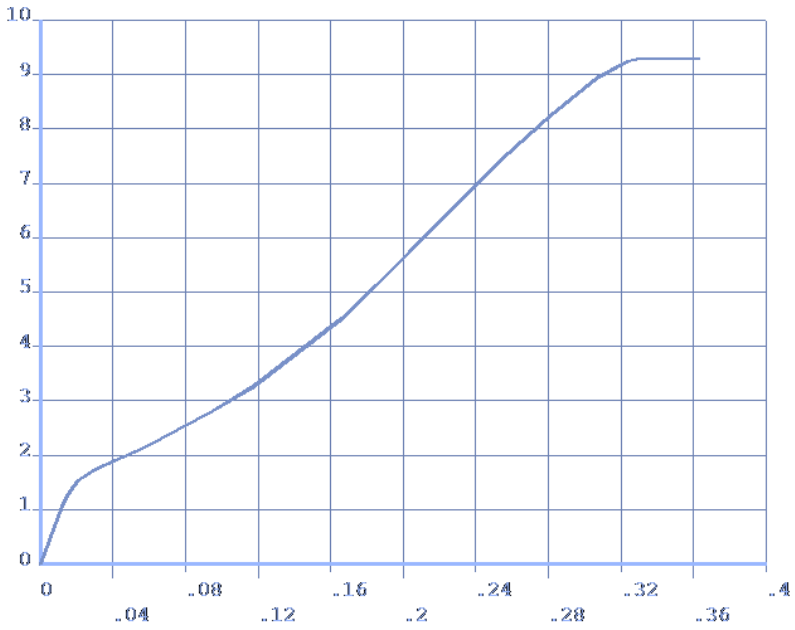

Figure 5-4: Nonlinear material properties

The shell element model found in the previous section is slightly modified to parallel the engineering model precisely. The point loads are removed and a pressure load of 16 pounds per

square foot is applied, staying consistent with the engineering model. Boundary conditions include fully fixing both ends of the element assuming no movement over the LAMSs arches once the fabric structure is loaded. The added restraint of deflection in the x-direction was applied to prevent a collapse of the finite element model due to out of plane action. The final shell element model used is shown in Figure 5-5.

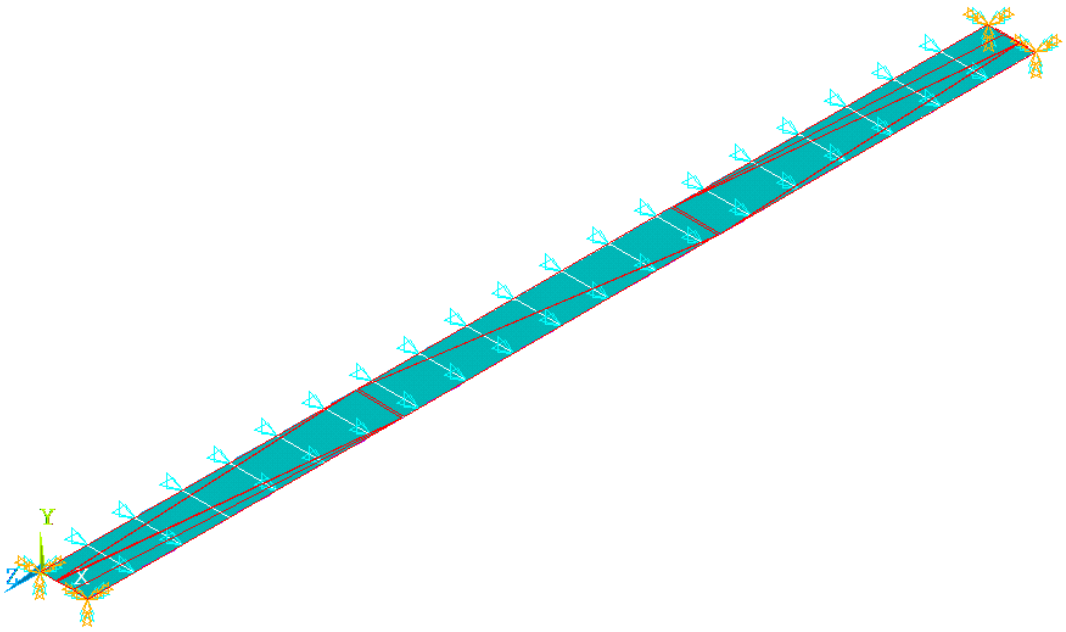

Figure 5-5: Nonlinear shell model with pressure applied

With nonlinear material properties inputted, solution controls are set to control the output. The amount of sub steps and iterations are set similar to that of the previous section. The model is run and allowed to converge on a solution. The results are then analyzed with the deflected shape shown in Figure 5-6 and the midspan deflection at the central node is exported for comparison to the engineering model. Figure 5-7 shows the deflection comparison of the finite element model to the engineering model.

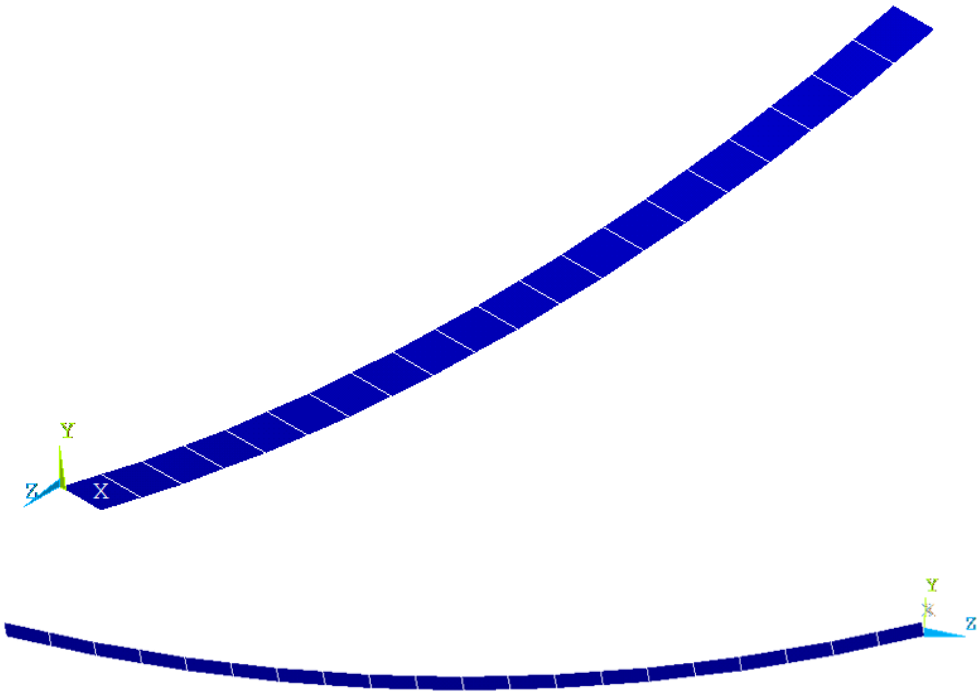

Figure 5-6: Deflected shape in isometric and side view

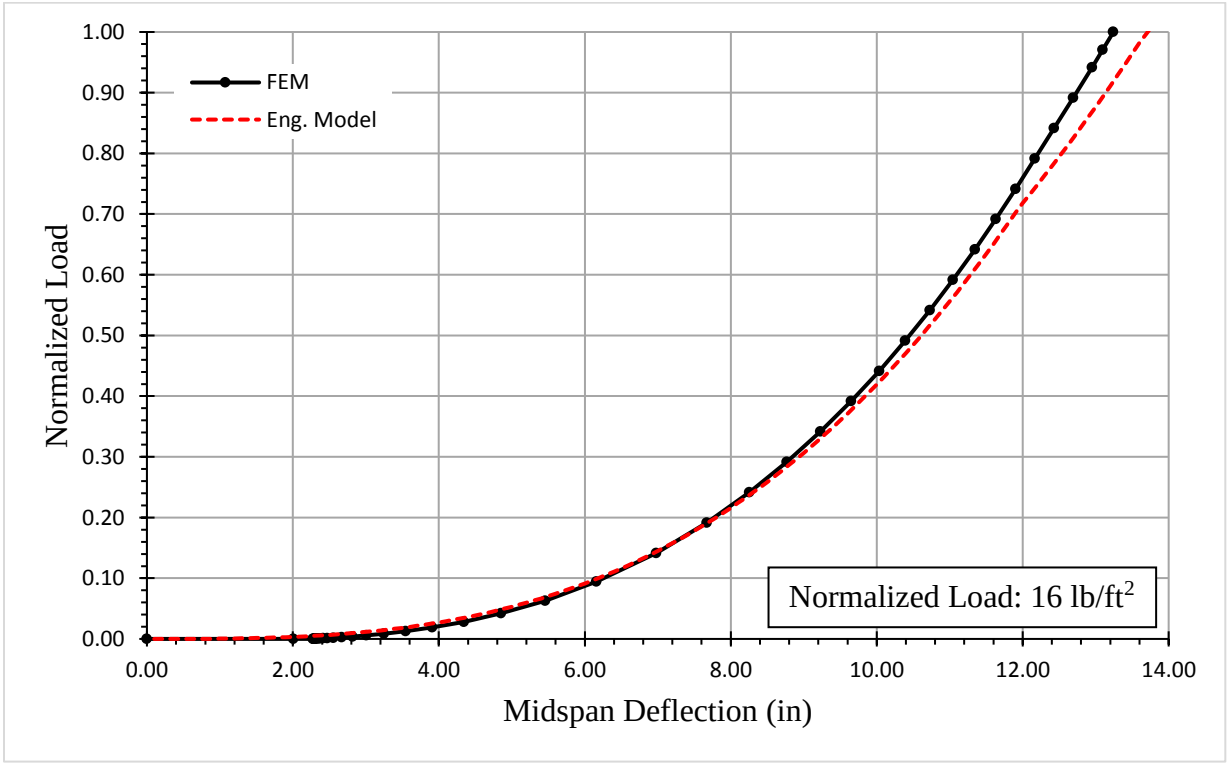

Figure 5-7: Nonlinear material properties deflection comparison

As observed, the engineering model is smooth when compared to the FEM model due to ANSYS Mechanical's and the engineering model's ability to interpolate between points on the nonlinear material properties plot. The von Mises stress at the supports is also exported form the finite element model for comparison to the engineering model, with the results shown in Figure 5-8.

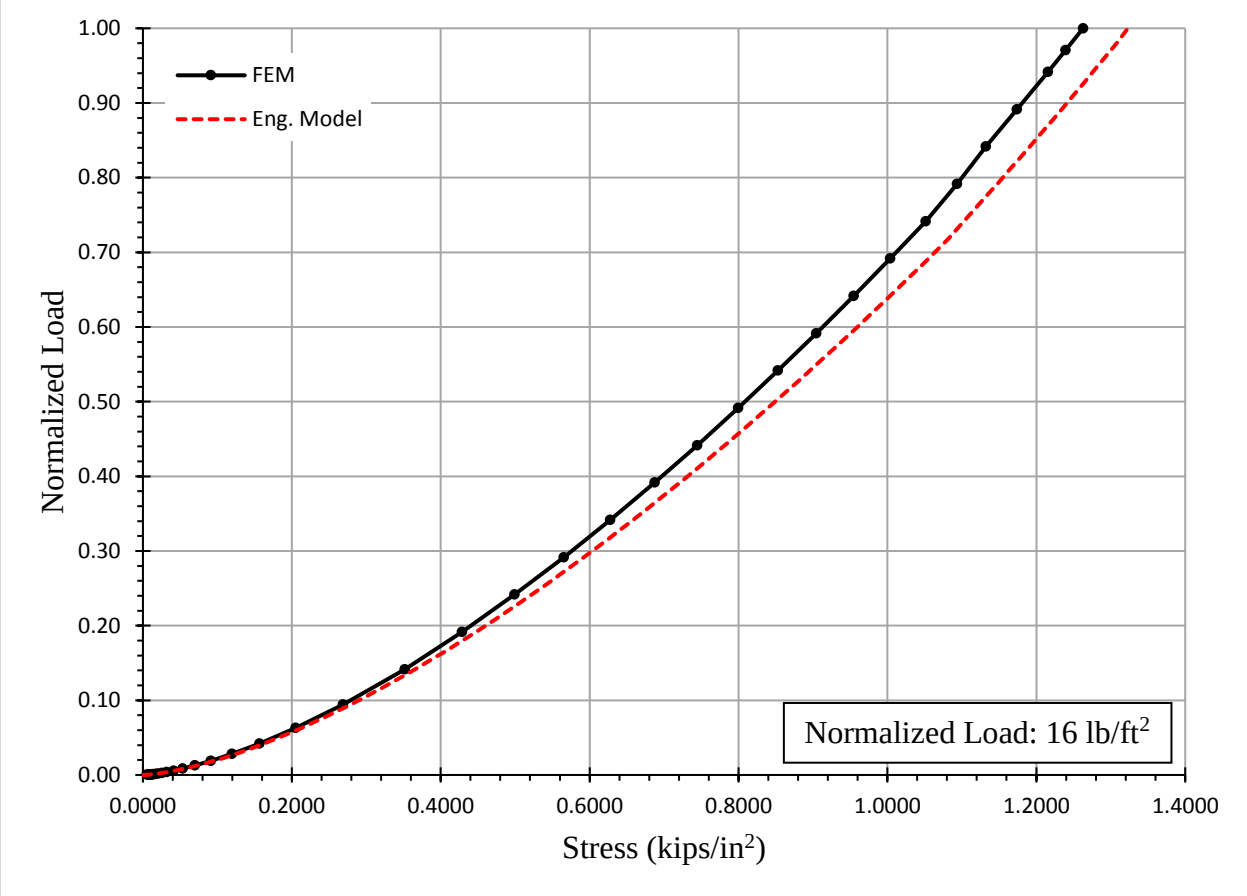

Figure 5-8: Nonlinear material properties stress comparison

As observed, the engineering model does a conservative job predicting the stress at each iterative step based on the true stress and true strain data available when compared to the finite element model stress results.

5.4. CONCLUSIONS

The work in chapter 5 of this research validated through finite element analysis the engineering model of Chapter 4 through finite element analysis. From the comparisons displayed in the previous sections, the engineering model has been validated through finite element modeling to mirror or conservatively predict results. Confirming the validity of the engineering model in this research is a major step in finalizing the engineering model. From field observations and tension the force analysis the fabric structure will break at the supports where it's radius of curvature is highest.

CHAPTER 6

ENGINEERING MODEL EXAMPLE

6.1. INTRODUCTION

Chapter 6 provides an engineering model example implementing the approached used in Chapter 3 to acquire material properties, along with operation of the engineering algorithm presented in Chapter 4. The goal of this chapter is to provide the reader with a proper example of the process required to fully implement the engineering model to predict a fabric structure's strength and deflection. The process of interpreting the material properties will be covered followed by the implementation of the engineering model, then finally the results will be analyzed.

6.2. EXAMPLE LAMS AND FABRIC STRUCTURE

The example LAMS has 10 bays, with a bay width of 12 feet 6 inches establishing an approximate length of 125 feet. The width of the LAMS is 75 feet and the height is 45 feet as seen in Figure 6-1. The manufacturer states that the LAMS will withstand 90 miles per hour sustained winds while sheltering vehicles and aircraft. One piece of fabric structure spans the full width of the LAMS between consecutive arches. Service loads shall be limited to 25 percent of the maximum breaking stress.

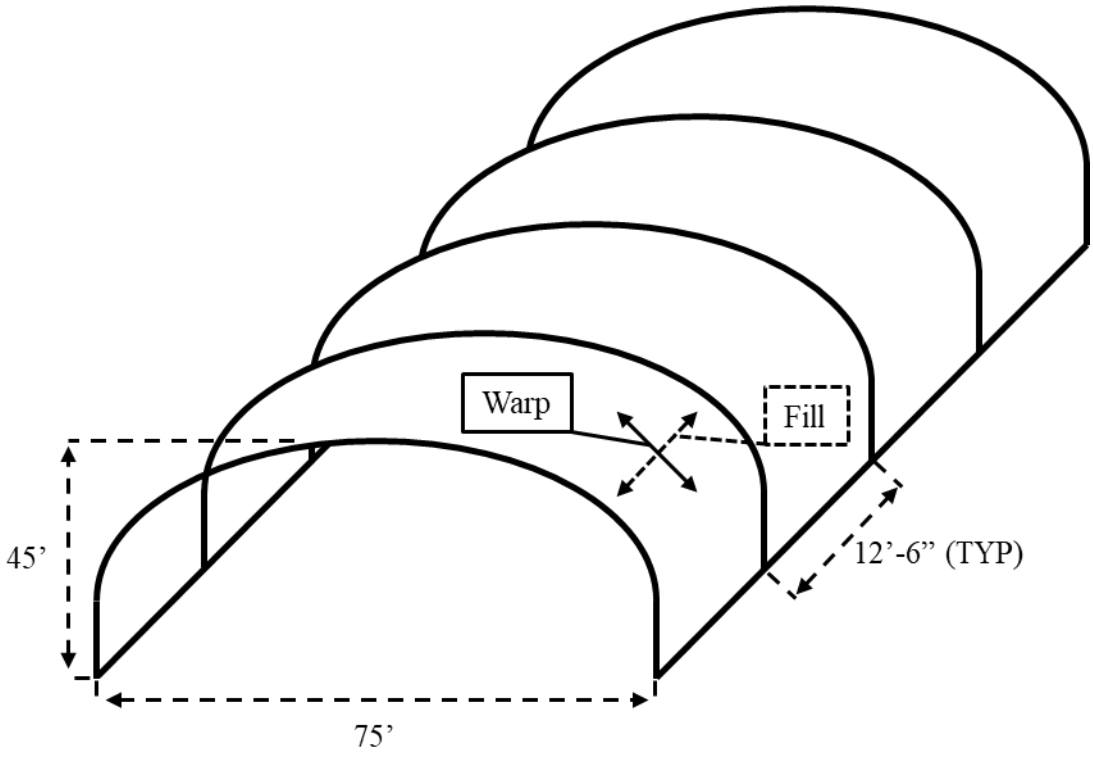

Figure 6-1: Partial isometric sketch of example structure (not to scale)

6.3. MATERIAL PROPERTIES

As stated by the manufacturer, the fabric structure spans the whole length of each bay. In terms of the fabric structure manufacturing process, the machine/warp direction spams the vertical support distance over the arch and the fill direction the longitudinal support distance between the arches as shown in Figure 6-2.

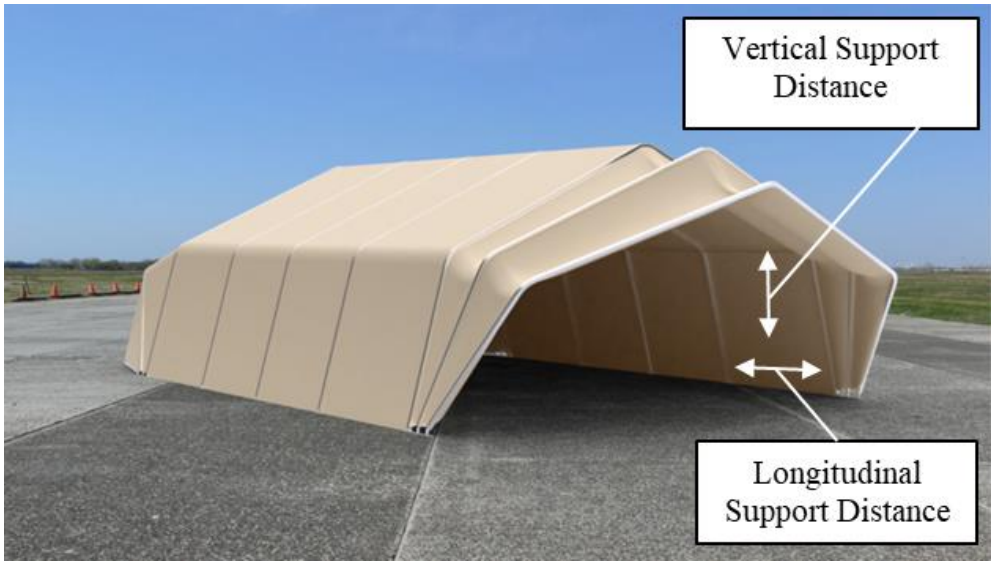

Figure 6-2: Direction of fabric and support distances (Celina Military Shelters n.d.)

This orientation calls for the material to undergo a uniaxial tension test covered in Chapter 3 in the fill direction of the fabric structure. If the material properties are provided as a simplified multilinear plot, they are ready for use in the engineering model. If only the raw test data is provided or testing is required, the following process must be carried out.

Once an UATT (UniAxial Tension Test) is preformed, the raw data will need the outlier data (a function of the initial slack in the specimen) removed from the test results and extrapolated to a simple multilinear plot. For this example, the material properties of Material 3 in the fill direction are used. From the UATT, the raw data will be returned in a similar fashion to Table 6-1, depending on the machine and software used for testing.

Table 6-1: Sample of raw data from a UATT

Gauge Length	3	in		
Thickness	0.64	mm		
Width	1	in		
Start Date	########			
Cross head speed	12	in/min		
Comments - 1				
Time	Extension	Load	Tensile strain	Tensile stress
(sec)	(in)	(lbf)	(%)	(ksi)
0	0	0.26	0	0.011
0.074	0.013	3.22	0.429	0.128
0.096	0.018	6.33	0.602	0.251
0.114	0.022	9.22	0.736	0.366
0.132	0.026	12.08	0.865	0.48
0.152	0.03	15.1	1.004	0.599
0.172	0.034	18.05	1.141	0.716
0.192	0.038	20.94	1.276	0.831
0.214	0.043	23.97	1.425	0.951

From the raw data, the tensile strain and stress is copied and pasted into a new Excel sheet to begin the process of converting the raw data into material properties usable by the engineering model. The strain is converted to a unitless value from a percentage and the stress remains the same as kips per square inch. Next, the outlier data (a function of the initial engagement of the specimen) present at the beginning of the UATT will need to be removed from the data. After plotting the raw data, the operator of the model needs to eliminate the outlier data illustrated by the red section highlighted in Figure 6-3. The numerical process of determining a constant slope between data points and offsetting the data is discussed in Chapter 3.

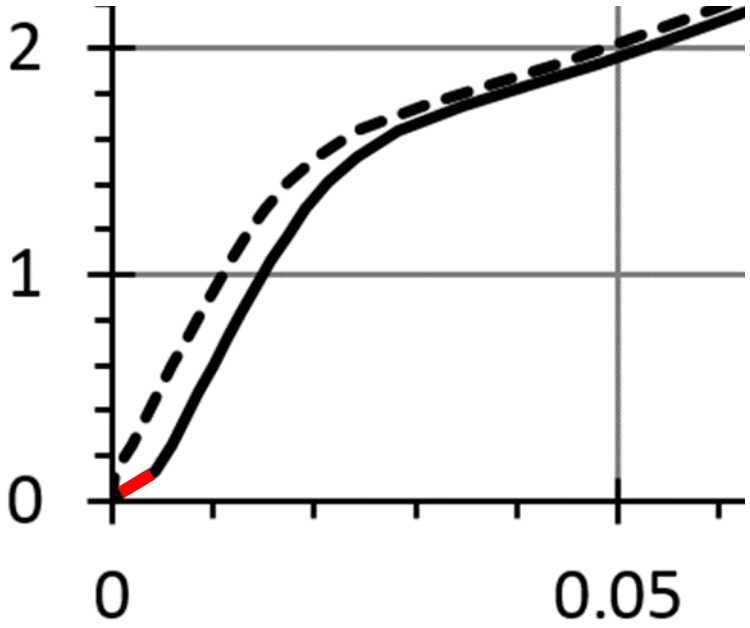

Figure 6-3: Removing slack

For this material, 0.004 inches per inch of strain is offset as represented by the dashed line when plotted in Figure 6-3. The raw data looks similar to the data shown in Table 6-2.

Table 6-2: Data after slack removal

No Slack	
Strain (in/in)	Stress (kips/in^2)
0	0
0.00029	0.128
0.00202	0.251
0.00336	0.366
0.00465	0.48
0.00604	0.599
0.00741	0.716
0.00876	0.831
0.01025	0.951

The final step is to simplify the raw data to a few transition points in order to create a multilinear plot for the engineering model and finite element model to use. This is accomplished by trial and error by copying and pasting points of interest from the data until a plot begins to mirror the data

represented by the no slack plot as seen in Figure 6-4. Table 6-3 shows the final simplified data used for the purpose of this example.

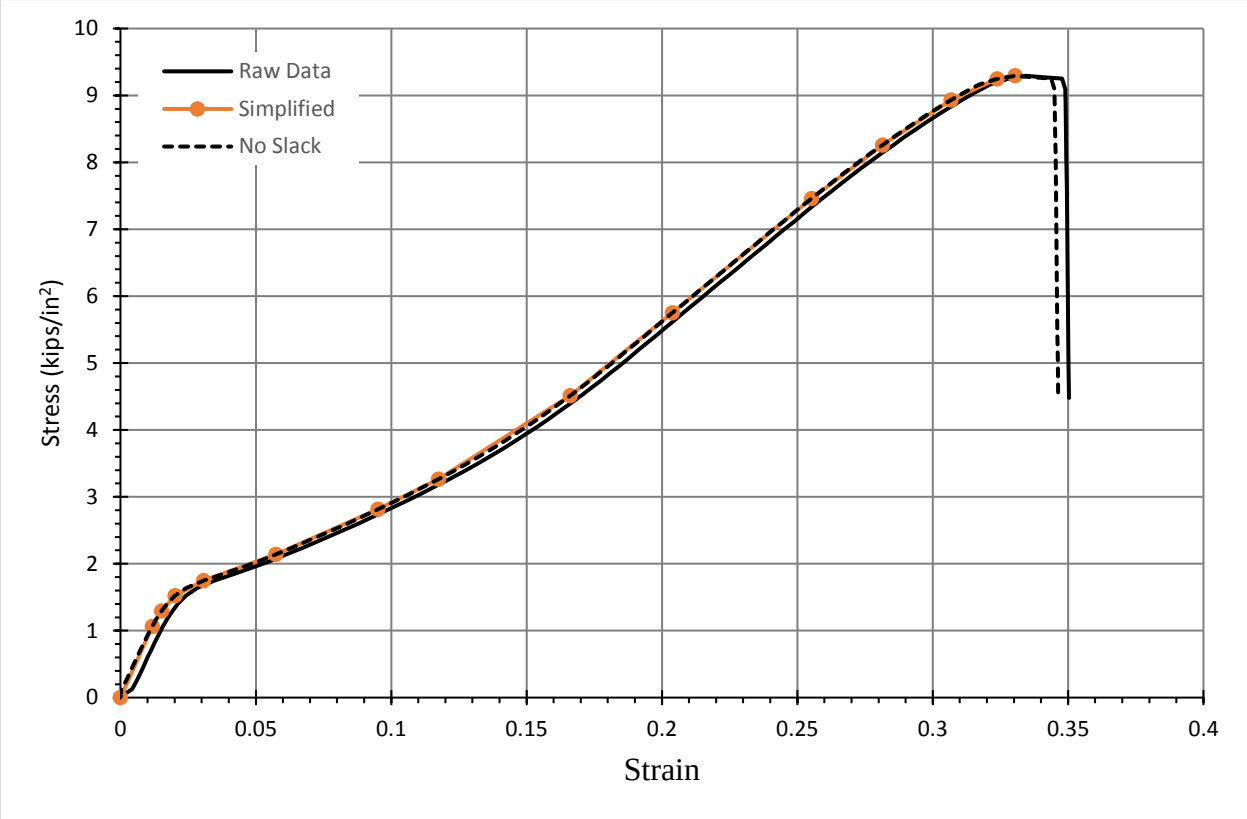

Figure 6-4: Simplifying the no slack data

Table 6-3: Simplified data

Simplified	
Strain (in/in)	Stress (kips/in^2)
0.0000	0.000
0.0117	1.064
0.0152	1.294
0.0201	1.522
0.0307	1.748
0.0573	2.138
0.0951	2.813
0.1175	3.264
0.1661	4.512
0.2039	5.751
0.2552	7.457
0.2815	8.259
0.3068	8.933
0.3237	9.246
0.3304	9.293

The material properties have now been simplified down to the data needed for the engineering model to operate properly.

6.4. INPUT INTO ENGINEERING MODEL

Having simplified the material property data, the engineering model can be then used. The first step is to import the simplified material property data into sheet 3 of the Excel file labeled “Raw Data” as shown in Figure 6-5. The engineering model then takes the material properties and convert them to true stress and true strain properties as discussed in Chapter 4. A graph also populates to the right of the material properties, plotting the material properties data points as a stress vs. strain curve.

	Simplified multi-linear material properties	
	Strain (in/in)	Stress (kips/in^2)
INSERT MATERIAL → PROPERTY DATA HERE	0	0
	0.01172	1.064
	0.01519	1.294
	0.02013	1.522
	0.03067	1.748
	0.05733	2.138
	0.09507	2.813
	0.11746	3.264
	0.16613	4.512
	0.20387	5.751
	0.25519	7.457
	0.28146	8.259
	0.3068	8.933
	0.32374	9.246
	0.3304	9.293

Figure 6-5: Raw data sheet example

Having inputted the "Raw Data," the next step is to select on the "Wind Analysis" tab to begin the process of inputting the wind pressure parameters as shown in Figure 6-6.

"Input cell"			
Initial properties from ASCE 7-10			
Risk category:	3	Table 1.5-1	1 for equipment / 3 for aircrafts
Wind Speed(mph):	136.8	http://windspeed.atcouncil.org/	
K_d:	0.85	Table 26.6-1	Components and Cladding
Exposure cat:	C	26.7	
K_{zt}:	1.00	Figure 26.8-1	
Gust Factor:	0.85	26.9	
GCp(+/-):	1.20	See Note 1	
GCpi(+/-):	0.55	Open: 0.00 / Partially Enclosed: 0.55	

Note 1
Open:
Figure 30.8-2 (Pitched free roofs)
Partially Enclosed:
Figure 30.4-2C (Gable roofs)
Fgure 30.4-7 (Domed roof)

Figure 6-6: Wind analysis sheet inputs

The inputs shown in Figure 6-6 are the same inputs used in this example. For guidance on selecting inputs, see Chapter 4. As stated in Section 6.2, the manufacturer states that the LAMS will withstand 90 miles per hour sustained winds while sheltering vehicles and aircraft. Sustained winds are winds measured on a one minute average, which is not what is required in the

engineering model. To convert the manufacturers claim to a 3 second gust wind used in ASCE 7-10, the Durst curve seen in Figure 6-7 must be consulted. The x-axis of the Durst curve displays the gust time desired while the y-axis displays the "amplification" factor to use. For this example, the sustained wind speed will be converted to a 3 second gust speed as shown in Equation 6-1 with the "amplification" factor taken as 1.216 from the Durst curve.

$$V = 90 * \left(\frac{1.52}{1.25} \right) = 109.44 \tag{6-1}$$

From Equation 6-1, the 3 second gust speed is found to be 109.44 miles per hour. If the manufacturer does not provide any wind speed limitations, the location of the LAMS will determine the wind speed based off the ASCE7-10 wind speed maps seen in Figure 4-1 or from the website http://windspeed.atcouncil.org/.

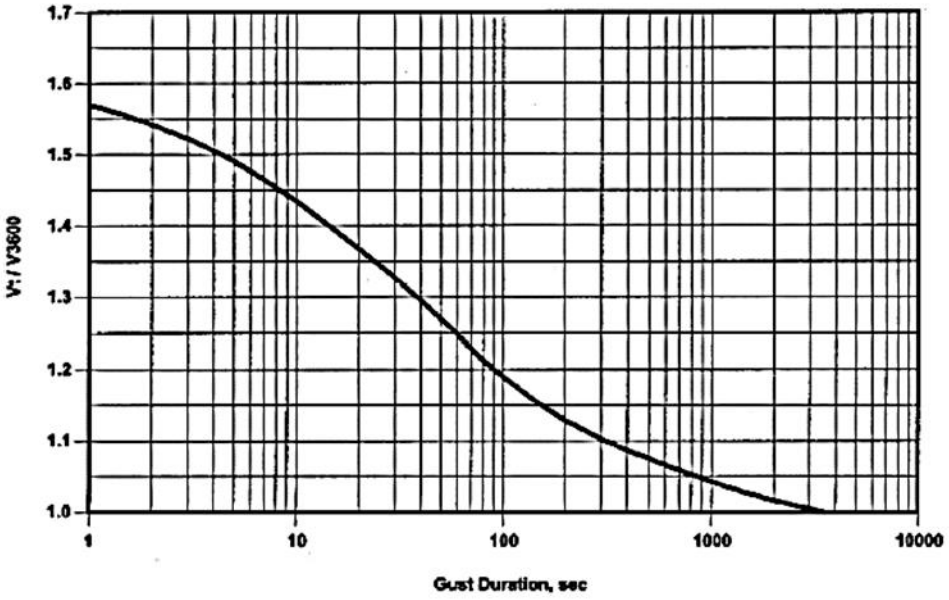

Figure 6-7: Durst curve (ASCE Standard ASCE/SEI 7-10. 2010)

Once all input cells in the "Wind Analysis" sheet are populated, the engineering model calculates the pressures at each elevation level. The final step in the process is to populate the "Iterative

Algorithm" sheet of the engineering model. The geometric properties of the LAMS in Section 6.2 are inputted along with the thickness of the fabric structure under consideration. The service values may change depending on the user input for the percent of maximum values Table 6-4 reflects the inputs of the example problem in this chapter.

Table 6-4: Iterative algorithm sheet inputs

"Input cell"	
Initial properties	
Thickness of material (in):	0.025197
Consistant Unit Width (ft):	1
Distance between longitudinal supports (ft):	12.5
Height of LAMS (ft):	40
Are max values below ASCE7-10 loads?:	YES
Are service values below ASCE7-10 loads?:	YES
Maximum Values	100%
Breaking Stress (kips/in^2):	12.36
Max Tension Force (kips/ft):	3.15
Max Midspan Deflection (in):	50.00
Service Values (% of Max):	25%
Service Stress (kips/in^2):	3.09
Service Tension Force (kips/ft):	0.93
Service Midspan Deflection (in):	28.80
Service Wind Pressure Failure (lb/ft^2)	103.74

Following the "Iterative Algorithm" inputs, the engineering model calculates the parabolic length, wind pressure, elevation, tension force, strain, and stress for each iterative step and return the maximum and service load values. The wind pressure calculation, according to the midspan deflection, is used to reference the "Wind Analysis" sheet to report an elevation associated with the calculated wind pressure. The elevation is referenced to report back if the fabric structure passes ASCE 7-10 standards. The strain calculation is used to reference the "Raw Data" sheet to report the stress.

6.5. ANALYZING RESULTS

The engineering model results are ready for analysis. From Table 6-4, the maximum and service values are displayed along with the service wind pressure at failure. Above the maximum values, the statements “Are max values below ASCE7-10 loads?” and “Are service values below ASCE7-10 loads?” are listed. These statements are followed by a simple YES or NO based on the height of the LAMS under consideration. The service value statement determines if the manufacturer’s claims pass the scrutiny of the engineering model and serves as a final answer on whether or not to trust the manufacturer’s claims. Table 6-4 also shows the results for the example problem in this chapter. Based on the engineering model, the fabric structure fails at a service wind pressure of 103.74 pounds per square foot with a midspan deflection of 28.8 inches and a tension force of 930 pounds per linear foot. Based on these values and the height of the LAMS, the fabric structure passes ASCE 7-10 requirements. With a dip to length ratio of 0.19, the fabric structure will produce a low tension force in conjunction with little to moderate curvature as seen in Figure 2-3.

CHAPTER 7

SUMMARY AND CONCLUSION

7.1. CONCLUDING REMARKS

LAMSs are very practical lightweight structures that have the ability to be easily shipped and constructed around the world as used by the Air Force. This research set out to develop an engineering model to predict the strength and serviceability of fabric structures in the LAMS. Following a thorough literature review of resources exploring the capabilities and limitations of LAMSs, this research applied ASTM test standards to quantify material properties of four different fabric structures through UTT (Uniaxial Tension Testing) .After gathering this crucial data, an engineering model was constructed utilizing Microsoft Excel and taking into account nonlinear material and geometric properties. This engineering model was then validated by finite element modeling with the use of ANSYS Mechanical APDL. Having validated the engineering model this research concluded with an example on evaluating fabric structures used on LAMSs. The purpose of the example is to guide the operator through the progression of filling out the engineering model to obtain valid results. From the primary objective of this research, the engineering model has the ability to validate claims of fabric manufacturers on their material characteristics. Using this engineering model, an operator has the ability to evaluate the validity of the manufacturer's claims on wind load resistance for the fabric structures used on LAMSs. Though wind load resistance is a crucial part of a LAMSs ability to function properly during the

entire lifespan, there are other factors involved in the strength and serviceability of a LAMS. Further research is recommended into LAMSs and the many causes of failure due to high wind events. A few areas of recommended research are discussed below.

7.1.1. EXPLICIT EQUATION

The explicit equation formulated in section 4.10 of Chapter 4 proves useful up to a certain applied wind pressure that varies dependent on the material properties of a fabric structure. Further research is recommended to validate the use and limitations of the explicit equation.

7.1.2. UV RAYS

Manufacturers recommend a life span for their fabric structures typically based on UV degradation characteristics. Most fabric structures have a life span of 5 to 8 years before the LAMS will need to be reskinned with a new fabric structure due to UV degradation. There will be visible discoloration of a highly degraded fabric structure as well.

The focus of this research has been to evaluate a fabric structure's strength and serviceability characteristics using an engineering model. These characteristics depend upon the material properties of the fabric structure under consideration. As a fabric structure ages due to UV degradation, the strength properties of the fabric structure will severely decrease thus calling for new material testing to quantify the material properties of the highly degraded fabric structure. Following the quantification of the degraded fabric structures material properties, the engineering model will run through the same calculations to determine if the degraded fabric structure will withstand wind loads prescribed in ASCE7-10. Overall, the engineering model has the ability to handle fabric structures degraded by UV rays through new material property testing. However, further research is recommended into UV degradation characteristics of fabric structures used on LAMSs.

7.1.3. FLUTTERING

From material testing covered in Chapter 3, it is observed that the fabric structure material is not stiff like steel. A consequence of this is the presence of residual strains after constant wind events or a relaxing of the material as it ages. When the fabric structure is not pulled taut over a metal frame, it will have the ability to flutter in the wind. This fluttering action may seem insignificant at first, but it will amplify over time as the fabric structure continues to gather up residual stains. In the case of a high wind event, the fluttering action will ultimately lead to a failure of the fabric structure. The elimination of fluttering action ultimately lies on the crew who are up-keeping the structure and on the reliability of scheduled inspections. The overall effects of fluttering action has not been explored in this research. Further research into this topic is recommended.

REFERENCES

ASCE Standard ASCE/SEI 7-10. 2010. "Minimum Design Loads for Buildings and Other Structures" *American Society of Civil Engineers*, Reston, Virginia.

ASCE Standard ASCE/SEI 55-16. 2017. "Tensile Membrane Structures" *American Society of Civil Engineers*, Reston, Virginia.

ASTM D751. 2006. "Standard Test Methods for Coated Fabrics" *ASTM International*, West Conshohocken, Pennsylvania.

ASTM E108 "Standard test methods for fire tests of roof coverings" *ASTM International*, West Conshohocken, Pennsylvania.

ASTM E84 "Standard test methods for surface burning characteristics of building materials" *ASTM International*, West Conshohocken, Pennsylvania.

Big Top Shelters (n.d.) "Large Area Maintenance Shelter (LAMS) Systems." <http://bigtopshelters.com/building-products/military/large-area-maintenance-shelter-lams-systems/> Web access January 2018.

Bridgens B., Birchall M. 2012. "Form and function: The significance of material properties in the design of tensile fabric structures" In *Engineering Structures*, Volume 44, Pages 1-12.

Celina Military Shelters (n.d.) "Large Area Maintenance Shelter" <https://www.celinamilitaryshelters.com/medium-shelter-1> Web access November 2018.

Fujikake Masahisa, Kojima Osamu, Fukushima Seiichiro 1989. "Analysis of fabric

tension structures". In *Computers & Structures*, Volume 32, Issues 3–4, Pages 537-547, ISSN 0045-7949.

Gagnet E,, Hoemann J., Davidson J. 2017. "Blast resistance of membrane retrofit unreinforced masonary walls with flexible connections" In *International Journal of Protective Structures,* I-21, DOI: 10.1177/2041419617729897.

Galliot C., Luchsinger R.H. 2009. "A simple model describing the non-linear biaxial tensile behavior of PVC-coated polyester fabrics for use in finite element analysis" In *Composite Structures*, Volume 90, Pages 438-447.

Huntington C. 2013. "Tensile Fabric Structures Design, Analysis, and Construction" American Society of Civil Engineers. Reston, VA. ISBN: 978-0-7844-1289-3.

Huntington C. 2004. "The tensioned fabric roof" American Society of Civil Engineers. Reston, VA. ISBN: 0-7844-428-3.

Masteikaite V., Sacevičiene V. 2004. "Study on tensile properties of coated fabrics and laminates" In *Indian Journal of Fiber & Textile Research*, Volume 30, Pages 267-272.

Microsoft (n.d.) "VLOOKUP function" < https://support.office.com/en-us/article/vlookup-function-0bbc8083-26fe-4963-8ab8-93a18ad188a1> Web access May 2018.

NFPA 701 "Standard methods of fire tests for flame propagation of textiles and films" *National Fire Protection Association*, Quincy, Massachusetts.

Sewingplums (2010) "Types of weaving/types of loom 3: yarn, heddles, cards" <https://sewingplums.com/2010/11/27/types-of-weaving-types-of-loom-3-yarn-heddles-cards/> Web access January 2018.

Shelter-Rite (n.d.) "Tensile Strength of Architectural Fabrics."

<https://cdn2.hubspot.net/hubfs/481608/Technical_Library/Fabric_Properties/Updated_Fabric_Properties/Fabric-Properties-01-Tensile-Strength-iv2.pdf?t=1514499793018> Web access January 2018.

SkySong Center (n.d.) "Overview." < http://skysong.com/about-skysong/overview/> Web access August 2018.

Unified Facilities Criteria (UFC) 2013. "UFC 3-301-01 Structural Engineering" *United States Department of Defense*, Washington, DC.

Young Warren, Rudynas Richard 2002. "Roark's Formulas for Stress and Strain" Seventh Edition. McGraw-Hill companies. New York, NY. ISBN 0-07-072542.

APPENDIX-A

This appendix contains test results discussed in Chapter 3.

Auburn University

Polymer and Fiber Engineering Department

Information Table

Operator	Preston
Cross head speed	12. in/min
Gauge Length	3. in
Width	1.00 in

Results Table

	Thickness (in)	Elongation at Maximum Load (%)	Maximum Load (lbf)	Tensile stress at Maximum Load (ksi)
1	0.031	27.61	404.7	13.18
2	0.030	29.88	438.5	14.46
3	0.030	27.04	407.3	13.43
4	0.030	30.23	460.7	15.20
5	0.030	29.09	453.6	14.96
6	0.030	29.68	472.0	15.57
Mean	0.030	28.92	439.5	14.47
CV%	0.53	4.50	6.4	6.72

Material 1: Warp

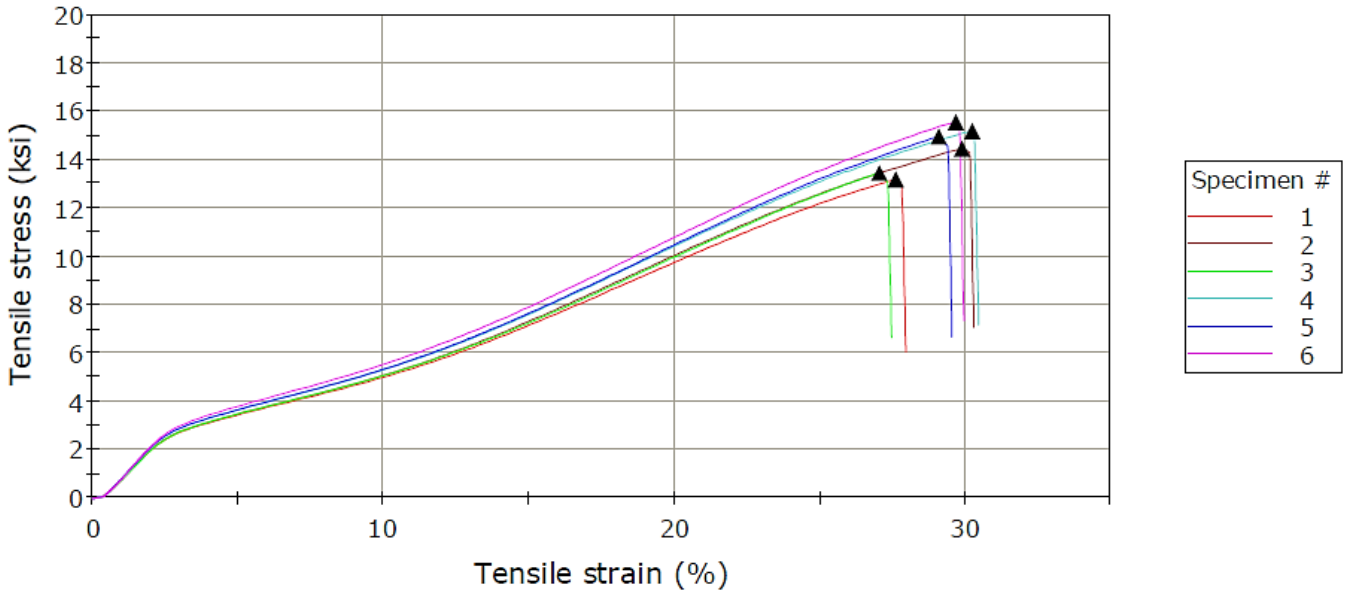

Auburn University

Polymer and Fiber Engineering Department

Information Table

Operator	Preston
Cross head speed	12. in/min
Gauge Length	3. in
Width	1.00 in

Results Table

	Thickness (in)	Elongation at Maximum Load (%)	Maximum Load (lbf)	Tensile stress at Maximum Load (ksi)
1	0.030	26.17	469.7	15.50
2	0.030	24.48	450.6	14.87
3	0.030	24.95	454.3	14.99
4	0.030	25.07	449.7	14.84
5	0.030	25.20	463.1	15.28
6	0.030	27.45	504.9	16.66
7	0.030	25.53	471.2	15.54
8	0.030	24.20	442.6	14.60
Mean	0.030	25.38	463.3	15.28
CV%	0.00	4.07	4.2	4.23

Material 1: Fill

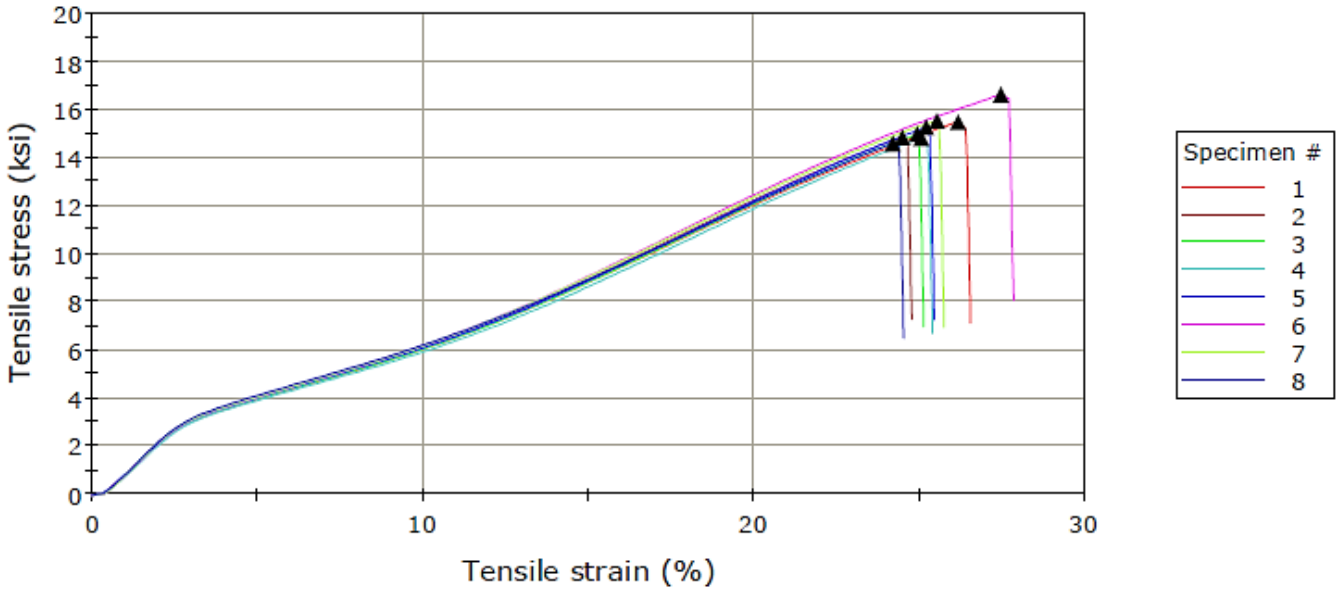

Auburn University

Polymer and Fiber Engineering Department

Information Table

Operator	Preston
Cross head speed	12. in/min
Gauge Length	3. in
Width	1.00 in

Results Table

	Thickness (in)	Elongation at Maximum Load (%)	Maximum Load (lbf)	Tensile stress at Maximum Load (ksi)
1	0.029	24.03	517.8	17.77
2	0.030	24.19	520.5	17.63
3	0.029	25.53	525.4	18.03
4	0.029	29.41	535.1	18.37
5	0.029	25.95	532.2	18.27
6	0.030	29.29	501.9	17.00
7	0.030	29.72	503.9	17.06
8	0.029	28.57	493.2	16.93
Mean	0.029	27.09	516.2	17.63
CV%	0.70	8.93	2.9	3.28

Material 2: Warp

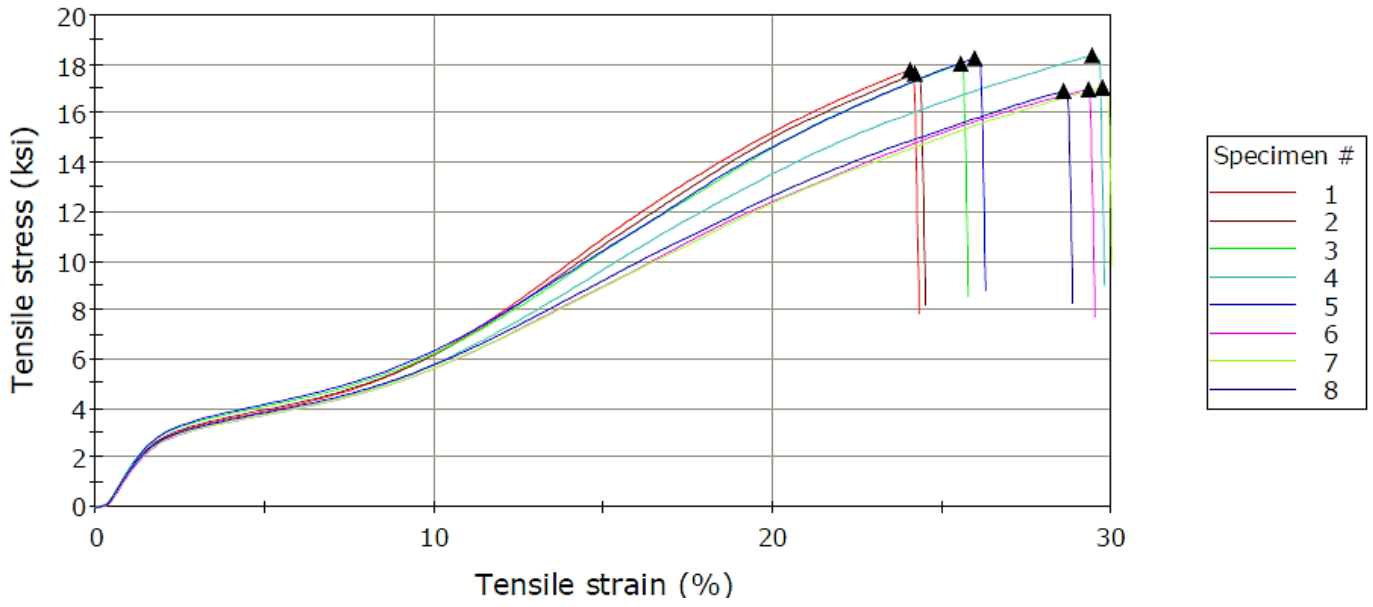

Auburn University

Polymer and Fiber Engineering Department

Information Table

Operator	Preston
Cross head speed	12. in/min
Gauge Length	3. in
Width	1.00 in

Results Table

	Thickness (in)	Elongation at Maximum Load (%)	Maximum Load (lbf)	Tensile stress at Maximum Load (ksi)
1	0.030	39.55	438.6	14.47
2	0.029	46.13	503.1	17.27
3	0.029	40.40	454.0	15.58
4	0.030	38.72	371.0	12.56
5	0.030	38.49	405.4	13.55
6	0.029	39.92	427.1	14.66
7	0.029	37.96	388.1	13.32
8	0.030	36.84	368.6	12.32
9	0.029	40.56	412.1	14.15
10	0.030	42.19	420.7	14.25
Mean	0.029	40.08	418.9	14.21
CV%	1.47	6.50	9.7	10.23

Material 2: Fill

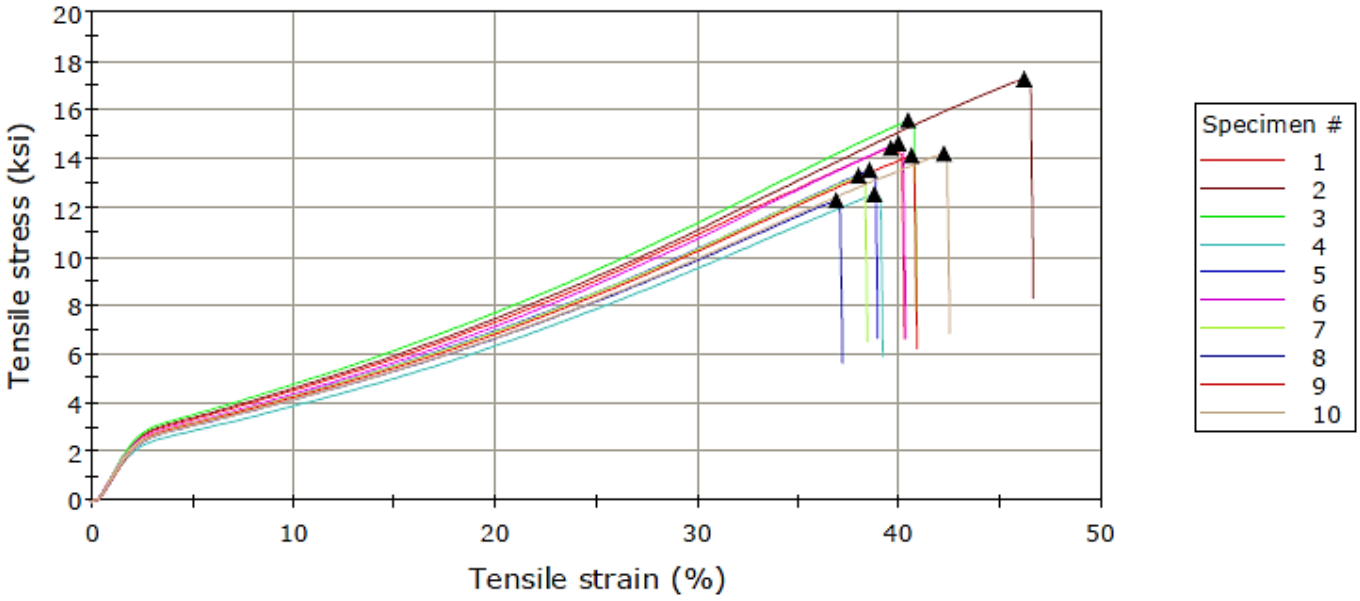

Auburn University

Polymer and Fiber Engineering Department

Information Table

Operator	Preston
Cross head speed	12. in/min
Gauge Length	3. in
Width	1.00 in

Results Table

	Thickness (in)	Elongation at Maximum Load (%)	Maximum Load (lbf)	Tensile stress at Maximum Load (ksi)
1	0.026	30.11	238.4	9.32
2	0.025	31.68	262.2	10.57
3	0.026	32.84	268.4	10.33
4	0.025	29.12	245.6	9.90
5	0.025	33.29	266.4	10.74
6	0.025	33.04	264.2	10.65
7	0.024	31.73	254.2	10.42
8	0.025	24.81	211.4	8.52
Mean	0.025	30.83	251.4	10.06
CV%	2.06	9.19	7.7	7.72

Material 3: Warp

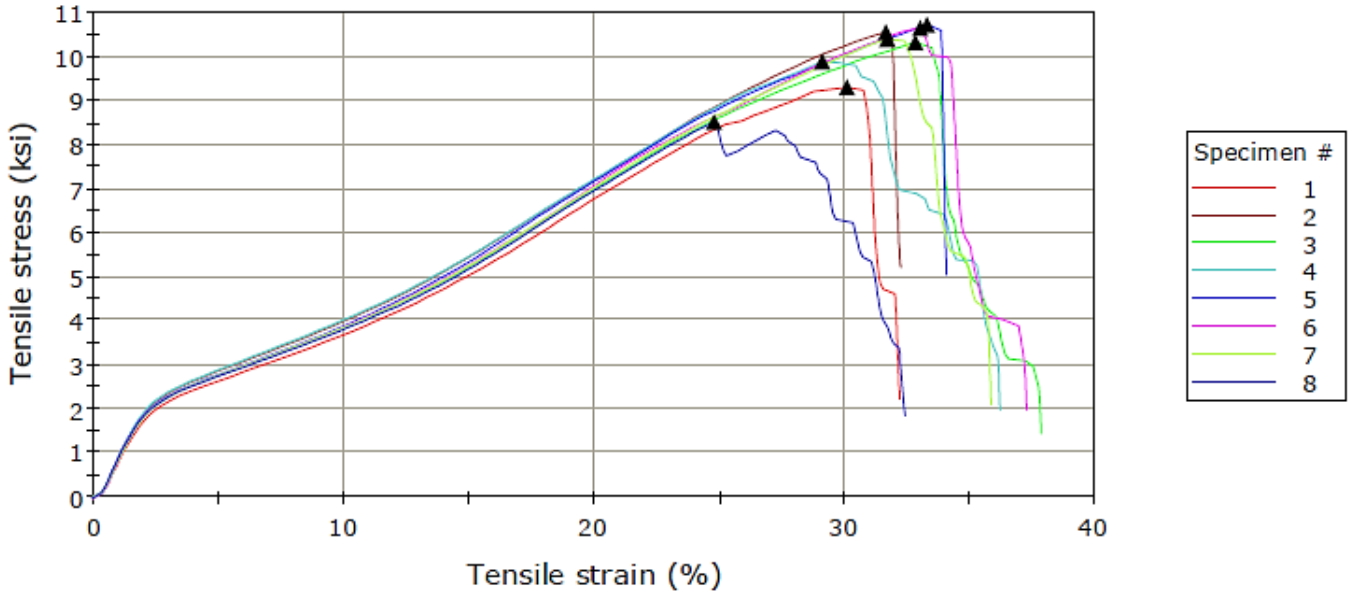

Auburn University

Polymer and Fiber Engineering Department

Information Table

Operator	Preston
Cross head speed	12. in/min
Gauge Length	3. in
Width	1.00 in

Results Table

	Thickness (in)	Elongation at Maximum Load (%)	Maximum Load (lbf)	Tensile stress at Maximum Load (ksi)
1	0.025	30.33	213.4	8.47
2	0.026	30.72	218.8	8.55
3	0.025	31.29	221.3	8.92
4	0.024	29.99	211.9	8.68
5	0.026	31.25	224.2	8.76
6	0.027	31.48	230.2	8.60
7	0.025	33.44	234.2	9.29
8	0.025	33.92	227.3	9.02
Mean	0.025	31.55	222.7	8.79
CV%	2.75	4.48	3.5	3.14

Material 3: Fill

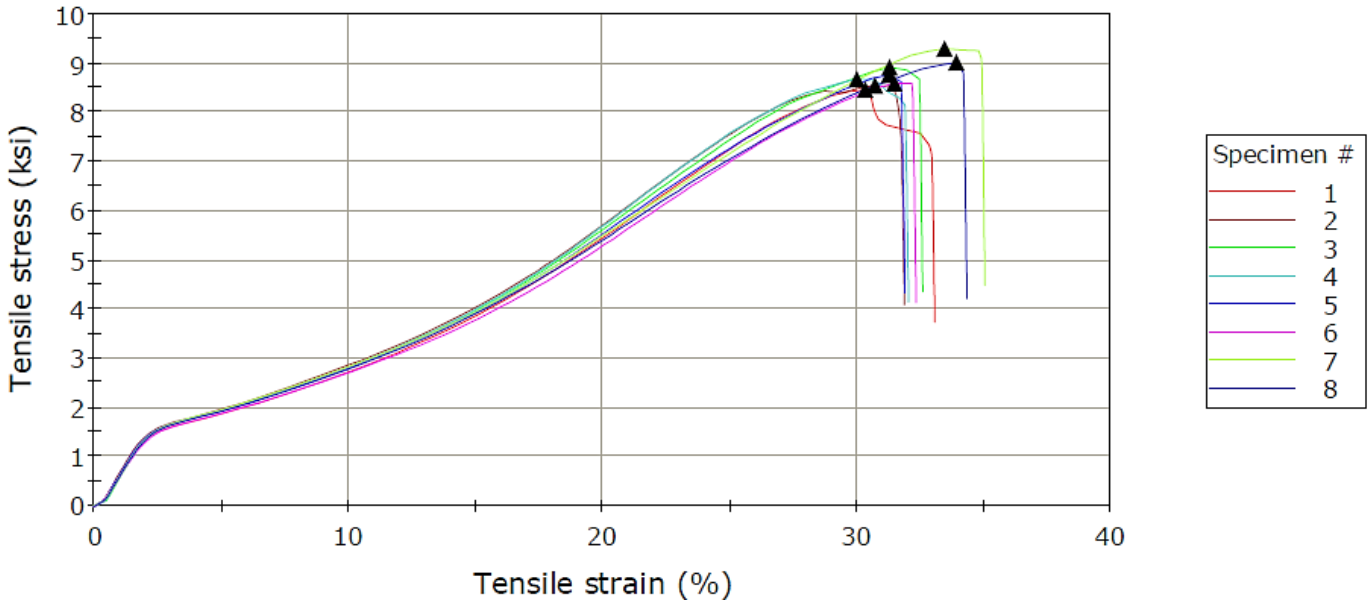

Auburn University

Polymer and Fiber Engineering Department

Information Table

Operator	Preston
Cross head speed	12. in/min
Gauge Length	3. in
Width	1.00 in

Results Table

	Thickness (in)	Elongation at Maximum Load (%)	Maximum Load (lbf)	Tensile stress at Maximum Load (ksi)
1	0.034	54.07	511.1	15.09
2	0.035	38.87	517.3	14.93
3	0.034	40.05	530.9	15.68
4	0.035	37.35	477.5	13.63
5	0.035	40.09	531.9	15.01
6	0.034	40.43	538.7	15.73
Mean	0.035	41.81	517.9	15.01
CV%	1.86	14.62	4.3	5.06

Material 4: Unknown Orientation

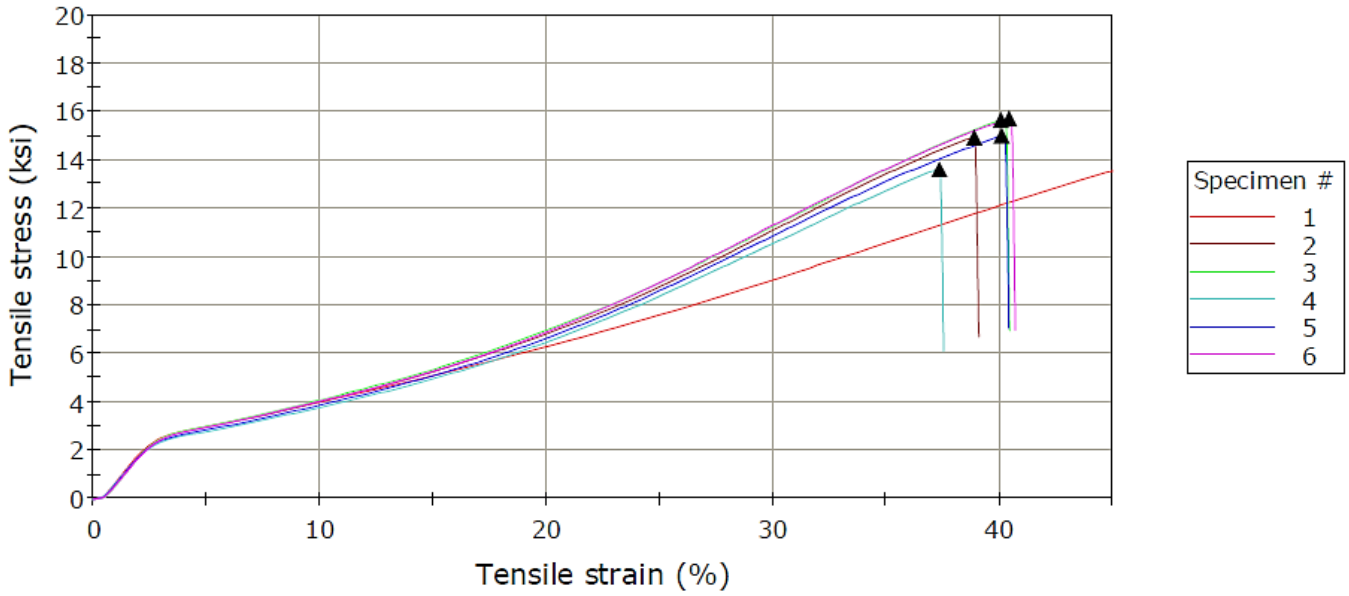

APPENDIX-B

This appendix contains the syntax used within excel to perform the equations discussed in Chapter 4 of this research. The variable excel is calculating will be called out followed by the syntax within excel. The example syntax provided will be pulled from the first iterative step.

SHEET 1 (WIND ANALYSIS)

K_z:

```
=IF($B$7="B",0.7,IF($B$7="C",0.85,1.03))
```

q_h:

```
=0.00256*G7*$B$8*$B$6*$B$5^2
```

p:

```
=H7*(($B$9*$B$10)+($B$9*$B$11))
```

SHEET 2 (ITERATIVE ALGORITHM)

Parabolic length:

```
=(4*(D3/12)/$B$5)*(((SQRT(($B$5^2/4)+($B$5^4/(64*(D3/12)^2))))+(($B$5^3/(32*(D3/12)^
2)))*LN(($B$5/2)+SQRT(($B$5^2/4)+($B$5^4/(64*(D3/12)^2))))-
(($B$5^3/(32*(D3/12)^2))*LN($B$5^2/(8*(D3/12))))))
```

Wind pressure:

=((2*J3*1000*$B$3)/($B$5*12))*(SIN((4*D3)/($B$5*12)))*144

Elevation:

=IF(F3>'Wind Analysis'!$I$28,500,(INDEX('Wind Analysis'!$F$6:$F$28,MATCH(F3,'Wind Analysis'!$I$6:$I$28,1)))+(((F3-(INDEX('Wind Analysis'!$I$6:$I$28,MATCH(F3,'Wind Analysis'!$I$6:$I$28,1))))*(((INDEX('Wind Analysis'!$F$6:$F$28,MATCH(F3,'Wind Analysis'!$I$6:$I$28,1)+1)))-((INDEX('Wind Analysis'!$F$6:$F$28,MATCH(F3,'Wind Analysis'!$I$6:$I$28,1))))))/((((INDEX('Wind Analysis'!$I$6:$I$28,MATCH(F3,'Wind Analysis'!$I$6:$I$28,1)+1)))-(INDEX('Wind Analysis'!$I$6:$I$28,MATCH(F3,'Wind Analysis'!$I$6:$I$28,1)))))))

Tension force:

=J3*$B$3*$B$4*12/$B$4

Strain:

=(E3-$B$5)/$B$5

Stress:

=(INDEX('Raw Data'!$C$3:$C$50,MATCH(I3,'Raw Data'!$B$3:$B$50,1)))+(I3-(INDEX('Raw Data'!$B$3:$B$50,MATCH(I3,'Raw Data'!$B$3:$B$50,1))))*((INDEX('Raw Data'!$C$3:$C$50,MATCH(I3,'Raw Data'!$B$3:$B$50,1)+1))-(INDEX('Raw Data'!$C$3:$C$50,MATCH(I3,'Raw Data'!$B$3:$B$50,1))))/((INDEX('Raw Data'!$B$3:$B$50,MATCH(I3,'Raw Data'!$B$3:$B$50,1)+1))-(INDEX('Raw Data'!$B$3:$B$50,MATCH(I3,'Raw Data'!$B$3:$B$50,1))))

Breaking stress:

=MAX('Raw Data'!C:C)

Max tension force:

=INDEX(H:H,MATCH(B11,J:J,1),1)

Max midspan deflection:

=INDEX(D:D,MATCH(B11,J:J,1),1)

Service stress:

=MAX('Raw Data'!C:C)*$B$15

Service tension force:

=INDEX(H:H,MATCH(B16,J:J,1),1)

Service midspan deflection:

=INDEX(D:D,MATCH(B16,J:J,1),1)

Service wind pressure:

=INDEX(F:F,MATCH(B16,J:J,1),1)

SHEET 3 (RAW DATA)

The material properties are pasted into sheet 3 for conversion to true stress and true strain.

True strain:

=LN(1+E3)

True stress:

=F3*(1+E3)